

University of Windsor

Scholarship at UWindor

Electronic Theses and Dissertations

Theses, Dissertations, and Major Papers

1984

Cold-formed angle columns under biaxial bending.

Sujit Kumar. Ray
University of Windsor

Follow this and additional works at: <https://scholar.uwindsor.ca/etd>

Recommended Citation

Ray, Sujit Kumar., "Cold-formed angle columns under biaxial bending." (1984). *Electronic Theses and Dissertations*. 1467.

<https://scholar.uwindsor.ca/etd/1467>

This online database contains the full-text of PhD dissertations and Masters' theses of University of Windsor students from 1954 forward. These documents are made available for personal study and research purposes only, in accordance with the Canadian Copyright Act and the Creative Commons license—CC BY-NC-ND (Attribution, Non-Commercial, No Derivative Works). Under this license, works must always be attributed to the copyright holder (original author), cannot be used for any commercial purposes, and may not be altered. Any other use would require the permission of the copyright holder. Students may inquire about withdrawing their dissertation and/or thesis from this database. For additional inquiries, please contact the repository administrator via email (scholarship@uwindsor.ca) or by telephone at 519-253-3000ext. 3208.



National Library
of Canada

Bibliothèque nationale
du Canada

Canadian Theses Service

Services des thèses canadiennes

Ottawa, Canada
K1A 0N4

CANADIAN THESES

THÈSES CANADIENNES

NOTICE

The quality of this microfiche is heavily dependent upon the quality of the original thesis submitted for microfilming. Every effort has been made to ensure the highest quality of reproduction possible.

If pages are missing, contact the university which granted the degree.

Some pages may have indistinct print especially if the original pages were typed with a poor typewriter ribbon or if the university sent us an inferior photocopy.

Previously copyrighted materials (journal articles, published tests, etc.) are not filmed.

Reproduction in full or in part of this film is governed by the Canadian Copyright Act, R.S.C. 1970, c. C-30. Please read the authorization forms which accompany this thesis.

AVIS

La qualité de cette microfiche dépend grandement de la qualité de la thèse soumise au microfilmage. Nous avons tout fait pour assurer une qualité supérieure de reproduction.

S'il manque des pages, veuillez communiquer avec l'université qui a conféré le grade.

La qualité d'impression de certaines pages peut laisser à désirer, surtout si les pages originales ont été dactylographiées à l'aide d'un ruban usé ou si l'université nous a fait parvenir une photocopie de qualité inférieure.

Les documents qui font déjà l'objet d'un droit d'auteur (articles de revue, examens publiés, etc.) ne sont pas microfilmés.

La reproduction, même partielle, de ce microfilm est soumise à la Loi canadienne sur le droit d'auteur, SRC 1970, c. C-30. Veuillez prendre connaissance des formules d'autorisation qui accompagnent cette thèse.

THIS DISSERTATION
HAS BEEN MICROFILMED
EXACTLY AS RECEIVED

LA THÈSE A ÉTÉ
MICROFILMÉE TELLE QUE
NOUS L'AVONS REÇUE

Canada

COLD-FORMED ANGLE COLUMNS UNDER BIAXIAL BENDING

by

SUJIT KUMAR RAY

A thesis
presented to the University of Windsor
in partial fulfillment of the
requirements for the degree of
Master of Applied Science
in
Civil Engineering

Windsor , Ontario, 1984

(c) SUJIT KUMAR RAY, 1984

~~I hereby declare that I am the sole author of this thesis.~~

I authorize the University of Windsor to lend this thesis to other institutions or individuals for the purpose of scholarly research.

SÚJIT KUMAR RAY

I further authorize the University of Windsor to reproduce this thesis by photocopying or by other means, in total or in part, at the request of other institutions or individuals for the purpose of scholarly research.

SUJIT KUMAR RAY

The University of Windsor requires the signatures of all persons using or photocopying this thesis. Please sign below, and give address and date.

ABSTRACT

Cross-sectional properties, including cross-sectional area, location of centroid, moments of inertia, torsional and warping constants and location of the shear centre, of both equal and unequal-leg cold-formed angle sections are presented. Two important properties, β_1 and β_2 , required for the calculation of theoretical buckling load of eccentrically loaded columns, are also listed.

The computational difficulties encountered in the exact solution of differential equations of equilibrium of columns under biaxial bending are pointed out and theoretical load-deflection relationships using the Galerkin method are presented. These theoretical relationships are then compared with experimental ones, obtained from the tests carried on fifteen 65 X 50 X 4 mm (nine specimens with long leg connected and six with long leg out) and nine 55 X 55 X 4 mm eccentrically loaded cold-formed single angles. The test specimens were connected at ends to the test frame by bolts on one leg and were subjected to eccentric thrust (eccentricity about both principal axes). Three different nominal slenderness ratios (80, 120 and 170) and three different end connections (one-, two- and three-bolt end connections) were used in the test program.

A computer program for pinned-end boundary conditions was developed to predict the load-deflection relationships of cold-formed angles under biaxial bending. This program was also used to estimate the ultimate compressive strengths of such sections connected by one leg. A table giving the ultimate compressive strengths of two commonly used cold-formed angles for various gauge distances is included. Failure is assumed to have occurred when the total stress (compressive or tensile) at any point on the cross-section reaches the value of yield stress or when there is a change of sign for at least one of the deflection components. These predicted loads together with those obtained from ASCE Manual No. 52 and the ECCS Recommendations are compared with experimental failure loads.

The effects of the location of shear centre and magnitude of warping constant on the ultimate compressive strength of cold-formed single angles have been discussed.

ACKNOWLEDGEMENTS

The author wishes to take this opportunity to express his sincerest gratitude to his advisor Dr. Murty K. S. Madugula for his continuous encouragement, guidance, advice and valuable suggestions throughout the preparation of this thesis.

The author is also grateful to Sidbec-Dosco, Montreal, for supplying the cold-formed angles used in this investigation.

The financial support provided by the Natural Sciences and Engineering Research Council of Canada under grant number A1194 is gratefully acknowledged.

Many thanks are also due to :

- Messrs. K. M. Chong and S. P. Khor for carrying out a portion of the experimental work.
- Mr. S. G. Ekhande and other graduate students of the Department of Civil Engineering for their often useful advices.
- Technicians of the Civil Engineering Department for their assistance during the experimental work.
- Computer Centre Staff of the University of Windsor for the help in running the computer program.

LIST OF SYMBOLS

- A = area of the cross-section
 C_w = warping constant of the cross-section
 E = modulus of elasticity

 e_x, e_y = x- and y- coordinates of point of application of eccentric thrust with reference to the centroidal principal axes
 e_1 = effective eccentricity about the x-x axis
 $\quad = e_y - v - (e_x - x_0) \phi$
 e_2 = effective eccentricity about the y-y axis
 $\quad = e_x - u + (e_y - y_0) \phi$
 G = modulus of rigidity = $\frac{E}{2(1 + \nu)}$
 I_x, I_y = moments of inertia of the cross-section about the major and minor centroidal principal axes (x-x and y-y axes) respectively
 $I_{x'}, I_{y'}$ = moments of inertia of the cross-section about the centroidal axes parallel and perpendicular to short leg, x'-x' and y'-y' axes respectively
 I_o = polar moment of inertia of the cross-section about the shear centre
 J = torsional constant of the cross-section
 K_x, K_y = effective length factors for flexural buckling about the x- axis and y- axis respectively
 l = length of the member

- P = external applied load
- P_x = flexural buckling load about x-x axis = $\frac{\pi^2 EI_x}{(K_x \cdot l)^2}$
- P_y = flexural buckling load about y-y axis = $\frac{\pi^2 EI_y}{(K_y \cdot l)^2}$
- $P_{x'y'}$ = product of inertia of the cross-section about $x'-x'$ and $y'-y'$ axes
- P_ϕ = torsional buckling load parameter = $(4EC_w \pi^2 / l^2 + GJ) / r_o^2$
- r_y = minimum radius of gyration
- r_o^2 = $\beta_1 e_y^2 + \beta_2 e_x^2 + I_o / A$
- u, v, ϕ = deflections of the shear centre (u and v) along major and minor centroidal principal axes respectively and rotation of the shear centre (ϕ) about the longitudinal axis (z-z axis)
- u_o, v_o, ϕ_o = co-efficients in the expressions for deflections to be determined by the application of the Galerkin method
- x, y = x- and y- coordinates of the point at which the stress is being calculated
- x', y' = perpendicular distances of the centroid from the outside of the long leg and short leg respectively
- x_s, y_s = perpendicular distances of the shear centre from $y'-y'$ and $x'-x'$ axes respectively

x_o, y_o = x- and y- coordinates of the shear centre with reference to the centroidal principal axes

z = location of the cross-section along the length of the member, where the deflection is being calculated

b/t = width-to-thickness ratio

Kl/r_y = largest effective slenderness ratio according to ASCE Manual No. 52

l/r_y = maximum slenderness ratio

α = angle of inclination of major principal axis with respect to the x'-x' axis

$$\alpha' = \frac{\sinh \lambda - \sin \lambda}{\cosh \lambda - \cos \lambda} = 1.0178$$

$$\beta_1 = \frac{1}{I_x} \left(\int_A y^3 dA + \int_A x^2 y dA \right) - 2y_o$$

$$\beta_2 = \frac{1}{I_y} \left(\int_A x^3 dA + \int_A xy^2 dA \right) - 2x_o$$

λ = 4.73004, an eigenvalue satisfying the characteristic equation $\cos \lambda \cosh \lambda = 1$

ν = poisson's ratio

σ_{cr} = ultimate maximum stress according to the ASCE Manual No. 52

σ_T = total normal stress at any point

σ_y = yield stress of the material

σ_1 = uniform axial compressive stress = P/A

σ_2 = linearly varying stress due to bending about the major centroidal principal axis (x-x axis)

$$\sigma_3 = \frac{Pe_1}{I_x} \cdot y$$

σ_3 = linearly varying stress due to bending about the minor centroidal principal axis (y-y axis)

$$= \frac{Pe_2}{I_y} \cdot x$$

σ_4 = warping normal stress due to non-uniform torsion

$$= E(\bar{\omega}_s - \omega_s)\phi''$$

ω_s = warping function according to Timoshenko and Gere

$\bar{\omega}_s$ = average value of ω_s

λ/λ_y = slenderness ratio according to ECCS Recommendations

LIST OF CONTENTS

ABSTRACT	iv
ACKNOWLEDGEMENTS	vi
LIST OF SYMBOLS	vii

<u>Chapter</u>	<u>page</u>
I. INTRODUCTION	1
General	1
Objectives	2
II. LITERATURE SURVEY	4
General	4
Theoretical Solution of Differential Equations of Equilibrium	5
Cold-Formed Angle Sections	6
Hot-Rolled Angle Sections	7
Design Specifications	10
III. THEORETICAL FORMULATION	12
General Theory of Torsional-Flexural Buckling	12
ASCE Manual No. 52	19
ECCS Recommendations	21
IV. COMPUTER PROGRAM	23
General	23
Description of the Computer Program	23
Main Program	24
Subroutines	25
Advantages of the Program	26
Limitations of the Program	27
Failure Criteria	27
Results	28
V. EXPERIMENTAL INVESTIGATION	29
General	29
Test Set-up	29
Lateral Support	30
Deflection Dial Gauges	30

/ Supports for Dial Gauges	30
Testing Procedure	31
VI. DISCUSSION OF RESULTS	32
Cross-Sectional Properties	32
Ultimate Compressive Strengths	32
Load-Deflection Relationships	34
Experimental Results	34
Exact Solution of Differential Equations	35
Solution of Differential Equations applying the Galerkin method	35
Comparison of Exact and Galerkin Solutions	37
Comparison of Experimental Failure Loads with the Predicted Loads	37
General	37
ASCE Manual No. 52	38
Slenderness ratios less than 120	38
Slenderness ratios exceeding 120	39
ECCS Recommendations	39
General Theory of Torsional-Flexural Buckling	39
Long Leg Connected versus Long Leg Out	40
Effect of the Other Variables	40a
VII. CONCLUSIONS AND RECOMMENDATIONS	41
General	41
Conclusions	41
Recommendations for Future Research	43
LIST OF REFERENCES	44
VITA AUCTORIS	50

<u>Appendix</u>	<u>page</u>
1. THEORETICAL FORMULATION FOR THE CROSS-SECTIONAL PROPERTIES OF COLD-FORMED ANGLES	83
2. FLOW CHART OF COMPUTER PROGRAM	118
3. SOURCE LISTING OF COMPUTER PROGRAM	120
4. DEFINITE INTEGRALS	144
5. SAMPLE CALCULATION FOR COMPUTATION OF ACTUAL DIMENSIONS OF TEST SPECIMENS	146
6. TYPICAL CALCULATIONS FOR THE DETERMINATION OF FAILURE LOADS	149

LIST OF TABLES

<u>Table</u>	<u>page</u>
6.1 Cross-sectional Properties (Full Section) of Cold- Formed Angles — Equal Leg Angles	51
6.2 Cross-sectional Properties (Full Section) of Cold- Formed Angles — Unequal Leg Angles	54
6.3 Ultimate Compressive Strength of Cold-Formed Angle Columns Under Biaxial Bending	59
6.4 Dimensional Buckling Curve, B3	60
6.5 Cross-sectional Properties of Test Specimens	61
6.6 Lengths & Slenderness Ratios of the Test Specimens	62
6.7a Experimental & Theoretical Failure Loads	63
6.7b Predicted Failure Loads for Test Specimens	63a
6.8 Effect of Variables on the Ultimate Compressive Strength of 65 X 50 X 4 mm Cold-Formed Angle (Long Leg Connected)	64
6.9 Comparison of Exact and Galerkin Solutions	65

LIST OF FIGURES

<u>Figure</u>	<u>page</u>
4.1 Location of Critical Points and the Load on the Cross-section	66
4.2 Cross-section of Cold-Formed Angle	67
4.3 Assumed Locations of Shear Centre	68
5.1 Schematic Diagram of Test Set-up	69
5.2 Arrangement for Load Application at joint B	70
5.3 Lateral Support at joint B	71
5.4 Lateral Support at joint C	72
5.5 Arrangement of Dial Gauges at Midspan of the Test Specimen	73
5.6 L-shaped Extension Piece at Midspan	74
5.7 Gauge Support Bracket	75
6.1 Load-Deflection and Load-Rotation Curves at Midspan for specimen ES55-3-1	76
6.2 Load-Deflection and Load-Rotation Curves at Midspan for specimen ES65-3-2	77
6.3 Load-Deflection and Load-Rotation Curves at Midspan for specimen ES65-2-2	78
6.4 Load-Deflection and Load-Rotation Curves at Midspan for specimen ES55-1-1	79
6.5 Load-Deflection and Load-Rotation Curves at Midspan for specimen ES55-2-2	80
6.6 Load-Deflection and Load-Rotation Curves at Midspan for specimen ES55-2-1	81
6.7 Load-Deflection and Load-Rotation Curves at Midspan for specimen ES65-5-1	82

Chapter I

INTRODUCTION

1.1 GENERAL

Structural steel angles are used extensively as leg and diagonal members of latticed towers, as chord and web members of trusses, as bracing members providing lateral support to beams and columns, etc.; they are easy to fabricate and erect because of the basic simplicity of their cross-section. In many of their potential uses, it is often required to use thin bar size angles. However, due to economic reasons, the manufacturers are reluctant to produce thin bar size hot-rolled angles unless the demand is appreciable. In such circumstances, cold-formed angle sections, made from hot-rolled sheet or plate, find their use when they are substituted for hot-rolled angles.

In a majority of the cases, the angles are connected to main members by one leg only, which gives rise to the biaxial bending of the angles. Cold-formed angles being open and thin, have low torsional rigidity and as such, are susceptible to torsional-flexural buckling which greatly reduces their load carrying capacities. For such uses, non-availability of well-formulated and sufficiently established guidelines make proper substitution and independent usage of

cold-formed angles difficult, if not altogether impossible.

Realising such an information gap, a research project has been undertaken to gain some insight into the behaviour of cold-formed angle columns under biaxial bending.

1.2 OBJECTIVES

The objectives of this investigation are :

1. To compute all the cross-sectional properties of equal and unequal-leg cold-formed angles that a designer may need.
2. To estimate ultimate compressive strengths of equal-leg and unequal-leg cold-formed angle sections under biaxial bending, using the general theory of torsional-flexural buckling.
3. To compare experimental load-deflection relationships with theoretical ones, obtained from the basic differential equations of equilibrium using the Galerkin method.
4. To compare experimental failure loads with the ultimate compressive loads computed from the general theory of torsional-flexural buckling, ASCE Manual No. 52 and ECCS Recommendations.
5. To study the effects of the number of bolts in the end connections on the ultimate strength of the member.

6. To investigate the difference in strengths of unequal-leg angles with long leg connected and with long leg out.
7. To study the effects of the location of the shear centre and the magnitude of the warping constant on the buckling load predicted by the general theory of torsional-flexural buckling.

Chapter II

LITERATURE SURVEY

2.1 GENERAL

The steel angle is a common and almost traditional member in building and industrial construction ---- its popularity can be attributed to its relative lightness, ease of fabrication and connection to the other members of the structure. Its use could be traced since the early days of the construction history. However, in view of its long and widespread use, it is quite surprising to find how little is known of many major aspects of its behaviour as a structural member. In some areas, design information is only available for limited use and often consists of conclusions drawn from the investigation done on other types of cross-section. For some other cases, the design manuals and specifications refer to the use of suitable rational theory or structural performance tests.

The question remains why the problem of single angle columns, under biaxial bending, has not been fully taken care of and the answer is that even though the angle is a very simple section to the common man and the manufacturer, it is not simple for the stress analyst. The principal axes of the cross-section do not coincide with the usual

loading directions and any routine loading will cause biaxial bending deflections which are not in the same plane as applied loads. Furthermore, the shear centre does not lie at the centroid due to the lack of symmetry in the cross-section and also is not in the line of action of more commonly applied loads. Thus any loading will force the cross-section to twist, causing torsional-flexural buckling in the angle section.

These angle sections can be broadly classified as hot-rolled or cold-formed depending upon the manufacturing process. However, cold-formed angle sections are relatively new, and as such, very little information on them exists. In the following sections, the available literature is briefly surveyed. For a detailed review of literature, reference may be made to Kennedy and Madugula (1982).

2.2 THEORETICAL SOLUTION OF DIFFERENTIAL EQUATIONS OF EQUILIBRIUM

The differential equations of equilibrium for the general case of biaxial eccentricities were solved by Bleich (1952), Vlasov (1961), Thurlimann (1953), Dabrowski (1961), Prawel and Lee (1964), Culver (1966) and Peköz and Celebi (1969), each using a different approach. Timoshenko and Gere (1961) defined the warping function and also solved the differential equations. They, however, neglected the effect of pre-critical deflections and therefore, the critical load obtained from their solution is higher than the expected ones, i.e., an upper bound solution results from their approach.

2.3 COLD-FORMED ANGLE SECTIONS

Torsional-flexural buckling of concentrically loaded thin-walled singly-symmetrical columns was first investigated by Chajes and Winter (1965) and Chajes, Fang and Winter (1966). They proposed a simple method of calculating torsional-flexural buckling load of such columns which was also extended to the inelastic range. An interaction equation, accompanied by sets of curves for design use, was suggested. Tests were also done for checking the analytical procedures developed.

In 1969, Peköz and Celebi studied the general behaviour of thin-walled singly-symmetrical open sections under eccentric axial loading in the plane of symmetry. The effect of precritical deflections and other modifications were introduced to the basic theory and the complete range of behaviour of such eccentric members was explored. Simplified design procedures and graphs for some complex parameters were presented together with experimental confirmation of theory. Tests carried out by Carpena, Cauzillo and Nicolini (1976) showed that cold-formed angles had an average buckling strength greater than that of hot-rolled angles.

It is therefore quite clear that the behavioural information available for cold-formed angle sections, connected by one leg, is scarce. That's why the cold-formed design codes and manuals (CSA 1974, Schuster 1975, AISI 1980, Winter 1977) do not give any ultimate strength formula or tables but simply refer the designer to the use of any rational theory or tests for determining structural performance.

All of the required cross-sectional properties of cold-formed sections, to the best of the author's knowledge, are not readily available. Formulas for β_1 and β_2 were developed for equal-leg angles only (Peköz and Celebi 1969). It is also common to use the magnitude of warping constant as zero and location of shear centre at SC_1 or SC_2 , as shown in Fig. 4.3.

2.4 HOT-ROLLED ANGLE SECTIONS

Chen and Atsuta (1972) developed exact interaction equations for biaxially loaded doubly symmetrical cross-sections. This was done by curve fitting. In 1974, they extended this method to the case of an unsymmetrical section composed of rectangular elements which meet each other at right angle. This method is applicable to any equal, unequal and built-up angle and is considered powerful and efficient.

The use of angles as laterally unsupported beams was investigated by Leigh and Lay (1970). The solutions are also applicable for restrained beams between the restraint points. The angles were loaded with a uniform moment over the entire span which simulated the most critical lateral buckling situation. The design of the ~~equal-leg and unequal-leg~~ angles --- approximated by the dual rectangle idealization, neglecting the fillet and toe radii --- were found to be governed by stress and deflection criteria rather than by buckling. Safe load tables were also presented. Tests were

undertaken by Thomas and Leigh (1970) to compare the theory developed which showed that the angle of twist normally reduces the maximum section stress produced.

Haaijer, Carskaddan and Grubb (1981) studied the feasibility of using finite-element analysis instead of a physical test. Only elastic behaviour was considered, thereby limiting its application to the slender angle columns only.

A total of fifty-seven 90 X 90 X 7 mm angle sections, with eccentricities in the plane of symmetry and also about both the principal axes, were tested by Yokoo, Wakabayashi and Nonaka (1968). Initially twisted specimens were included in test program. It was shown that the buckling behaviour and strength were not affected significantly by the boundary condition for twisting. Considerable torsional deformation was observed for the angles with eccentric loading in the minor principal axis of the cross-section. Also, initial twisting did not affect the buckling behaviour of angles. For the load acting on the major principal axis, bending was predominant resulting in a smaller failure load. On the other hand, in case of load acting on the minor principal axis, failure of the short angles was caused by local buckling or torsional deformation. Long angles were, however, concerned with bending about the major principal plane.

Ishida (1965) carried out tests on a total of 33 concentric and 7 eccentric specimens of 75 X 75 X 6 mm and 65 X 65 X 6 mm semi-killed high strength steel angles, hav-

ing slenderness ratios from 20 to 100. It was found that the behaviour of rolled high strength steel angles was different from that of rolled mild steel angles due to the presence of higher residual stresses. Correspondingly, the load carrying capacities were lower.

Marsh (1969), after testing 25 X 25 X 2.5 mm and 38 X 38 X 2.5 mm aluminium angles, found that the use of proper effective length factor provided good agreement between the theory he had developed and the experiments carried out.

Eccentrically loaded single angle columns were also investigated theoretically and experimentally by Trahair, Usami and Galambos (1969, 1970) and by Usami and Galambos (1971). The single angle compression members were treated as end-restrained columns with biaxially eccentric load and an elastic-plastic behaviour was determined by a numerical analysis which takes the effect of residual stress and initial imperfections of the angle columns into account. Forty-five tests were also done on 51 X 51 X 6.3 and 76 X 51 X 6.3 mm angles to substantiate the proposed numerical procedure. It was observed that the theoretical and experimental results were in good agreement. Load-deflection curves were also presented. AISC Beam-Column interaction equation was found to be a good basis for design recommendations. This numerical procedure also agreed quite well with the tests done on 100 X 100 X 10 mm and 130 X 130 X 9 mm angles by Usami and

Fukumoto (1972), intended to study the behaviour of bracing members of steel bridges. It was also found that the effect of residual stresses was not significant.

Based on the tests of single angle single-bolted connections, Kennedy and Sinclair (1972) developed empirical formulas for ultimate load of bolted connections, for both end- and edge- type failures.

Kennedy and Murty (1972) tested 72 angle struts, with both hinged and fixed end conditions and subjected to axial compressive load. All specimens failed in the inelastic range and a procedure, to estimate the realistic permissible buckling stress for a given angle, was outlined.

A total of 153 equal-leg and unequal-leg angles were tested by the Working Group 08 of Study Committee no. 22 of the International Conference on Large High Voltage Electric Systems (Wood 1975) and it was shown that the critical buckling stress for slenderness ratios between 120 and 250 for crossed diagonals was higher than the Euler critical stress. However, the ratio of the two increased with increasing slenderness ratio.

2.5 DESIGN SPECIFICATIONS

ASCE Manual No. 52 entitled "Guide for the Design of Steel Transmission Tower (1971)" is used extensively for the design of hot-rolled angle members in latticed steel transmission towers. These recommendations, however, have certain limita-

tions. The formula for ultimate compressive stress is based on Euler formula in the elastic range and Column Research Council's basic strength curve in the inelastic range.

AISC Manual of Steel Construction (1980) gives an approximate procedure for the design of single-angle struts, connected by one leg. However, this does not include the effect of torsion caused by the twist of the section and the Manual refers the designer to the appropriate technical publications, if its effect is to be considered.

The European practice for the design of angle members can be found in the Introductory Report of the European Convention for Constructional Steelwork (ECCS 1976). Design procedures were outlined for concentrically and eccentrically loaded angles used in transmission towers or in other structures. It takes into account the effect of the stiffnesses of the other connecting members and reduced torsional rigidity and increase of yield stress at the corners of cold-formed angles.

Chapter III

THEORETICAL FORMULATION

3.1 GENERAL THEORY OF TORSIONAL-FLEXURAL BUCKLING

The basic differential equations of equilibrium of a column, loaded with axial end loads and biaxial eccentricities, are (Timoshenko and Gere, 1961) :

$$EI_y u^{iv} + Pu'' + P(y_o - e_y)\phi'' = 0 \quad [3.1]$$

$$EI_x v^{iv} + Pv'' - P(x_o - e_x)\phi'' = 0 \quad [3.2]$$

$$EC_w \phi^{iv} - (GJ - Pe_y \beta_1 - Pe_x \beta_2 - P \frac{I_o}{A})\phi'' + P(y_o - e_y)u'' - P(x_o - e_x)v'' = 0 \quad [3.3]$$

where,

E = modulus of elasticity

I_x, I_y = moments of inertia of the cross-section about the major and minor centroidal principal axes (x-x axis and y-y axis) respectively.

P = external applied load

x_o, y_o = x- and y- coordinates of the shear centre with reference to the centroidal principal axes.

e_x, e_y = x- and y- coordinates of point of application of eccentric thrust with reference to the centroidal principal axes.

C_w = warping constant of the cross-section

G = modulus of rigidity = $\frac{E}{2(1 + \nu)}$

ν = poisson's ratio

I_o = polar moment of inertia of the cross-section about the shear centre.

A = area of the cross-section.

u, v, ϕ = deflection of the shear centre (u and v) along major and minor centroidal principal axes respectively and rotation of the shear centre (ϕ) about the longitudinal axis ($z-z$ axis).

J = torsional constant of the cross-section.

$$\beta_1 = \frac{1}{I_x} \left(\int_A y^3 dA + \int_A x^2 y dA \right) - 2y_o$$

$$\beta_2 = \frac{1}{I_y} \left(\int_A x^3 dA + \int_A xy^2 dA \right) - 2x_o$$

The above differential equations of equilibrium were formulated on the basis of the following assumptions :

1. The column is initially straight.
2. Effects of the residual stresses are negligible.
3. The geometry of the cross-section of the member does not change during buckling. This basic assumption implies that the displacement of the each point in the cross-section can be specified in terms of the displacement components, u , v and ϕ of the shear centre.

4. Shear and axial deformations are insignificant.
5. Deflection components are small (u and v in comparison with the length of the member and ϕ in comparison with $\pi/2$).
6. The material is linearly elastic and the stress-strain curve is elastic-perfectly plastic, having a well-defined yield point.

Exact and approximate solutions of these equations have been given by Vlasov (1961), Culver (1966), Dabrowski (1961), Thurliemann (1953) and Prawel and Lee (1964). However, the exact procedure (Culver 1966), involving twelve unknown integration constants in twelve simultaneous equations, are difficult, if not impossible, to use and therefore, an approximate solution has been resorted to. The Galerkin method, which is sufficiently accurate and simple (Chajes 1974), is used here to obtain a solution of these equations.

The boundary conditions for pinned-end columns can be expressed as follows :

Static:

$$u''_{zz} = 0, \quad l = \frac{Pe_x}{EI_y} \quad [3.4]$$

$$v''_{zz} = 0, \quad l = \frac{Pe_y}{EI_x} \quad [3.5]$$

Geometric:

$$u = v = \phi = \phi' = 0 \quad \text{at } z = 0, l \quad [3.6]$$

Since the point of load application is not a point of zero longitudinal displacement, warping is considered to be restrained and the condition $\phi' = 0$ is used (Culver 1966).

Accordingly, the following functions for u, v and ϕ have been selected (Peköz and Celebi 1969) :

$$u = \frac{Pe_x}{2EI_y} (z^2 - lz) + u_o \sin \frac{\pi z}{l} \quad [3.7]$$

$$v = \frac{Pe_y}{2EI_x} (z^2 - lz) + v_o \sin \frac{\pi z}{l} \quad [3.8]$$

$$\phi = \phi_o \left[\sin \frac{\lambda z}{l} - \sinh \frac{\lambda z}{l} - \alpha' \left(\cos \frac{\lambda z}{l} - \cosh \frac{\lambda z}{l} \right) \right] \quad [3.9]$$

where,

l = length of the member.

z = location of the cross-section along the length of the member, where the deflection is being calculated.

u_o, v_o, ϕ_o = coefficients to be determined by the application of the Galerkin method.

λ = 4.73004, an eigenvalue satisfying the characteristic equation $\cos \lambda \cosh \lambda = 1$.

$$\alpha' = \frac{\sinh \lambda - \sin \lambda}{\cosh \lambda - \cos \lambda} = 1.0178$$

Using Eq. [3.7] to [3.9] and applying Galerkin method to the differential Eq. [3.1] to [3.3], the following algebraic equations are obtained :

$$\begin{aligned}
& u_0 \left(EI_y \frac{\pi^4}{l^4} \int_0^l \sin^2 \frac{\pi z}{l} dz - P \frac{\pi^2}{l^2} \int_0^l \sin^2 \frac{\pi z}{l} dz \right) \\
& + P(y_0 - e_y) \phi_0 \frac{\lambda^2}{l^2} \int_0^l \left[-\sin \frac{\lambda z}{l} - \sinh \frac{\lambda z}{l} - \alpha' \left(-\cos \frac{\lambda z}{l} \right. \right. \\
& \left. \left. - \cosh \frac{\lambda z}{l} \right) \right] \sin \frac{\pi z}{l} dz = - \frac{P^2 e_x}{EI_y} \int_0^l \sin \frac{\pi z}{l} dz \quad [3.10]
\end{aligned}$$

$$\begin{aligned}
& v_0 \left(EI_x \frac{\pi^4}{l^4} \int_0^l \sin^2 \frac{\pi z}{l} dz - P \frac{\pi^2}{l^2} \int_0^l \sin^2 \frac{\pi z}{l} dz \right) \\
& - P(x_0 - e_x) \phi_0 \frac{\lambda^2}{l^2} \int_0^l \left[-\sin \frac{\lambda z}{l} - \sinh \frac{\lambda z}{l} - \alpha' \left(-\cos \frac{\lambda z}{l} \right. \right. \\
& \left. \left. - \cosh \frac{\lambda z}{l} \right) \right] \sin \frac{\pi z}{l} dz = - \frac{P^2 e_y}{EI_x} \int_0^l \sin \frac{\pi z}{l} dz \quad [3.11]
\end{aligned}$$

$$\begin{aligned}
& \phi_0 \left\{ EC_w \frac{\lambda^4}{l^4} \int_0^l \left[\sin \frac{\lambda z}{l} - \sinh \frac{\lambda z}{l} - \alpha' \left(\cos \frac{\lambda z}{l} - \cosh \frac{\lambda z}{l} \right) \right]^2 dz \right. \\
& + (Pe_y \beta_1 + Pe_x \beta_2' + P \frac{I_0}{A} - GJ) \int_0^l \frac{\lambda^2}{l^2} \left[-\sin \frac{\lambda z}{l} - \sinh \frac{\lambda z}{l} \right. \\
& \left. \left. - \alpha' \left(-\cos \frac{\lambda z}{l} - \cosh \frac{\lambda z}{l} \right) \right] \left[\sin \frac{\lambda z}{l} - \sinh \frac{\lambda z}{l} - \alpha' \left(\cos \frac{\lambda z}{l} - \cosh \frac{\lambda z}{l} \right) \right] dz \right\} \\
& - P(y_0 - e_y) u_0 \frac{\pi^2}{l^2} \int_0^l \left[\sin \frac{\lambda z}{l} - \sinh \frac{\lambda z}{l} - \alpha' \left(\cos \frac{\lambda z}{l} - \cosh \frac{\lambda z}{l} \right) \right] \sin \frac{\pi z}{l} dz \\
& + P(x_0 - e_x) v_0 \frac{\pi^2}{l^2} \int_0^l \left[\sin \frac{\lambda z}{l} - \sinh \frac{\lambda z}{l} - \alpha' \left(\cos \frac{\lambda z}{l} - \cosh \frac{\lambda z}{l} \right) \right] \\
& \sin \frac{\pi z}{l} dz = - P^2 \left[\frac{e_x (y_0 - e_y)}{EI_y} - \frac{e_y (x_0 - e_x)}{EI_x} \right] \int_0^l \left[\sin \frac{\lambda z}{l} - \sinh \frac{\lambda z}{l} \right. \\
& \left. - \alpha' \left(\cos \frac{\lambda z}{l} - \cosh \frac{\lambda z}{l} \right) \right] dz \quad [3.12]
\end{aligned}$$

Carrying out the necessary integrations (as shown in Appendix 4) and simplifying, we get

$$\begin{bmatrix} P_y - P & 0 & -P(y_o - e_y)1.4196 \\ 0 & P_x - P & P(x_o - e_x)1.4196 \\ -P(y_o - e_y)0.5507 & P(x_o - e_x)0.5507 & 4.1302EC_w \frac{\pi^2}{l^2} + (GJ - Pr_o^2)1.0019 \end{bmatrix} \begin{Bmatrix} u_o \\ v_o \\ \phi_o \end{Bmatrix} = \begin{Bmatrix} -\frac{P^2 e_x}{P_y} 1.2732 \\ -\frac{P^2 e_y}{P_x} 1.2732 \\ -P^2 \left[\frac{e_x(y_o - e_y)}{P_y} - \frac{e_y(x_o - e_x)}{P_x} \right] 0.6561 \end{Bmatrix}$$

Substitution of the values of u_o , v_o and ϕ_o in Eq. [3.7] to [3.9] will give the desired deflection components of the shear centre, viz., u , v and ϕ at any particular location z along the longitudinal axis of the column, corresponding to a given applied load P .

Using these deflection components, stress at any point on the cross-section can be computed from (Culver 1966)

$$\sigma_T = \sigma_1 + \sigma_2 + \sigma_3 + \sigma_4 \quad [3.13]$$

where,

σ_1 = uniform axial compressive stress

$$= P/A$$

σ_2 = linearly varying stress due to bending about the major centroidal principal axis (x-x axis)

$$\begin{aligned} &= \frac{P \cdot e_1}{I_x} y \\ &= \frac{P[e_y - v - (e_x - x_o)\phi]}{I_x} y \end{aligned}$$

σ_3 = linearly varying stress due to bending about the minor centroidal principal axis (y-y axis)

$$\begin{aligned} &= \frac{P \cdot e_2}{I_y} x \\ &= \frac{P[e_x - u + (e_y - y_o)\phi]}{I_y} x \end{aligned}$$

σ_4 = warping normal stress due to non-uniform torsion

$$= E(\bar{\omega}_s - \omega_s)\phi''$$

where,

ω_s = warping function according to Timoshenko and Gere (1961)

$\bar{\omega}_s$ = average value of ω_s

3.2 ASCE MANUAL NO. 52

The American Society of Civil Engineers Manual No. 52, entitled "Guide for Design of Steel Transmission Towers" (ASCE 1971), has been the basis for the design of hot-rolled angle shapes used in latticed steel transmission towers. The recommendations are not to be used when the width-to-thickness ratio, b/t , exceeds 20; the width 'b' is the width measured from the toe of the angle to the root of the fillet. Since there are no fillets in cold-formed angles, the b/t ratio is taken as the flat width-to-thickness ratio for the purpose of calculating the critical stresses of test specimens. The equations given in ASCE Manual No. 52 are in Imperial System of units; in the following, the equations have been converted to SI system.

If the width-to-thickness ratio does not exceed the limiting b/t ratio given by

$$(b/t)_{\text{limit}} = 208/\sqrt{\sigma_y} \quad [3.14]$$

where σ_y is the yield stress of the material in MPa, then the member is sufficiently compact to develop its material yield stress and the ultimate maximum stress, σ_{cr} , is obtained from

$$\sigma_{cr} = \left[1 - \frac{(Kl/r_y)^2}{2C_c^2} \right] \sigma_y \quad \text{if } \frac{Kl}{r_y} \leq C_c \quad [3.15]$$

and

$$\sigma_{cr} = \frac{\pi^2 E}{(Kl/r_y)^2} \quad \text{if } \frac{Kl}{r_y} > C_c \quad [3.16]$$

in which

$$C_c = \pi \sqrt{\frac{2E}{\sigma_y}} \quad [3.17]$$

where,

E = modulus of elasticity of the material

= 205 GPa (assumed in the computation)

and Kl/r_y = largest effective slenderness ratio.

If the width-to-thickness ratio exceeds limiting b/t ratio, then Eq. [3.15] and [3.17] shall be modified by substituting $\sigma_{y,eff}$ for σ_y where

$$\sigma_{y,eff} = \left[1.8 - \frac{0.8(b/t)}{(b/t)_{limit}} \right] \sigma_y \quad [3.18]$$

$$\text{if } (b/t)_{limit} \leq (b/t) \leq 1.5(b/t)_{limit}$$

and

$$\sigma_{y,eff} = \frac{57900}{(b/t)^2} \quad \text{if } b/t > 1.5(b/t)_{limit} \quad [3.19]$$

For members with normal framing eccentricities at both ends and $l/r_y < 120$,

$$Kl/r_y = 60 + 0.50 l/r_y \quad [3.20]$$

For members unrestrained against rotation at both ends and $120 < l/r_y < 200$,

$$Kl/r_y = l/r_y \quad [3.21]$$

For members partially restrained against rotation at both ends and $120 < l/r_y < 250$,

$$Kl/r_y = 46.2 + 0.615 l/r_y \quad [3.22]$$

Furthermore, single-bolted connection shall not be considered as offering restraint against rotation, whereas a multiple-bolted connection properly detailed to minimise eccentricities shall be considered to offer partial restraint if the connection is made to a sufficiently strong member.

Failure loads computed according to ASCE Manual No. 52 for the specimens included in the experimental investigation are shown in Table 6.7a.

3.3 ECCS RECOMMENDATIONS

The loads in eccentrically loaded cold-formed angle struts are transmitted by bolts or other connectors on only one leg. When these members are the web members of latticed trusses and are relatively flexible, their compressive strength is influenced by the stiffness of the connections to the main members.

For these members, the critical stresses are calculated by entering the curve B3 (for thickness < 20 mm) (Annexure B of European Recommendations for Steel Construction, ECCS 1978) shown in Table 6.4, with :

$$\left(\frac{\lambda}{\lambda_y} \right)_{\text{eff}} = 0.60 + 0.57 \frac{\lambda}{\lambda_y} \quad \text{if } \frac{\lambda}{\lambda_y} \leq 1.41 \quad [3.23]$$

$$\left(\frac{\lambda}{\lambda_y} \right)_{\text{eff}} = \frac{\lambda}{\lambda_y} \quad \text{if } \frac{\lambda}{\lambda_y} > 1.41 \quad [3.24]$$

where

$$\frac{\lambda}{\lambda_y} = \frac{Kl/r_y}{\pi\sqrt{E/\sigma_y}} \quad [3.25]$$

where $E = 210$ GPa for cold-formed angles.

When the chords and the web members do not attain their maximum stress level for the same load conditions

$$\left(\frac{\lambda}{\lambda_y} \right)_{\text{eff}} = 0.35 + 0.75 \frac{\lambda}{\lambda_y} \quad \text{if } 1.41 \leq \frac{\lambda}{\lambda_y} \leq 3.5 \quad [3.26]$$

may be used if the chords give good end-restraints to the web members and at least two bolts or rivets in line are present at the end connections of the web members.

Failure loads computed according to ECCS Recommendations for the specimens included in the experimental investigation are shown in Table 6.7a.

Chapter IV

COMPUTER PROGRAM

4.1 GENERAL

Calculation of the deflection components (i.e., u , v and ϕ) from the general theory of torsional-flexural buckling using the Galerkin method is a complicated procedure. This is further aggravated by the need of the actual cross-sectional properties of the specimen. A computer program was developed not only to calculate the actual cross-sectional properties including area, moments of inertia, location of the centroid, warping and torsional constants, minimum radius of gyration, location of the shear centre, β_1 and β_2 , but also to estimate the deflection components and calculate the stresses at any point on the cross-section. It then predicts the ultimate compressive strengths based on the failure criteria.

4.2 DESCRIPTION OF THE COMPUTER PROGRAM

The computer program was written in FORTRAN IV language and run on IBM/3031 system. The program can be broadly divided into three parts:

1. Calculation of the actual cross-sectional properties.

2. Estimation of the deflection components using the Galerkin method.
3. Calculation of the total stress, σ_T at any point at any cross-section.

The flow chart of the program is given in Appendix 2 and a complete listing of it is given in Appendix 3. The details of the program are discussed in the following sections.

4.2.1 Main Program

The main program can be broadly divided into the following:

1. Input the data
 - a) Width of the long leg
 - b) Width of the short leg
 - c) Thickness
 - d) Inside bend radius
 - e) Thickness of the connecting gusset plate
 - f) Connected leg
 - g) Gauge distance.
 - h) Assumed yield stress
2. Calculate the cross-sectional properties (i.e., A , $I_{x'}$, $I_{y'}$, I_x , I_y , $P_{x'y'}$, I_o , x' , y' , α , r_y , J , C_w , x_s , y_s , β_1 , β_2), for which the theoretical formulation is shown in Appendix 1.
3. Compute P_x , P_y and P_ϕ .

4. Start the iterations at 0.1% of minimum of P_x , P_y and P_ϕ .
5. Find the deflection components (u, v and ϕ) corresponding to this load.
6. Calculate the total stress at each of the 16 points (as shown in Fig. 4.1) for each of the 11 cross-sections (the whole column length being divided into 10 equal segments).
7. Check the failure criteria.
 - a) If satisfied, write the input data, calculated cross-sectional properties and estimated ultimate compressive strength.
 - b) If not, modify the failure load and repeat the calculations.
8. Exit when all the required information have been obtained.

Output of this program consists of cross-sectional properties and the ultimate compressive strengths for e/r_y ratios ranging from 20 to 240. Ultimate compressive strengths can also be obtained for $C_w = 0$ and two approximate locations of the shear centre, SC_1 and SC_2 (Fig. 4.3).

4.2.2 Subroutines

1. MXCP12, MXCP34, MXCP78: Compute the moment of the shear flow in the curved portion for different conditions.

2. CWACTL: Calculates the magnitude of the actual warping constant.
3. INTGRL: Estimates the value of an integral by adaptive quadrature technique using Simpson's rule (Johnson and Riess 1982).
4. ADSIMP: Estimates the value of an integral in the sub-interval.
5. DEFROT: Calculates the deflection components at any cross-section using the Galerkin method.
6. SIGMA: Computes the stresses at each of the 16 different points of each of the 11 cross-sections and returns the maximum and minimum stresses at any of those 11 X 16 points.
7. SOLVE: Solves the linear equation $A \sin \theta + B \cos \theta + C = 0$ in order to determine the point of maximum or minimum stress, if any, in the curved portion of the angle.

4.3 ADVANTAGES OF THE PROGRAM

This program needs very few input data. For each specimen, only one card is required to feed the program. It generates all the cross-sectional properties and other information required in order to estimate the ultimate compressive strength. It has several built-in error messages so that the user can be warned against some unusual occurrences. This program can be run for any leg size, thickness, inside bend

radius, thickness of gusset plate, gauge distance and yield stress. An iterative approach is used for the calculation of ultimate strength and the smallest load increment in the final steps of iteration is taken as 0.001% of the minimum of P_x , P_y and P_ϕ . However, the accuracy of the failure load depends also on the functions used for the deflection components.

With minor modifications, this program is capable of providing load-deflection relationships for cold-formed angles under biaxial bending.

4.4 LIMITATIONS OF THE PROGRAM

This program does not take the effect of material non-linearity and initial out-of-straightness of the columns into account. Also, it is not possible to trace the unloading part of the load-deflection curves.

4.5 FAILURE CRITERIA

It has been assumed that the column has failed if the maximum total stress (tensile or compressive) at any point in the column reaches the yield stress level or at least one of the deflection components changes its sign.

4.6 RESULTS

All the cross-sectional properties are presented in Tables 6.1 and 6.2. Ultimate compressive strengths for two commonly used cold-formed angle sections for l/r_y ratios varying from 20 to 240 for different gauge distances are presented in Table 6.3. Theoretical load-deflection relationships for pinned-end boundary conditions are compared with experimental results and are shown in Fig. 6.1 through 6.7.

Chapter V

EXPERIMENTAL INVESTIGATION

5.1 GENERAL

Tests were carried out on fifteen 65 X 50 X 4 mm and nine 55 X 55 X 4 mm cold-formed angles. Since these thin bar size angle members are principally used as web members in latticed towers, the lower limit of slenderness ratio was set at 80.

Table 6.5 gives the cross-sectional properties while Table 6.6 shows the lengths and slenderness ratios of the cold-formed angles used in this program. These angles were roll-formed from CSA G40.21M 300W grade sheet. The test specimens are cut from fairly straight portion of the factory supplies. However, specific data regarding the magnitude of initial imperfections and residual stress are not available.

5.2 TEST SET-UP

The test set-up shown in Fig. 5.1 consists of four angle members (including the test specimen) connected to the wide flange column of the main test facility. The arrangement resembles one panel of one face of a latticed tower. Load was applied through a ball bearing at joint B (Fig. 5.1). To

prevent the transmission of load to member AB, the gusset plate at joint A was loosely connected to the steel wide flange column of the main test facility so that member AB is free to rotate about joint A.

5.2.1 Lateral Support

The test set-up was laterally supported at joints B and C as shown in Fig. 5.3 and 5.4. Rollers were used in the lateral supports to allow vertical but not the lateral movement. However, there could be some out-of-plane rotation of the test specimens.

5.2.2 Deflection Dial Gauges

Four deflection dial gauges with 25 mm travel and a least reading of 0.01 mm were used at midspan of the test specimens. Their arrangement is shown in Fig. 5.5. Two of the dial gauges were used to measure horizontal deflection and twist of the vertical leg, while the other two were used to measure vertical deflection and twist of the horizontal leg.

5.2.3 Supports for Dial Gauges

A specially designed L-shaped extension piece was constructed from metal strips, allowing easy fastening and removal from the specimen by means of a long bolt as shown in Fig. 5.6. This extension piece enabled the measurement of deflection and rotation at midspan. The gauge support bracket,

as shown in Fig. 5.7, was made from angle section. This bracket allowed fast and simple attachment of the dial gauges as well as their adjustment on the L-shaped extension piece.

5.3 TESTING PROCEDURE

Test specimens were connected either with one, two or three 16mm diameter ASTM A325M high strength bolts at both ends at a gauge distance of one-half the nominal width of the connected leg. Fig. 5.2 shows the arrangement for load application.

The compressive load was applied by means of a 445 kN mechanical jack. The load was applied in increments of approximately one-twentieth of the predicted ultimate load until failure of the test specimen occurred. The load on the specimen was measured with the help of a previously calibrated load cell. Deflections at each load increment were recorded.

The experimental failure loads are listed in Table 6.7a while the typical load-deflection curves at mid-span for some of the test specimens are presented in Fig. 6.1 through 6.7 and compared with the theoretical results obtained earlier.

Chapter VI.

DISCUSSION OF RESULTS

6.1 CROSS-SECTIONAL PROPERTIES

The angles included in the theoretical investigation have a maximum leg width of 200 mm and correspond to the sizes of hot-rolled angles (CISC 1980). The maximum thickness is limited to 25 mm, it being the upper limit for the applicability of cold-formed steel design specifications (AISI 1980).

The inside bend radius is taken as ' $2t$ ' for $t \leq 4$ mm, and ' $3t$ ' for $t > 4$ mm, where t is the thickness of the leg of the angle. These bend radii are satisfactory for steels having guaranteed minimum yield stress of 300 MPa (Algoma Steel 1978). For higher strength steels, larger bend radii are required.

6.2 ULTIMATE COMPRESSIVE STRENGTHS

Table 6.3, which shows the ultimate compressive strengths of cold-formed angle sections for λ/r_y ratios ranging from 20 to 240 under pinned-end boundary conditions for different gauge distances, is based on an assumed yield stress level of 300 MPa, modulus of elasticity of cold-formed steels of 205 GPa and modulus of rigidity of 77 GPa. In addition, the

load is assumed to be acting along the centre-line of the bolt (defined by the gauge distance) on the outer face of the connected leg.

As expected, it can be seen from Table 6.3 that ultimate compressive strength reduces gradually and continuously for increasing l/r_y ratio for a majority of the cases. However, for certain gauge distances, the compressive strength remains more or less constant over a certain range of l/r_y ratio. This can be understood if one bears in mind the coupling of the bending about the x-x axis and y-y axis and twisting about longitudinal z-z axis. This can further be attributed to the nature of the assumed deflection functions.

The effective eccentricities, e_1 and e_2 , depend on the variables u , v and ϕ in addition to the constants e_x , e_y , x_0 and y_0 . For certain combinations of e_x , e_y , u and v , e_2 becomes negative in sign, while e_1 remains positive. Sometimes, the increase of e_2 is much more than that of e_1 (because of the larger increase in the u -component of the deflection) and therefore, the total compressive stress, tends to remain the same. This leads to the almost constant ultimate compressive strength over a certain range of l/r_y ratios for certain gauge distances.

The same trend (i.e., greater increase in e_2 over e_1) is also confirmed by the numerical results presented by Culver (1966). For identical boundary conditions, in his inves-

tigation, it was found that the rate of increase of σ_3 is much more than that of σ_2 when l/r_y ratio was increased from 60 to 140, due to the rapid increase in the u-component of the deflection together with the rotation, ϕ .

This behaviour occurs only when the point of load application is close to the point of intersection of the y-y axis and the centre-line of the connected leg.

It is to be noted that the failure criterion adopted here, viz. failure at first yield, leads to a lower bound solution. However, if the residual stresses are considered, the critical point, i.e., the point at which the resultant total stress reaches the yield stress, may be different from the one determined from theoretical formulation. In some cases, this may lead to actual failure loads being less than those predicted by the present theory.

Angles with large width-to-thickness ratio tend to fail by local buckling of the legs, much before their overall failure. Such local instability can be taken into account by appropriately modifying the yield stress of the material, as is done in ASCE Manual No. 52.

6.3 LOAD-DEFLECTION RELATIONSHIPS

6.3.1 Experimental Results

The experimental results, consisting of horizontal and vertical deflections and twists of the legs, are resolved into three deflection components, u, v and ϕ with respect to

shear centre and are shown in Fig. 6.1 through 6.7. Results shown here are those at mid-span only.

6.3.2 Exact Solution of Differential Equations

Culver's exact solution of differential equations, involving twelve unknown constants of integration in twelve simultaneous equations, includes trigonometric and hyperbolic functions. The hyperbolic functions are difficult to evaluate for large values of arguments making the use of the exact solution computationally impossible. When the author tried to use this method for the test specimens under investigation, for some combinations of load, length and flexural rigidities, algorithmic singularity was encountered in the solution of those twelve equations.

6.3.3 Solution of Differential Equations applying the Galerkin method

A close observation of Fig. 6.1 through 6.7 will reveal that, for a given load, two of three experimental deflection components (usually the u-component and rotation, ϕ) are less than the theoretically computed values which establishes the fact that the experimental set-up offers a boundary condition which is different from pinned-ends, probably due to the rigidity of the connection and the influence of the other members of the test frame. In general, the experimental v-components of deflection are more than those of the theoretical deflections. Besides the usual assumptions in-

volved in the theoretical formulation, some of the parameters possibly influencing the experimental results are discussed below.

Eccentricity: Depending on the gauge distance, the shape of the load-deflection curve changes. It can be shown theoretically that the load-deflection curve is quite sensitive to the gauge distance.

Effect of the test setup: In all these comparisons, the length of the member is assumed to be the distance from gauge to gauge of the connecting members. However, the test specimen actually includes a gusset plate at both ends. Since the properties of the gusset plate are quite different from those of the test specimen, ignoring the presence of the gusset plate and assuming the test specimen to be a member having uniform cross-sectional properties from gauge to gauge of the connecting members, results in discrepancies between theoretical and experimental load-deflection curves.

The most important feature of this comparison is the confirmation of the theoretical load-deflection curves by experimental results. So far, to the best of author's knowledge, no such information exists for cold-formed angles. In spite of some discrepancies, the trends of the respective curves are all alike. The shapes of all these load-deflection curves are very much similar to the corresponding curves of hot-rolled angle sections reported by Usami (1970).

6.3.4 Comparison of Exact and Galerkin Solutions

Table 6.9 shows a comparison of results obtained from exact and Galerkin solutions for 65 X 50 X 4 mm (long leg out) angle with a gauge distance of 25 mm and slenderness ratio of 20. This is one of the few cases for which the "exact" method worked, except for the smallest load. Loads shown in the table are those which the program calculated at each step of iteration, hence the decimal fractions. For the range of loading shown, per cent error varies from 0.0 to -2.0 for u - and v - components showing that the Galerkin method is sufficiently accurate. However, the error in the evaluation of ϕ is surprisingly high. But, the values of ϕ being very small, it is quite unlikely that such an error will have any significant effect on the eccentricities, e_1 and e_2 . Therefore, it can be assumed that the calculated stresses would hardly differ from the exact stresses. Differences, if any, would be acceptable for all practical purposes.

6.4 COMPARISON OF EXPERIMENTAL FAILURE LOADS WITH THE PREDICTED LOADS

6.4.1 General

From a study of Table 6.5, it can be seen that the actual cross-sectional areas were 3-4% less than the nominal areas while the actual moments of inertia were about 9-10% less than those specified.

The experimental and theoretical loads are summarized in Table 6.7a. The computed failure loads based on actual dimensions are 5-8% less than those based on nominal dimensions. In the following sections, the predicted failure loads according to ASCE Manual No. 52, ECCS Recommendations and the general theory of torsional-flexural buckling are compared with the experimental failure loads.

6.4.2 ASCE Manual No. 52

6.4.2.1 Slenderness ratios less than 120

The calculated failure load is based only on eccentricity of loads; the number of bolts does not enter the computations. However, experimental failure loads for two- and three- bolted end connections are significantly higher than those for single-bolted end connections. An examination of Table 6.7a reveals that for two- and three- bolted end connections, the computed loads are in reasonable agreement with the experimental failure loads.

For single-bolted connections, the computed loads are upto 30% higher than the experimental failure loads. The discrepancy between the computed and experimental failure loads is higher for specimens having smaller slenderness ratios. This point should be kept in mind if ASCE Manual is applied for the design of cold-formed angles.

6.4.2.2 Slenderness ratios exceeding 120

For all the nine specimens tested, the experimental failure loads are 10-50% higher than the computed loads; therefore, the ASCE Manual can be safely used in the design of slender members. For such members, the Manual distinguishes between single- and multiple- bolted connections, higher values being allowed for multiple-bolted connections. However, the Manual does not make any distinction between two-bolted and three-bolted connections, whereas the experimental failure loads of specimens with three bolts are in all cases higher than the failure loads of specimens with two bolts.

6.4.3 ECCS Recommendations

For all slenderness ratios, the computed failure loads are either less or very close to the experimental failure loads. They are more conservative than ASCE Manual No. 52 and can be applied with confidence to the design of cold-formed angles connected by one leg.

6.4.4 General Theory of Torsional-Flexural Buckling

The failure loads according to the general theory of torsional-flexural buckling are given in Table 6.7b for all single-bolted columns included in the test program. Single-bolted connections are assumed to provide insignificant restraint to bending and therefore, pinned-end connections are assumed in the analysis. This is also in conformity

with ASCE Manual No. 52 (1971). Since the line of action of the eccentric thrust does not pass through the point of zero longitudinal displacement (defined by the warping function), warping is restrained (Culver 1966).

A study of Tables 6.7a and 6.7b shows that the theoretical failure loads vary from 55-90% of the experimental failure loads. The discrepancy is more for slender columns compared to others. One possible reason for this discrepancy is the fact that slender columns are more sensitive to the end connections than stocky or intermediate columns. In the theoretical computations, the ends are conservatively assumed as pinned while for the test columns, the rigidity of the steel frame may have provided partial restraint.

Also, one end of the test specimens was allowed to move in the vertical plane while the other end, being connected to a rigid wide flange column, could be considered as partially fixed. This differential movement of the joints probably has produced additional curvature, and therefore bending moments, in the test specimens which has not been considered in the theoretical formulation.

6.5 LONG LEG CONNECTED VERSUS LONG LEG OUT

Neither the ASCE Manual No. 52 nor ECCS Recommendations makes any distinction in the failure loads of the angles with long leg connected or long leg out. However, tests carried on 65 X 50 X 4 mm cold-formed angles show that the fai-

Failure loads are 8-30% higher if the long leg is out. Failure loads based on the general theory of torsional-flexural buckling also lead to the same conclusion.

6.6 EFFECT OF THE OTHER VARIABLES

To study the effect of the location of the shear centre and the magnitude of warping constant, failure loads are computed according to the general theory of torsional-flexural buckling for the following cases :

1. Exact location of the shear centre
 - a) warping constant = 0
 - b) warping constant calculated according to Timoshenko and Gere (1961)
2. Shear centre assumed at point 'SC₁' (Fig. 4.3)
 - a) warping constant = 0
 - b) warping constant calculated according to Timoshenko and Gere (1961)
3. Shear centre assumed at point 'SC₂' (Fig. 4.3)
 - a) warping constant = 0
 - b) warping constant calculated according to Timoshenko and Gere (1961)

The results for 65 X 50 X 4 mm cold-formed angle with long leg connected are summarized in Table 6.8.

A study of Table 6.8 shows that the effect of all these

Chapter VII

CONCLUSIONS AND RECOMMENDATIONS

7.1 GENERAL

Though cold-formed angles are currently available only in thin bar-size sections, the properties of heavier sections are also included here for use in future, when cold-formed angles might become competitive with hot-rolled angles.

Cold-formed angles connected by one leg generally have decreasing strengths with increasing l/r_y ratios, except when the point of load application is close to the point of intersection of the minor principal axis (y-y axis) with the centre-line of the connected leg. In such cases, ultimate compressive strength may remain more or less constant over a certain range of l/r_y ratios. This behaviour could be attributed to the nature of assumed deflection functions.

7.2 CONCLUSIONS

From the theoretical and limited experimental study and for the test condition specified herein, the following conclusions can be drawn about the behaviour of thin bar-size cold-formed angles :

1. For certain combinations of load, length and bending rigidities of the member, computational problems will

arise in the determination of the constants of integration if Culver's "exact" procedure is followed for the solution of differential equations of equilibrium for columns under biaxial bending.

2. The application of the Galerkin method to predict theoretical load-deflection relationships is a simple, fast and sufficiently accurate alternative to the exact solution.
3. Failure loads computed according to ECCS Recommendations are, in general, conservative.
4. For stocky and intermediate specimens with single-bolted end connection, ASCE Manual No. 52 predicts failure loads which are higher than the experimental failure loads. For multiple-bolted connection, the predicted failure loads are either less than or very close to the experimental failure loads.
5. Loads computed according to general theory of torsional-flexural buckling (assuming pinned-end connection and warping restrained) are approximately 55-90% of experimental failure loads; the discrepancy is more for slender columns.
6. For all slenderness ratios, the strength of member increases when the number of bolts in the end connection is increased from one to three.
7. Unequal leg cold-formed angles are capable to carry higher loads when the long leg is out.

8. The usual assumptions regarding the location of the shear centre (SC_1 and SC_2 , as shown in Fig. 4.3) and the magnitude of warping constant ($C_w = 0$) are sufficiently accurate to predict failure loads according to the general theory of torsional-flexural buckling.

7.3 RECOMMENDATIONS FOR FUTURE RESEARCH

Based on the experience gained during the investigation, the following recommendations are being made :

1. Further research may be directed to include the effect of residual stresses in the calculation of ultimate strengths.
2. Initial out-of-straightness could also be investigated in order to estimate its effect on the ultimate compressive strength.
3. Finally, a simple and useful interaction type formula may be obtained for cold-formed angle sections under biaxial bending.

LIST OF REFERENCES

1. Algoma Steel Corporation Limited. 1978. Guide to Steel Standards and Specifications. Toronto, Ontario. pp. 1B-18, 1B-19.
2. American Institute of Steel Construction. 1980. Manual of Steel Construction. Chicago, Illinois, U.S.A. p. 3-48.
3. American Iron and Steel Institute. 1980. Specifications for the Design of Cold-Formed Steel Structural Members. Washington, D.C., U.S.A.
4. American Society of Civil Engineers (ASCE). 1971. Guide for the Design of Steel Transmission Towers. ASCE Manuals and Reports on Engineering Practice, No. 52, New York, N.Y., U.S.A.
5. Bleich, F. 1952. Buckling Strength of Metal Structures, McGraw Hill Book Co. Inc., New York, N.Y., U.S.A.
6. Canadian Institute of Steel Construction. 1980. Handbook of Steel Construction. Willowdale, Ontario. pp. 6-68 to 6-71.
7. Canadian Standards Association. 1974. Cold-Formed Steel Structural Members, CSA S136. Rexdale, Ontario.
8. Carpena, A., Cauzillo, B.A. and Nicolini, P. 1976. Modern Technical and Constructional Solutions for the

New Italian Power Lines. Presented at the International Conference on Large High Voltage Electric Systems. Paris, France.

9. Chajes, A. 1974. Principles of Structural Stability Theory. Prentice-Hall, New Jersey, N.Y., U.S.A. pp. 103-106.
10. Chajes, A., Pang, P.J. and Winter, G. 1966. Torsional-Flexural Buckling, Elastic and Inelastic, of Cold-Formed Thin-Walled Columns. Cornell Engineering Research Bulletin 66-1, Cornell University, Ithaca, N.Y., U.S.A.
11. Chajes, A. and Winter, G. 1965. Torsional-Flexural Buckling of Thin-Walled Members. Journal of the Structural Division, ASCE, Vol. 91, No. ST4, pp. 103-124.
12. Chen, W.F. and Atsuta, T. 1972. Interaction Equations for Biaxially Loaded Sections. Journal of the Structural Divisions, ASCE, Vol. 98, No. ST5, pp. 1035-1052.
13. Chen, W.F. and Atsuta, T. 1974. Interaction Curves for Steel Sections Under Axial Loading and Biaxial Bending. Engineering Journal, Montreal, Canada, Vol. 57, No. 3/4, pp. 49-56.
14. Culver, C.G. 1966. Exact Solution of Biaxial Bending Equations. Journal of the Structural Divisions, ASCE, Vol. 92, No. ST2, pp. 63-83.

15. Dabrowski, R. 1961. Dunnwandige Stabe Unter Zweiachsig Aussermittigen Druck. Der Stahlbau, Vol. 30, No. 12, Berlin, Germany, pp. 360-365.
16. European Convention for Structural Steelwork. 1978. European Convention for Steel Construction, Brussels, Belgium.
17. Haaijer, G., Carskaddon, P.S. and Grubb, M.A. 1981. Eccentric Load Test of Angle Column Simulated with MSC/NASTRAN Finite Element Program. Presented at the Annual Meeting of Structural Stability Research Council, Chicago, Illinois, U.S.A.
18. Ishida, A. 1968. Experimental Study on Column Carrying Capacity of 'SHY' Steel Angles. Yawata Technical Report No. 265, Yawata Iron and Steel Co. Ltd., Tokyo, Japan. pp. 8564-8582 and 8761-8763.
19. Johnson, L.W. and Riess, R.D. 1982. Numerical Analysis. Addison-Wesley Publishing Co., Don Mills, Ontario. pp. 313-317.
20. Kennedy, J.B. and Madugula, M.K.S. 1982. Buckling of Angles: State of the Art. Journal of the Structural Divisions, ASCE, Vol. 108, No. ST9, pp. 1967-1980.
21. Kennedy, J.B. and Murty, M.K.S. 1972. Buckling of Steel Angle and Tee Struts. Journal of the Structural Divisions, ASCE, Vol. 98, No. ST11, pp. 2507-2522.
22. Kennedy, J.B. and Sinclair, G.R. 1969. Ultimate Capacity of Single Bolted Angle Connections. Journal of the

Structural Division, ASCE, Vol. 95, No. ST8, pp. 1645-1660.

23. Leigh, J.M. and Lay, M.G. 1970. Laterally Unsupported Angles With Equal and Unequal Legs and Safe Load Tables for Laterally Unsupported Angles. Report No. 22/2 and 22/3. Broken Hill Proprietary Research Laboratory, Melbourne, Australia.
24. Marsh, C. 1969. Single Angle Members in Tension and Compression. Journal of the Structural Division, ASCE, Vol. 95, No. ST5, pp. 1043-1049.
25. Peköz, T.B. and Celebi, N. 1969. Torsional-Flexural Buckling of Thin-Walled Sections under Eccentric Load. Cornell Engineering Research Bulletin 69-1, Cornell University, Ithaca, New York, N.Y., U.S.A.
26. Prawel, S.P., Jr. and Lee, G.C. 1964. Biaxial Flexure of Columns by Analogue Computers. Journal of the Engineering Mechanics Division, ASCE, Vol. 90, No. EM1, pp. 83-111.
27. Schuster, R.M. 1975. Cold-Formed Steel Design Manual. Solid Mechanics Division, University of Waterloo, Waterloo, Canada.
28. Thomas, B.F. and Leigh, J.M. 1970. The Behavior of Laterally Unsupported Angles. Report No. 22/4, The Broken Hill Proprietary Co. Ltd., Melbourne, Australia.
29. Thurlimann, B. 1953. Deformations of and Stresses in Initially Twisted and Eccentrically Loaded Columns of

- Thin-Walled Open Cross-section. Report No. E696-3,
Brown University, Providence, R.I., U.S.A.
30. Timoshenko, S.P. and Gere, J.M. 1961. Theory of Elastic Stability. Mc-Graw Hill Book Co. Inc., New York, N.Y., U.S.A.
31. Trahair, N.S., Usami, T. and Galambos, T.V. 1969. Eccentrically Loaded Single Angle Columns. Research Report No. 11, Dept. of Civil and Environmental Engg., Washington University, St. Louis, Missouri, U.S.A.
32. Trahair, N.S., Usami, T. and Galambos, T.V. 1970. Eccentrically Loaded Single Angle Columns. Research Report No. 11A. Dept. of Civil and Environmental Engg. Washington University, St. Louis, Missouri, U.S.A.
33. Usami, T. 1970. Restrained Single Angle Columns under Biaxial Bending. Research Report No. 14, Dept. of Civil and Environmental Engg., Washington University, St. Louis, Missouri, U.S.A.
34. Usami, T. and Fukumoto, Y. 1972. Compressive Strength and Design of Bracing Members with Angle or Tee Section. Proceedings, Japan Society of Civil Engineers, No. 201, pp. 43-50.
35. Usami, T. and Galambos, T.V. 1971. Eccentrically Loaded Single Angle Columns. International Association for Bridge and Structural Engineering, Vol. 31-II, Zurich, Switzerland. pp. 153-184.

36. Vlasov, V.Z. 1961. Thin-Walled Elastic beams. National Science Foundation, Washington, D.C., U.S.A.
37. Winter, G. 1977. Cold-Formed Steel Design Manual, Part III and V. AISI, Washington, D.C., U.S.A.
38. Wood, A.B. 1975. Buckling Tests on Crossed Diagonals in Lattice Towers. Electra, Working Group 08 of Study Committee No. 22 of the International Conference on Large High Voltage Electric Systems, Vol. 38, Paris, France. pp. 89-99.
39. Yokoo, Y., Wakabayashi, M. and Nonaka, T. 1968. An Experimental Study on Buckling of Angles. Yawata Technical Report No. 265, Yawata Iron and Steel Co. Ltd., Tokyo, Japan. pp. 8543-8563 and 8759-8760.

VITA AUCTORIS

SUJIT KUMAR RAY

The author was born on January 2, 1959 in Burnpur, West Bengal, India. In 1975, he completed his higher secondary school education at Ballygunge Govt. High School, Calcutta, India. In 1980, he graduated from Jadavpur University, Calcutta, India, with a degree of Bachelor of Civil Engineering. Then he joined Development Consultants Pvt. Ltd., Calcutta, as a Structural Engineer.

In 1982, he joined the Civil Engineering Department at the University of Windsor, Windsor, Ontario, Canada. The author prepared this thesis in partial fulfillment for the requirements for the degree of Master of Applied Science in Civil Engineering at the University of Windsor.

Table 61 Cross-Sectional Properties (full section) of Cold-Formed Angles - Equal Angles

Size mm x mm	Long Leg x Short Leg	Thickness mm	Radius Inside Bend	Mass kg/m	Dead Load kN/m	Area mm ²	Axis x'-x'		Axis y'-y'		Product of Inertia mm ⁶	Axis x-x		Axis y-y		J mm ⁴ 10 ³	Location of Shear Center		C _w mm ⁶ 10 ⁶	β ₁ [*] mm	β ₂ [*] mm
							I _{x'} mm ⁴ 10 ⁶	y' mm	I _{y'} mm ⁴ 10 ⁶	x' mm		I _x mm ⁴ 10 ⁶	α Deg.	I _y mm ⁴ 10 ⁶	r _y mm		x _s mm	y _s mm			
200 x 200	25	75		66.2	0.649	8440	31.3	66.0	31.3	66.0	-23.1	54.4	45.0	8.24	31.3	1760	41.3	41.3	90.9	0.00	292
	20	60		54.9	0.539	7000	26.7	62.5	26.7	62.5	-18.8	45.5	45.0	7.90	33.6	933	44.5	44.5	81.0	0.00	290
	16	48		45.2	0.443	5760	22.4	59.8	22.4	59.8	-15.2	37.7	45.0	7.19	35.3	491	46.6	46.6	69.8	0.00	288
	13	39		37.5	0.368	4780	18.9	57.8	18.9	57.8	-12.5	31.4	45.0	6.39	36.6	269	47.9	47.9	59.7	0.00	287
	10	30		29.4	0.289	3750	15.0	55.9	15.0	55.9	-9.69	24.7	45.0	5.33	37.7	125	48.9	48.9	48.0	0.00	286
150 x 150	20	60		39.2	0.385	5000	10.3	50.5	10.3	50.5	-7.72	18.1	45.0	2.61	22.8	667	30.0	30.0	29.5	0.00	220
	16	48		32.7	0.320	4160	8.86	47.6	8.86	47.6	-6.32	15.2	45.0	2.55	24.7	355	32.8	32.8	26.6	0.00	218
	13	39		27.3	0.268	3480	7.57	45.5	7.57	45.5	-5.21	12.8	45.0	2.36	26.1	196	34.5	34.5	23.4	0.00	217
	10	30		21.6	0.212	2750	6.10	43.5	6.10	43.5	-4.05	10.2	45.0	2.05	27.3	91.7	35.8	35.8	19.3	0.00	216
125 x 125	16	48		26.4	0.259	3360	4.85	41.6	4.85	41.6	-3.59	8.44	45.0	1.26	19.4	287	25.5	25.5	14.0	0.00	183
	13	39		22.2	0.218	2830	4.20	39.4	4.20	39.4	-2.98	7.17	45.0	1.22	20.8	159	27.5	27.5	12.6	0.00	181
	10	30		17.7	0.173	2250	3.42	37.4	3.42	37.4	-2.33	5.75	45.0	1.10	22.1	75.0	29.2	29.2	10.7	0.00	180
	8	24		14.4	0.142	1840	2.84	36.1	2.84	36.1	-1.88	4.72	45.0	0.965	22.9	39.3	30.0	30.0	8.99	0.00	180
100 x 100	16	48		20.1	0.197	2560	2.27	35.7	2.27	35.7	-1.78	4.05	45.0	0.495	13.9	218	17.9	17.9	6.12	0.00	149
	13	39		17.1	0.168	2180	2.01	33.4	2.01	33.4	-1.49	3.50	45.0	0.515	15.4	123	20.3	20.3	5.78	0.00	146
	10	30		13.7	0.135	1750	1.67	31.2	1.67	31.2	-1.18	2.84	45.0	0.494	16.8	58.3	22.3	22.3	5.06	0.00	145
	8	24		11.3	0.111	1440	1.40	29.9	1.40	29.9	-0.953	2.35	45.0	0.450	17.7	30.7	23.3	23.3	4.37	0.00	144

Table 6.1 cont'd

Size mm x mm	Long leg x Short leg	Thickness mm	Inside Bend Radius mm	Mass kg/m	Dead Load kN/m	Area mm ²	Axis x'-x'		Axis y'-y'		Product of Inertia 10^6 mm^4	Axis x-x		Axis y-y		J 10^3 mm^4	Location of Shear Center		C_w 10^6 mm^6	β_1^* mm	β_2^* mm
							$I_{x'}$	y'	$I_{y'}$	x'		I_x	α	I_y	z_y		x_e	y_e			
90 x 90		6	18	8.71	0.085	1110	1.10	28.6	1.10	28.6	-0.723	1.82	45.0	0.379	18.5	13.3	24.1	24.1	3.49	1.45	0.00
		13	39	15.0	0.148	1920	1.41	31.0	1.41	31.0	-1.07	2.48	45.0	0.335	13.2	108	17.2	17.2	3.93	18.8	0.00
		10	30	12.2	0.119	1550	1.18	28.8	1.18	28.8	-0.850	2.03	45.0	0.333	14.7	51.7	19.4	19.4	3.52	8.66	0.00
		8	24	10.0	0.099	1280	1.00	27.4	1.00	27.4	-0.691	1.69	45.0	0.310	15.6	27.3	20.6	20.6	3.08	3.86	0.00
		6	18	7.77	0.076	990	0.791	26.1	0.791	26.1	-0.525	1.32	45.0	0.266	16.4	11.9	21.5	21.5	2.50	1.21	0.00
75 x 75		13	39	12.0	0.118	1530	0.748	27.6	0.748	27.6	-0.597	1.35	45.0	0.151	9.94	86.0	12.3	12.3	1.94	9.12	0.00
		10	30	9.81	0.096	1250	0.646	25.2	0.646	25.2	-0.483	1.13	45.0	0.163	11.4	41.7	15.0	15.0	1.85	5.10	0.00
		8	24	8.16	0.080	1040	0.554	23.8	0.554	23.8	-0.395	0.949	45.0	0.159	12.4	22.2	16.4	16.4	1.66	2.52	0.00
		6	18	6.36	0.062	810	0.444	22.4	0.444	22.4	-0.301	0.745	45.0	0.142	13.3	9.72	17.5	17.5	1.30	0.857	0.00
		5	15	5.40	0.053	687	0.381	21.8	0.381	21.8	-0.253	0.635	45.0	0.128	13.7	5.73	17.9	17.9	1.20	0.405	0.00
65 x 65		10	30	8.24	0.081	1050	0.397	22.9	0.397	22.9	-0.307	0.704	45.0	0.090	9.24	35.0	12.0	12.0	1.09	3.07	0.00
		8	24	6.91	0.068	880	0.346	21.4	0.346	21.4	-0.254	0.599	45.0	0.092	10.2	18.8	13.5	13.5	1.01	1.71	0.00
		6	18	5.42	0.053	690	0.280	20.0	0.280	20.0	-0.195	0.475	45.0	0.086	11.1	8.28	14.8	14.8	0.855	0.633	0.00
		5	15	4.61	0.045	587	0.242	19.3	0.242	19.3	-0.164	0.406	45.0	0.079	11.6	4.90	15.3	15.3	0.757	0.310	0.00

Table 6.1 con'td

Size Long Leg x Short Leg	Thickness mm	Inside Radii mm	Mass kg/m	Dead Load kN/m	Area mm ²	Axis x'-x'		Axis y'-y'		Product of Inertia I_{xy}	Axis x-x		Axis y-y		J 10^3 mm^4	Location of Shear Center		C_v 10^3 mm	β_1^* mm	β_2^* mm
						$I_{x'}$ 10^6 mm^4	y' mm	$I_{y'}$ 10^6 mm^4	x' mm		I_x 10^6 mm^4	α Deg.	I_y 10^6 mm^4	r_y mm		x_s mm	y_s mm			
55 x 55	10	30	6.67	0.065	850	0.221	20.6	0.221	20.6	-0.179	0.400	45.0	0.042	7.06	20.3	8.52	8.52	1.52	0.00	83.1
	8	24	5.65	0.055	720	0.197	19.0	0.197	19.0	-0.150	0.347	45.0	0.047	8.05	15.4	10.5	10.5	0.994	0.00	81.1
	6	18	4.47	0.044	570	0.163	17.5	0.163	17.5	-0.117	0.279	45.0	0.046	9.01	6.84	11.9	11.9	0.424	0.00	79.9
	5	15	3.83	0.038	487	0.142	16.8	0.142	16.8	-0.090	0.240	45.0	0.044	9.46	4.06	12.5	12.5	0.219	0.00	79.9
	4	8	3.19	0.031	407	0.121	15.9	0.121	15.9	-0.078	0.199	45.0	0.043	10.2	2.17	13.3	13.3	0.100	0.00	77.9
	3	6	2.44	0.024	311	0.094	15.3	0.094	15.3	-0.059	0.153	45.0	0.034	10.5	0.934	13.5	13.5	0.008	0.00	77.9
45 x 45	8	24	4.39	0.043	560	0.098	16.7	0.098	16.7	-0.079	0.177	45.0	0.019	5.06	11.9	7.16	7.16	0.251	0.00	67.7
	6	18	3.53	0.035	450	0.084	15.1	0.084	15.1	-0.063	0.146	45.0	0.021	6.85	5.40	9.01	9.01	0.239	0.00	66.0
	5	15	3.04	0.030	387	0.074	14.4	0.074	14.4	-0.053	0.127	45.0	0.021	7.33	3.23	9.71	9.71	0.220	0.00	65.4
	4	8	2.57	0.025	327	0.064	13.4	0.064	13.4	-0.042	0.106	45.0	0.022	8.17	1.74	10.7	10.7	0.202	0.00	63.7
	3	6	1.97	0.019	251	0.050	12.8	0.050	12.8	-0.032	0.082	45.0	0.018	8.45	0.754	10.9	10.9	0.160	0.00	63.7

*For the definition of β_1 and β_2 , refer to Timoshenko and Gere, 1951.

Table 6.2 Cross-Sectional Properties (full section) of Cold-Formed Angles - Unequal Angles

Size mm x mm	Long Leg x Short Leg	Thickness mm	Radius Inside Bend mm	Mass kg/m	Dead Load kN/m	Area mm ²	Axis x'-x'		Axis y'-y'		Product of Inertia mm ⁴	Axis x-x		Axis y-y		J 10 ³ mm ⁴	Location of Shear Center		C _w 10 ⁶ mm ⁴	A ₁ [*] mm ²	A ₂ [*] mm ²
							I _{x'}	y'	I _{y'}	x'		I _x	α	I _y	z _y		x _s	y _s			
200 x 150		25	75	56.4	0.553	7190	27.0	75.4	13.6	47.1	-14.5	36.3	32.6	4.35	24.6	1500	22.5	39.0	1680	65.7	215
							23.5	71.2	11.7	43.7	-11.9	30.9	31.9	4.31	26.8	800	25.9	46.3	690	69.2	231
							19.9	68.1	9.93	41.2	-9.70	25.8	31.4	4.02	28.5	423	28.1	50.7	281	73.2	237
							16.9	65.9	8.41	39.4	-7.97	21.7	31.0	3.62	29.6	232	29.9	53.5	103	76.2	240
200 x 100		20	60	39.2	0.385	5000	18.9	83.5	3.59	27.5	-5.95	21.0	18.9	1.55	17.6	667	18.8	47.8	464	123	-12.2
							16.5	79.7	3.06	25.1	-4.89	18.1	18.1	1.46	18.8	355	17.6	55.4	214	128	85.0
							14.2	77.0	2.61	23.3	-4.04	15.4	17.5	1.34	19.6	196	17.1	59.9	96.2	132	127
							11.5	74.4	2.12	21.7	-3.16	12.4	17.0	1.15	20.5	91.7	16.9	63.3	37.1	136	152
150 x 100		16	48	26.4	0.259	3360	7.30	57.0	2.76	29.1	-3.28	9.02	27.7	1.03	17.6	287	15.1	33.5	132	65.8	139
							6.34	54.5	2.38	27.2	-2.73	7.73	27.0	0.991	18.7	159	17.4	30.4	45.7	69.1	156
							5.19	52.1	1.94	25.4	-2.13	6.25	26.3	0.885	19.8	75.0	19.2	41.9	18.6	72.8	165
							4.32	50.6	1.61	24.3	-1.72	5.16	25.9	0.776	20.5	39.3	19.4	43.3	7.39	75.1	166

Table 62 cont'd

Size mm x mm	Long Leg x Short Leg	Thickness	Inside Bend Radius	Mass kg/m	Dead Load kN/m	Area mm ²	Axis x'-x'		Axis y'-y'		Product of Inertia mm ⁴	Axis x-x		Axis y-y		J 10 ³ mm ⁴	Location of Shear Center		C _w 10 ⁶ mm ⁶	I ₀ 10 ⁸ mm ⁴	β_1° mm	β_2° mm
							I _{x'} 10 ⁶ mm ⁴	y' mm	I _{y'} 10 ⁶ mm ⁴	x' mm		I _x 10 ⁶ mm ⁴	α Deg.	I _y 10 ⁶ mm ⁴	r _y mm		x _s mm	y _s mm				
125 x 90	16	48		22.0	0.216	2800	4.08	48.3	1.87	28.4	-2.11	5.36	31.2	0.599	14.6	239	12.8	23.6	7.91	100	45.5	120
				18.6	0.183	2370	3.60	45.7	1.63	26.3	-1.76	4.64	30.4	0.600	15.9	134	14.6	28.3	7.62	47.1	47.4	136
				14.9	0.146	1900	2.99	43.3	1.35	24.4	-1.39	3.78	29.7	0.558	17.1	63.3	16.6	32.2	6.81	14.4	50.5	143
				12.2	0.120	1560	2.50	41.8	1.13	23.2	-1.12	3.13	29.3	0.500	17.9	33.3	17.9	34.2	5.95	5.23	52.7	146
125 x 75	13	39		17.1	0.168	2180	3.27	49.2	0.960	21.3	-1.29	3.85	24.1	0.301	13.2	123	11.5	20.8	6.29	22.7	64.2	85.1
				13.7	0.135	1750	2.75	46.6	0.796	19.5	-1.02	3.18	23.2	0.358	14.3	58.3	13.6	34.1	5.89	11.6	67.8	114
				11.3	0.111	1440	2.32	45.0	0.669	18.3	-0.830	2.66	22.6	0.323	15.0	30.7	13.8	36.3	5.15	5.39	70.6	122
				8.71	0.085	1110	1.82	43.4	0.527	17.2	-0.631	2.08	22.1	0.271	15.6	13.3	13.8	37.8	4.15	1.59	73.0	126
100 x 90	13	39		16.1	0.158	2050	3.91	35.1	1.48	29.5	-1.26	2.97	40.2	0.413	14.2	115	16.4	19.8	4.71	25.6	13.5	136
				13.0	0.127	1650	3.60	32.8	1.24	27.4	-0.998	2.43	39.9	0.402	15.6	55.0	18.2	22.5	4.20	11.5	14.6	135
				10.7	0.105	1360	3.34	31.4	1.04	26.1	-0.810	2.02	39.7	0.370	16.5	29.0	19.3	23.9	3.66	5.14	15.4	135
				8.24	0.081	1050	3.06	30.1	0.821	24.8	-0.615	1.57	39.5	0.314	17.3	12.6	20.1	25.0	2.96	1.63	16.2	135

Table 6.2 cont'd

Size mm x mm	Long leg x Short leg	Thickness mm	Radius mm	Mass kg/m	Dead Load kN/m	Area mm ²	Axis x'-x'		Axis y'-y'		Product of Inertia I_{xy}	Axis x-x		Axis y-y		J	Location of Shear Center		C_w	β_1^*	β_2^*	
							$I_{x'}$	y'	$I_{y'}$	x'		I_x	α	I_y	r_y		x_s	y_s				
mm	mm	mm	mm	kg/m	kN/m	mm ²	10^{-6} mm ⁴	mm	10^{-6} mm ⁴	mm	10^{-6} mm ⁴	Deg.	10^{-6} mm ⁴	mm	10^{-6} mm ⁴	10^{-6} mm ⁴	mm	10^{-6} mm ⁴	mm	mm	mm	
100 x 75		13	39	14.5	0.143	1850	1.73	38.1	0.872	23.9	-0.936	2.33	32.7	0.270	12.1	104	11.0	18.7	3.44	29.3	32.7	105
		10	30	11.8	0.115	1500	1.47	35.6	0.733	21.9	-0.745	1.93	31.9	0.269	13.4	50.0	12.9	23.1	3.24	10.8	34.6	116
		8	24	9.73	0.095	1240	1.25	34.1	0.621	20.6	-0.606	1.62	31.4	0.251	14.2	26.5	14.1	25.4	2.90	4.40	36.6	119
		6	18	7.54	0.074	960	0.988	32.6	0.492	19.4	-0.461	1.26	30.9	0.216	15.0	11.5	15.3	27.2	2.41	1.10	38.6	121
90 x 75		13	39	13.5	0.133	1720	1.27	33.8	0.828	25.2	-0.798	1.88	37.2	0.222	11.4	97.0	11.5	15.5	2.72	20.8	19.7	110
		10	30	11.0	0.108	1400	1.09	31.4	0.702	23.1	-0.630	1.56	36.6	0.228	12.8	46.7	13.6	19.4	2.57	8.08	20.8	114
		8	24	9.10	0.089	1160	0.927	29.9	0.597	21.7	-0.520	1.31	36.2	0.216	13.7	24.7	14.7	21.4	2.30	4.21	22.1	115
		6	18	7.06	0.069	900	0.738	28.4	0.474	20.5	-0.396	1.02	35.8	0.189	14.5	10.8	15.7	22.9	1.90	1.34	23.5	116
90 x 65		5	15	5.99	0.059	762	0.632	27.7	0.407	19.9	-0.332	0.870	35.6	0.169	14.9	6.35	16.1	23.5	1.66	0.579	24.1	116
		10	30	10.2	0.100	1300	1.01	33.4	0.454	19.5	-0.504	1.31	30.7	0.164	11.2	43.3	10.1	19.4	2.09	0.82	33.3	95.6
		8	24	8.48	0.083	1080	0.869	31.8	0.396	18.2	-0.413	1.11	30.1	0.157	12.1	23.0	11.5	22.2	1.94	3.27	35.3	102
		6	18	6.59	0.065	840	0.696	30.2	0.316	16.9	-0.315	0.874	29.5	0.138	12.8	10.1	12.7	24.4	1.65	0.858	37.5	105
		5	15	5.59	0.055	712	0.598	29.5	0.272	16.3	-0.265	0.746	29.2	0.124	13.2	5.94	13.2	25.1	1.44	0.422	38.5	106

56

Table 6.2 cont'd

Size mm x mm	Thickness mm	Inside Band Radius	Mass kg/m	Dead Load kN/m	Area mm ²	Axis x'-x'		Axis y'-y'		Product of Inertia I _{xy}	Axis x-x		Axis y-y		J 10 ⁶ mm ⁴	Location of Shear Center			C _w	β ₁	β ₂		
						I _{x'}	y'	I _{y'}	x'		I _x	α	I _y	r _y		x _s	y _s	I ₀				10 ⁶ mm ⁴	10 ⁶ mm ⁴
80 x 60	10	30	9.03	0.089	1150	0.692	30.1	0.349	18.8	-0.371	0.929	32.6	0.111	9.84	38.3	8.98	15.6	1.40	6.86	26.3	86.0		
	8	24	7.53	0.074	960	0.601	28.5	0.300	17.5	-0.305	0.791	31.9	0.110	10.7	20.5	10.4	18.5	1.33	2.83	27.7	92.5		
	6	18	5.89	0.058	750	0.485	26.9	0.242	16.2	-0.234	0.627	31.2	0.100	11.5	9.00	11.5	20.7	1.14	0.855	29.7	95.4		
	5	15	5.00	0.049	637	0.419	26.2	0.208	15.6	-0.196	0.536	30.9	0.091	11.9	5.31	12.1	21.6	1.02	0.348	30.7	96.3		
75 x 50	8	24	6.59	0.065	840	0.456	28.5	0.172	14.6	-0.205	0.564	27.7	0.065	8.77	17.9	7.57	16.8	0.909	2.06	32.9	69.7		
	6	18	5.18	0.051	660	0.374	26.8	0.140	13.3	-0.158	0.454	26.8	0.060	9.55	7.92	9.05	19.9	0.826	0.509	35.2	79.9		
	5	15	4.42	0.043	562	0.325	26.0	0.121	12.7	-0.133	0.390	26.3	0.055	9.92	4.69	9.60	21.0	0.744	0.291	36.4	82.3		
65 x 50	8	24	5.96	0.058	760	0.303	24.1	0.162	15.7	-0.167	0.413	33.5	0.052	8.25	16.2	7.77	12.9	0.634	1.90	19.9	73.5		
	6	18	4.71	0.046	600	0.250	22.5	0.133	14.3	-0.129	0.333	32.7	0.050	9.13	7.20	9.06	15.5	0.576	0.637	21.4	77.9		
	5	15	4.02	0.039	512	0.218	21.8	0.116	13.7	-0.109	0.287	32.4	0.047	9.54	4.27	9.61	16.5	0.520	0.301	22.3	78.8		
	4	8	3.35	0.033	427	0.185	20.7	0.098	12.9	-0.086	0.238	31.5	0.045	10.2	2.28	10.5	17.9	0.466	0.031	24.0	78.8		
55 x 35	6	18	3.53	0.035	450	0.130	21.4	0.044	10.2	-0.056	0.158	26.2	0.017	6.08	5.40	5.16	12.1	0.251	0.282	25.9	43.7		
	5	15	3.04	0.030	387	0.116	20.5	0.039	9.57	-0.048	0.139	25.5	0.016	6.46	3.23	5.81	13.8	0.241	0.122	26.9	52.0		
	4	8	2.57	0.025	327	0.101	19.3	0.033	8.73	-0.038	0.118	24.0	0.017	7.13	1.74	6.54	15.9	0.232	0.022	29.3	57.2		
	3	6	1.97	0.019	251	0.080	18.6	0.026	8.24	-0.029	0.092	23.7	0.014	7.37	0.755	6.52	16.4	0.184	0.006	30.2	58.0		

Table 6.2 cont'd.

Size mm x mm	Long leg x Short leg	Thickness mm	Inside Bend Radius mm	Mass kg/m	Dead Load kN/m	Area mm ²	Axis x'-x'		Axis y'-y'		Product of Inertia mm ⁴	Axis x-x		Axis y-y		Location of Shear Center		C _w 10 ⁶ mm ⁶	β ₁ [*] mm	β ₂ [*] mm
							I _{x'} 10 ⁶ mm ⁴	y' mm	I _{y'} 10 ⁶ mm ⁴	x' mm		I _x 10 ⁶ mm ⁴	α Deg.	I _y 10 ⁶ mm ⁴	r _y mm	x _s mm	y _s mm			
45 x 30				2.83	0.028	360	0.067	18.2	0.026	9.55	-0.032	0.084	28.7	0.008	4.78	4.07	7.92	0.120	19.3	29.3
				2.45	0.024	312	0.061	17.3	0.023	8.86	-0.028	0.075	27.8	0.008	5.18	4.43	9.72	0.119	19.6	40.3
				2.09	0.021	267	0.054	16.0	0.020	7.96	-0.022	0.065	26.0	0.009	5.93	5.68	12.4	0.124	21.7	48.3
				1.62	0.016	206	0.043	15.3	0.016	7.45	-0.017	0.051	25.6	0.008	6.18	5.78	13.0	0.101	22.6	49.0
*For the definition of β ₁ and β ₂ , refer to Timoshenko and Gere, 1961.																				

Table 6.3 Ultimate Compressive Strength of Cold-Formed Angle Columns Under Biaxial Bending

Slenderness Ratio	ULTIMATE COMPRESSIVE STRENGTH (KN)											
	55 x 55 x 3 x 6				55 x 35 x 4 x 8 [Long Leg Connected]				55 x 35 x 4 x 8 [Long Leg Out]			
	g=15	g=20	g=25	g=30	g=35	g=40	g=20	g=25	g=30	g=35	g=15	g=20
20	32.5	40.4	51.0	35.7	27.1	21.7	35.1	44.1	51.4	37.6	42.6	27.8
30	31.9	39.4	50.4	35.6	26.9	21.5	34.3	42.8	51.3	37.5	42.4	27.5
40	30.9	38.0	48.3	35.6	26.6	21.3	33.2	41.2	51.1	37.5	41.9	27.2
50	29.8	36.4	45.9	35.5	26.3	20.9	31.9	39.2	49.7	37.5	41.1	26.9
60	28.5	34.6	43.1	35.5	25.9	20.5	30.5	37.0	46.2	37.5	40.2	26.4
70	27.1	32.6	40.2	35.5	25.4	20.1	28.9	34.7	42.3	37.4	39.0	25.8
80	25.6	30.5	37.2	35.5	24.8	19.5	27.2	32.3	37.9	37.3	37.5	25.2
90	24.1	28.5	34.3	35.5	24.1	18.9	25.5	29.6	34.1	37.2	35.8	24.4
100	22.6	26.4	31.4	35.4	21.0	18.3	23.9	26.9	30.7	35.8	33.7	23.2
110	21.1	24.4	28.7	33.0	17.0	17.6	21.9	24.5	27.8	32.1	31.5	19.2
120	19.6	22.6	26.2	29.9	14.1	16.8	20.1	22.4	25.2	28.9	29.2	16.1
130	18.3	20.8	23.9	27.1	12.0	16.0	18.5	20.4	22.9	26.0	26.9	13.7
140	17.0	19.2	21.8	24.5	10.3	15.2	17.1	18.7	20.8	23.5	24.6	11.8
150	15.8	17.7	19.9	22.2	8.82	14.4	15.8	17.2	19.0	21.3	22.5	10.3
160	14.7	16.3	18.1	20.2	7.71	13.6	14.6	15.9	17.4	19.4	20.5	9.07
170	13.2	15.1	16.6	18.4	6.81	12.8	13.5	14.6	16.0	17.7	18.7	8.03
180	12.7	13.9	15.2	16.7	6.05	12.1	12.6	13.5	14.7	16.2	17.1	7.16
190	11.9	12.9	14.0	15.3	5.43	11.4	11.7	12.5	13.6	14.8	15.7	6.43
200	11.1	11.9	12.9	14.0	4.90	10.7	10.9	11.6	12.5	13.7	14.4	5.80
210	10.3	11.1	11.9	12.9	4.44	10.0	10.2	10.8	11.6	12.6	13.3	5.26
220	9.65	10.3	11.0	11.8	4.05	9.43	9.51	10.1	10.8	11.6	12.2	4.80
230	9.03	9.61	10.2	10.9	3.70	8.86	8.91	9.44	10.1	10.8	11.3	4.39
240	8.47	8.96	9.50	10.1	3.40	8.34	8.36	8.84	9.38	10.0	10.5	4.03

Note: 1. The size of angle is expressed as: Width of Long Leg (mm) x Width of Short Leg (mm) x Thickness (mm) x Inside Bend Radius (mm)

2. g = gauge distance (mm)

Table 6.4 Dimensional Buckling Curve, B3 (Limiting Stress in MPa)

λ	0	1	2	3	4	5	6	7	8	9	λ
0	250.0	250.0	250.0	250.0	250.0	250.0	250.0	250.0	250.0	250.0	0
10	250.0	250.0	250.0	250.0	250.0	250.0	250.0	250.0	250.0	249.3	10
20	248.4	247.4	246.5	245.5	244.6	243.6	242.6	241.6	240.5	239.5	20
30	238.4	237.3	236.2	235.1	234.0	232.8	231.7	230.6	229.5	228.5	30
40	227.4	226.3	225.2	224.1	223.0	221.9	220.7	219.5	218.2	217.0	40
50	215.7	214.4	213.1	211.7	210.4	209.0	207.6	206.2	204.7	203.3	50
60	201.5	200.4	198.9	197.4	195.8	194.3	192.8	191.2	189.6	188.0	60
70	186.4	184.8	183.1	181.5	179.8	178.1	176.4	174.7	173.0	171.2	70
80	169.4	167.6	165.7	163.9	162.1	160.3	158.5	156.7	155.0	153.2	80
90	151.5	149.8	148.0	146.3	144.6	142.9	141.2	139.6	137.9	136.3	90
100	134.7	133.1	131.5	129.9	128.3	126.7	125.2	123.7	122.1	120.6	100
110	119.1	117.6	116.2	114.7	113.3	111.8	110.4	109.1	107.1	106.4	110
120	105.0	103.8	102.5	101.2	100.0	98.7	97.5	96.3	95.2	94.0	120
130	92.8	91.7	90.6	89.5	88.4	87.3	86.1	85.2	84.2	83.2	130
140	82.2	81.3	80.3	79.4	78.5	77.6	76.7	75.8	74.9	74.0	140
150	73.2	72.3	71.5	70.5	69.6	69.0	68.2	67.4	66.7	65.8	150
160	65.1	64.5	63.8	63.1	62.5	61.8	61.2	60.5	59.9	59.3	160
170	58.7	58.0	57.4	56.8	56.2	55.6	55.1	54.5	53.9	53.4	170
180	52.8	52.3	51.8	51.3	50.8	50.3	49.9	49.4	48.9	48.5	180
190	48.0	47.5	47.1	46.6	46.2	45.8	45.4	45.0	44.6	44.2	190
200	43.8	43.3	42.9	42.5	42.2	41.8	41.5	41.1	40.7	40.3	200
210	40.0	39.6	39.2	38.9	38.5	38.2	37.9	37.6	37.2	36.9	210
220	36.6	36.3	36.0	35.7	35.4	35.1	34.9	34.6	34.3	34.0	220
230	33.7	33.5	33.2	33.0	32.8	32.6	32.3	32.0	31.7	31.5	230
240	31.2	31.0	30.8	30.6	30.4	30.1	29.9	29.7	29.5	29.3	240
250	29.0										250

Table 6.5 Cross-Sectional Properties of Test Specimens

Property	Nominal Size of Angle (mm)	
	65 x 50 x 4	55 x 55 x 4
Actual Width of Long Leg (mm)	63.30	53.20
Actual Width of Short Leg (mm)	48.80	53.20
Thickness (mm)	4.00	3.96
Inside Bend Radius (mm)	8.00	8.00
Nominal Area (mm ²)	427	407
Actual Area, A (mm ²)	415	389
Maximum Moment of Inertia, I_x (mm ⁴)	219600	177400
Nominal Minimum Moment of Inertia (mm ⁴)	44790	42670
Minimum Moment of Inertia, I_y (mm ⁴)	40990	37620
Torsional Constant, J (mm ⁴)	2210	2030
Polar Moment of Inertia about the Shear Centre, I_o (mm ⁴)	428960	342430
x-Coordinate of Shear Centre, x_o (mm)	-17.82	-18.10
y-Coordinate of Shear Centre, y_o (mm)	-9.37	0.00
β_1 (mm)	23.19	0.00
β_2 (mm)	76.84	75.35
Warping Constant, C_w (mm ⁶)	29890	27600

Table 6.6. Lengths and Slenderness Ratios of the Test Specimens

62

Angle Size (mm)	Specimen No.	No. of bolts at each end-connection	Length (mm)	Maximum Slenderness Ratio	
				Nominal	Actual
65 x 50 x 4 Long Leg Connected	ES65-1-1	1	838	82	84
	1-2	2			
	1-3	3			
	2-1	1	1218	119	122
	2-2	2			
	2-3	3			
	3-1	1	1752	171	176
	3-2	2			
	3-3	3			
65 x 50 x 4 Long Leg Out	ES65-4-1	1	838	82	84
	4-2	2			
	4-3	3			
	5-1	1	1752	171	176
	5-2	2			
	5-3	3			
55 x 55 x 4	ES55-1-1	1	838	82	85
	1-2	2			
	1-3	3			
	2-1	1	1218	119	123
	2-2	2			
	2-3	3			
	3-1	1	1752	171	178
	3-2	2			
	3-3	3			

Table 6.7a Experimental and Theoretical Failure Loads

Specimen Number	Experimental Failure Load in kN	Computed Failure Load (kN) based on			
		Nominal Dimensions		Actual Dimensions	
		ASCE	ECCS	ASCE	ECCS
ES65-1-1	59.5	76.7	59.8	74.8	57.4
1-2	71.0	76.7	59.8	74.8	57.4
1-3	75.0	76.7	59.8	74.8	57.4
2-1	45.7	60.4	45.4	56.4	42.6
2-2	56.8	60.4	45.8	57.2	43.3
2-3	59.2	60.4	45.8	57.2	43.3
3-1	37.0	29.5	24.8	27.1	22.9
3-2	37.0	37.7	28.7	35.2	26.8
3-3	40.0	37.7	28.7	35.2	26.8
ES65-4-1	57.0	76.7	59.8	74.8	57.4
4-2	81.0	76.7	59.8	74.8	57.4
4-3	81.0	76.7	59.8	74.8	57.4
5-1	40.0	29.5	24.8	27.1	22.9
5-2	44.0	37.7	28.7	35.2	26.8
5-3	51.5	37.7	28.7	35.2	26.8
ES55-1-1	58.0	75.9	57.0	71.2	53.4
1-2	70.0	75.9	57.0	71.2	53.4
1-3	75.0	75.9	57.0	71.2	53.4
2-1	54.5	57.6	43.3	52.0	39.3
2-2	58.6	57.6	43.6	53.0	40.2
2-3	63.8	57.6	43.6	53.0	40.2
3-1	40.5	28.1	23.6	24.8	21.0
3-2	40.0	35.9	27.3	32.5	24.6
3-3	43.8	35.9	27.3	32.5	24.6

Table 6.7b Predicted Failure Loads for Test Specimens

Specimen Number	Computed Failure Loads (kN) based on General Theory of Torsional-Flexural Buckling
ES65-1-1	49.8
2-1	34.2
3-1	21.2
4-1	50.4
5-1	27.5
ES55-1-1	52.5
2-1	37.6
3-1	22.6

Table 6.8 Effect of Variables on the Ultimate Compressive Strength of
65 x 50 x 4 mm Cold-Formed Angle (Long Leg Connected)

Slenderness Ratio	Failure Loads (kN) based on					
	Exact Shear Centre		Shear Centre at SC ₁		Shear Centre at SC ₂	
	$C_w = 0$	Actual C_w	$C_w = 0$	Actual C_w	$C_w = 0$	Actual C_w
20	71.8	70.1	71.8	70.3	71.8	70.0
30	71.0	70.0	71.2	70.2	70.8	69.8
40	67.6	68.5	67.9	68.8	67.4	68.4
50	63.6	64.4	64.1	64.7	63.4	64.1
60	59.3	59.8	59.8	60.3	59.0	59.6
70	54.8	55.2	55.3	55.7	54.6	55.0
80	50.4	50.7	50.8	51.1	50.2	50.4
90	46.1	46.0	46.5	46.6	45.9	45.7
100	41.5	41.4	42.0	41.9	41.3	41.2
110	37.5	37.4	37.8	37.8	37.3	37.2
120	33.9	33.9	34.2	34.1	33.8	33.7
130	30.8	30.7	31.0	31.0	30.6	30.6
140	28.0	28.0	28.2	28.1	27.9	27.9
150	25.5	25.5	25.7	25.7	25.5	25.4
160	23.4	23.4	23.5	23.5	23.3	23.3
170	21.4	21.4	21.5	21.5	21.4	21.3
180	19.7	19.7	19.8	19.8	19.6	19.6
190	18.1	18.1	18.2	18.2	18.1	18.1
200	16.8	16.8	16.8	16.8	16.7	16.7
210	15.5	15.5	15.6	15.6	15.5	15.5
220	14.4	14.4	14.4	14.4	14.4	14.4
230	13.4	13.4	13.4	13.4	13.4	13.4
240	12.5	12.5	12.5	12.5	12.5	12.5

Table 6.9 Comparison of Exact and Galerkin Solutions

Size of the angle = $65 \times 50 \times 4$ mm (Long Leg Out)

Gauge Distance = 25 mm

Length of the member = 189.6 mm ($l/r_y = 20$)

Load kN	u-component			v-component			rotation, $\phi \times 10^3$		
	Exact mm	Galerkin mm	% error	Exact mm	Galerkin mm	% error	Exact rad	Galerkin rad	% error
1.3276	-	0.0014	-	-	0.0025	-	-	0.0002	-
14.6036	0.0150	0.0150	0.0	0.0273	0.0273	0.0	-0.1314	0.0202	-115.4
27.8796	0.0287	0.0288	0.0	0.0522	0.0522	0.0	-0.0753	0.0742	-198.5
41.1556	0.0427	0.0427	0.0	0.0771	0.0771	0.0	0.0163	0.1630	900.0
54.4316	0.0568	0.0567	-0.2	0.1020	0.1020	0.0	0.1452	0.2875	98.0
67.7076	0.0711	0.0708	-0.4	0.1270	0.1270	0.0	0.3131	0.4485	43.2
69.0352	0.0726	0.0723	-0.4	0.1295	0.1295	0.0	0.3321	0.4666	40.5
70.3629	0.0740	0.0737	-0.4	0.1320	0.1320	0.0	0.3515	0.4852	38.0
80.9837	0.0856	0.0851	-0.6	0.1521	0.1521	0.0	0.5215	0.6470	24.1
134.0877	0.1460	0.1432	-2.0	0.2528	0.2525	-0.1	1.7959	1.8376	2.3

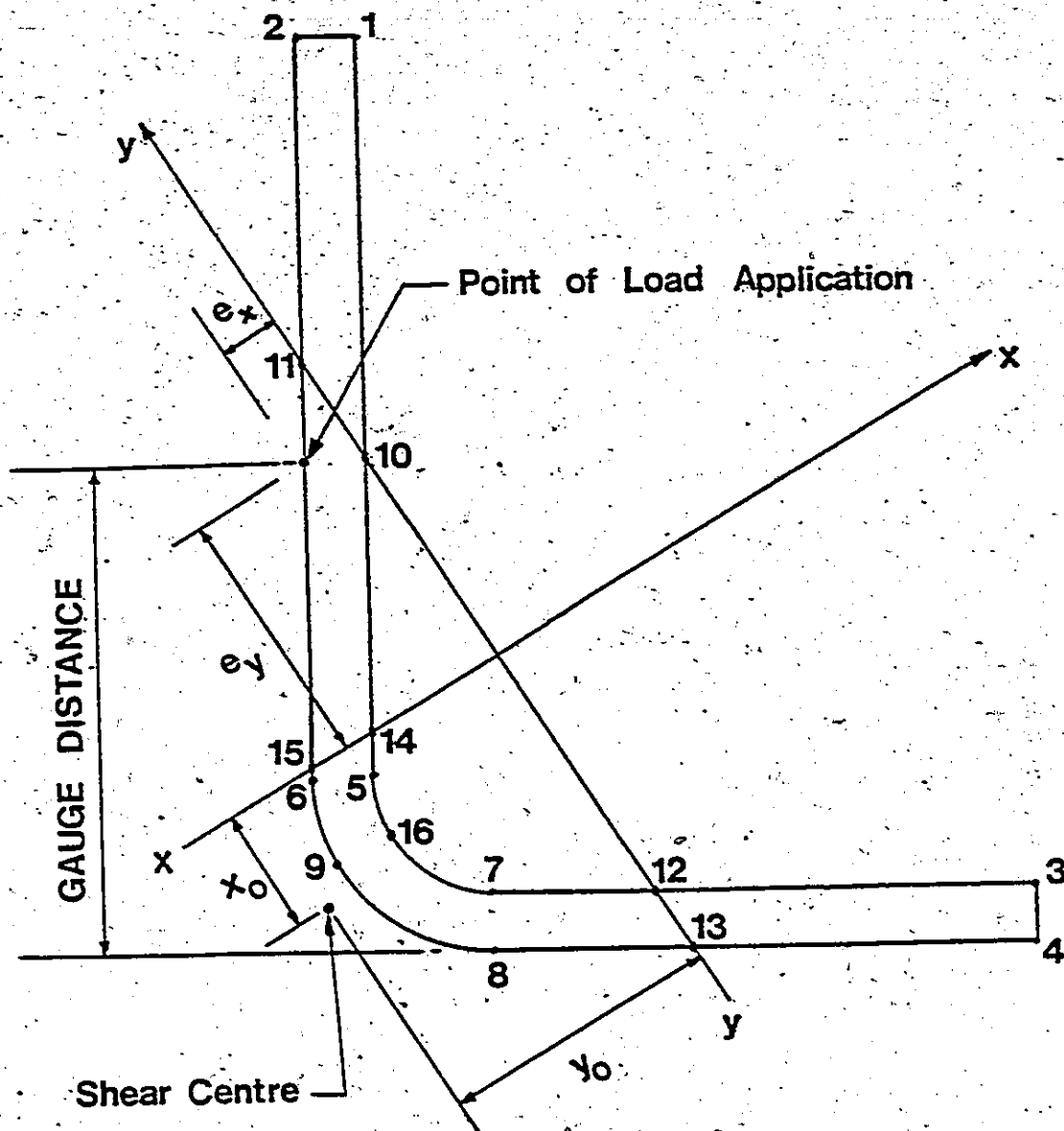


Figure 4.1 Location of critical points and the load on the cross-section.

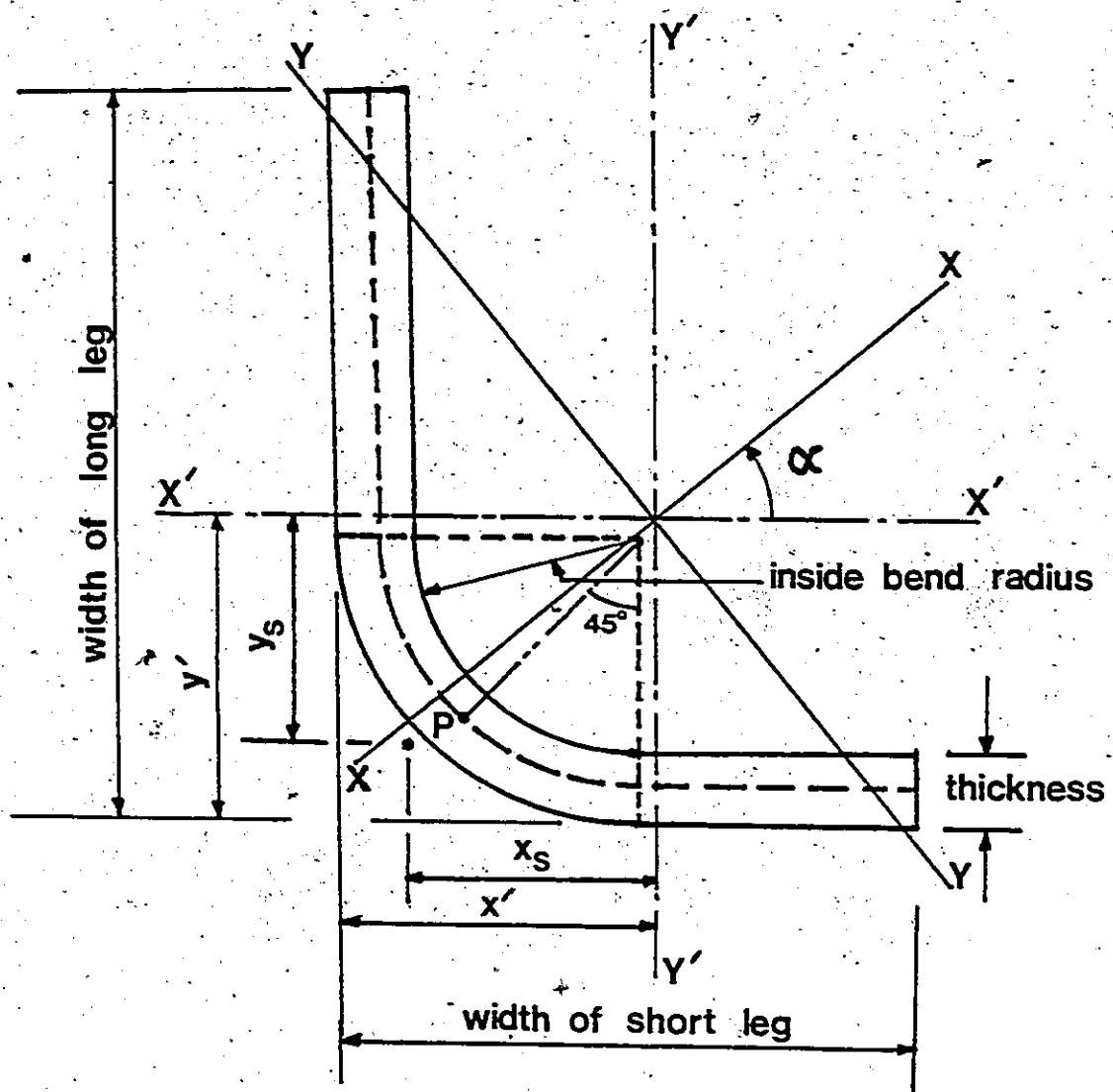


Figure 4.2 Cross-section of cold-formed angle.

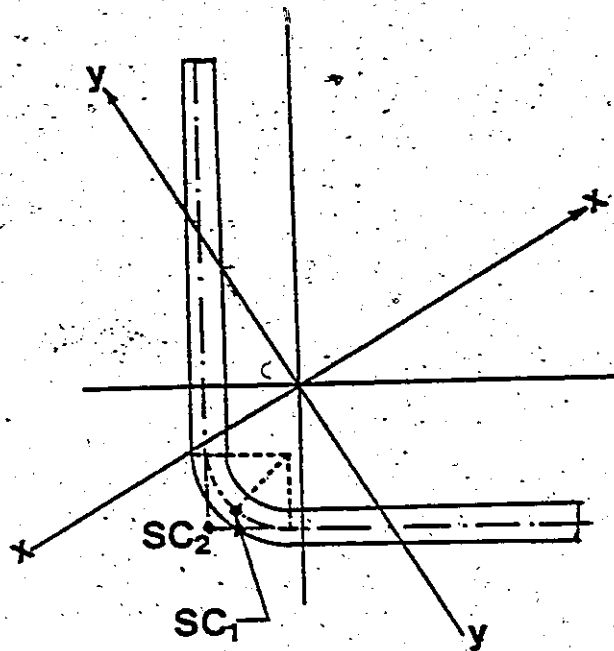


Figure 4.3 Assumed locations of shear centre.

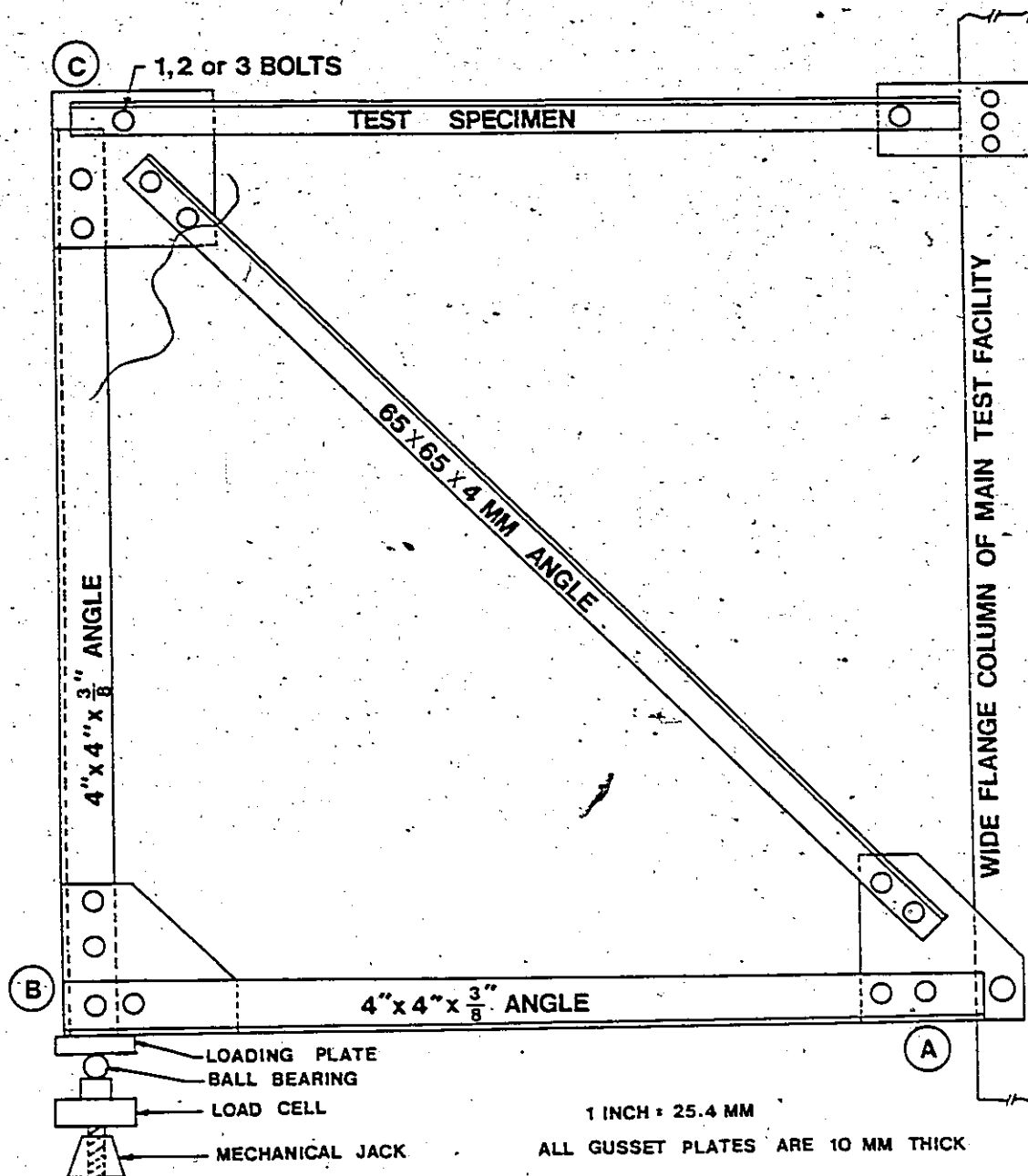


Figure 5.1 Schematic diagram of test set-up.



Figure 5.2 Arrangement for load application at joint B.



Figure 5.3 Lateral support at joint B.



Figure 5.4 Lateral support at joint C.

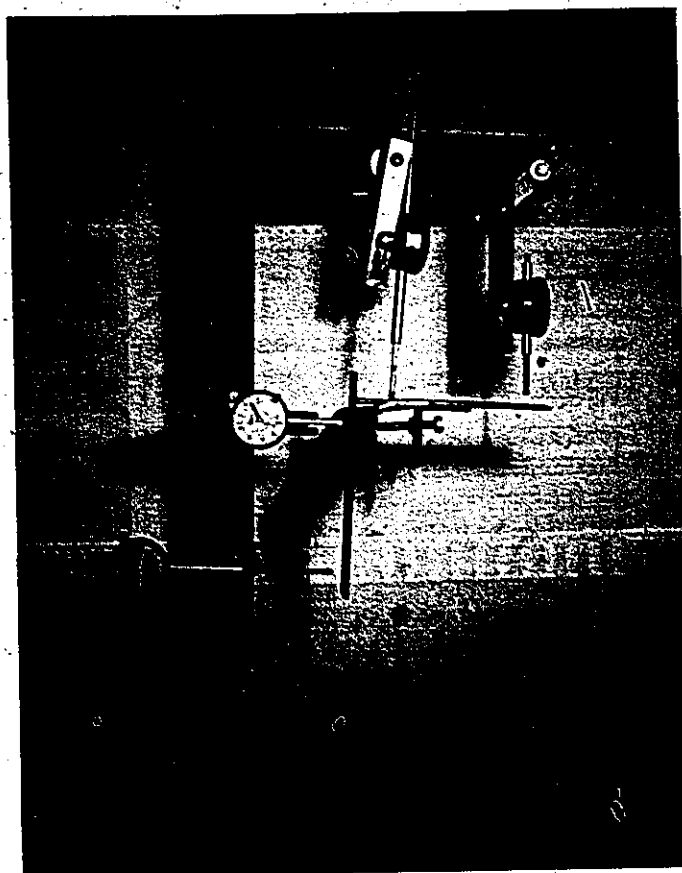


Figure 5.5 Arrangement of dial gauges at midspan of the test specimen.

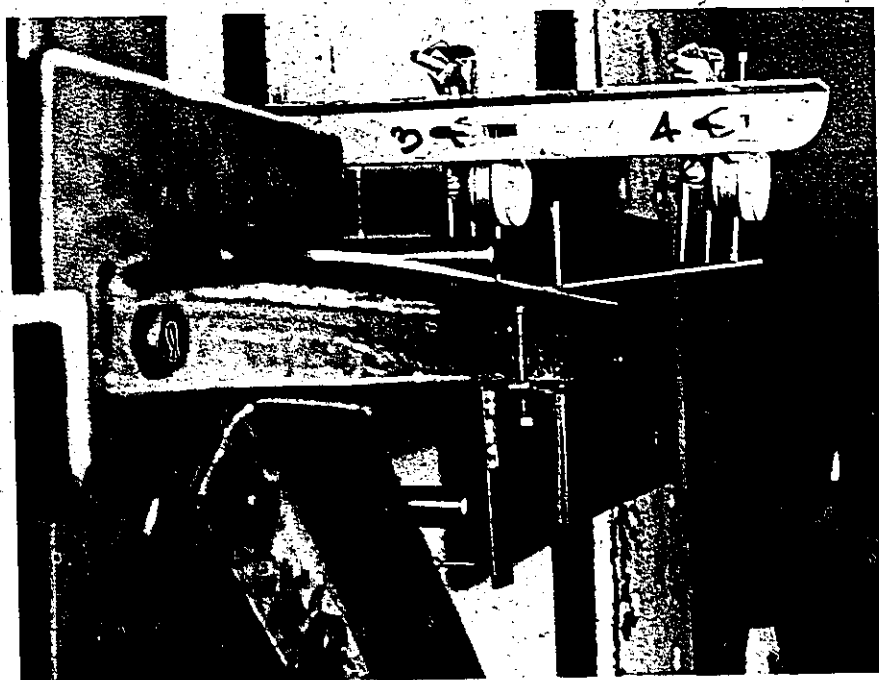


Figure 5.6 L-shaped extension piece at midspan.

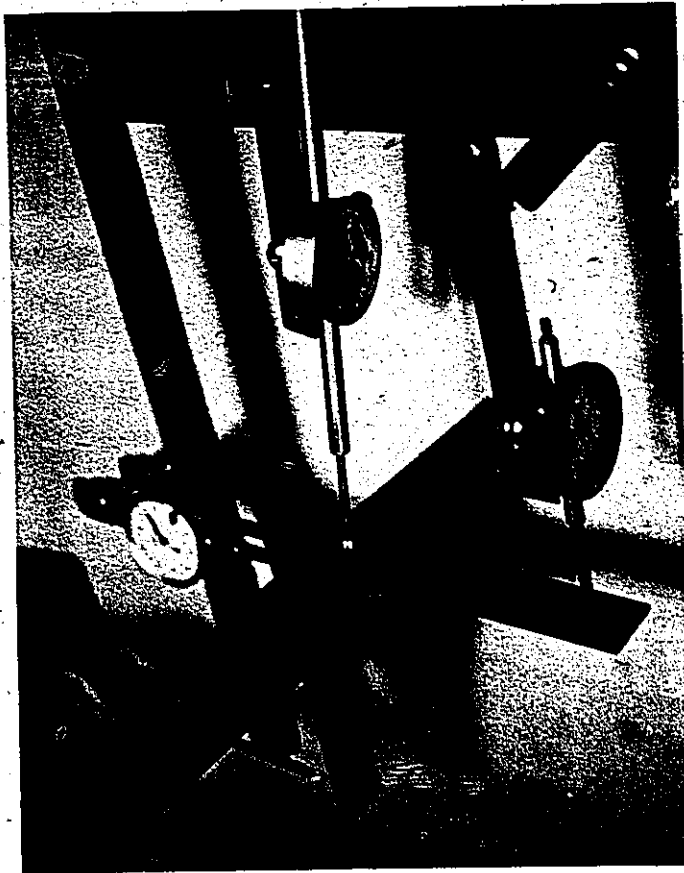


Figure 5.7 Gauge support bracket.

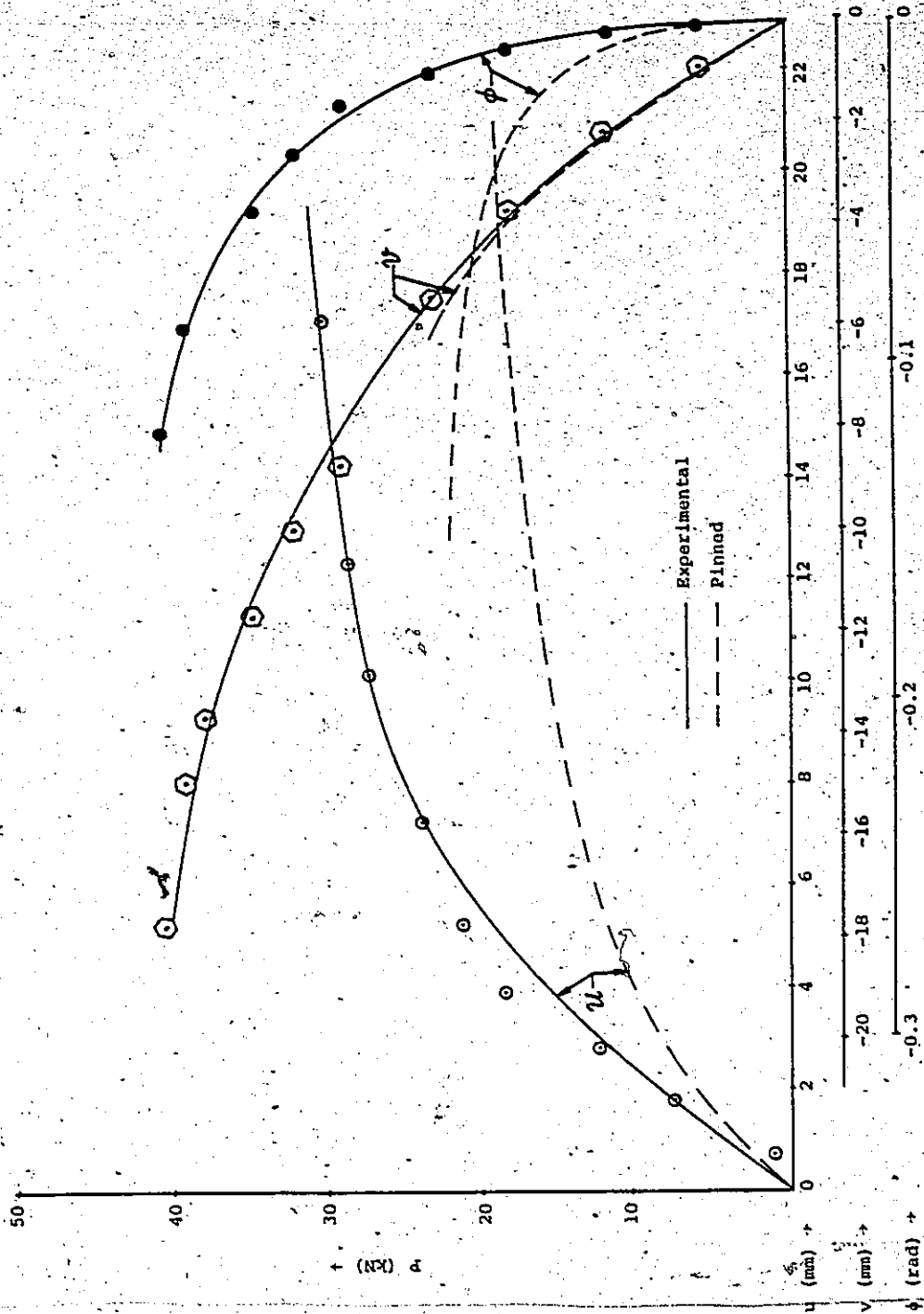


Figure 6.1 Load-deflection and load-rotation curves at midspan for Specimen ES55-3-1

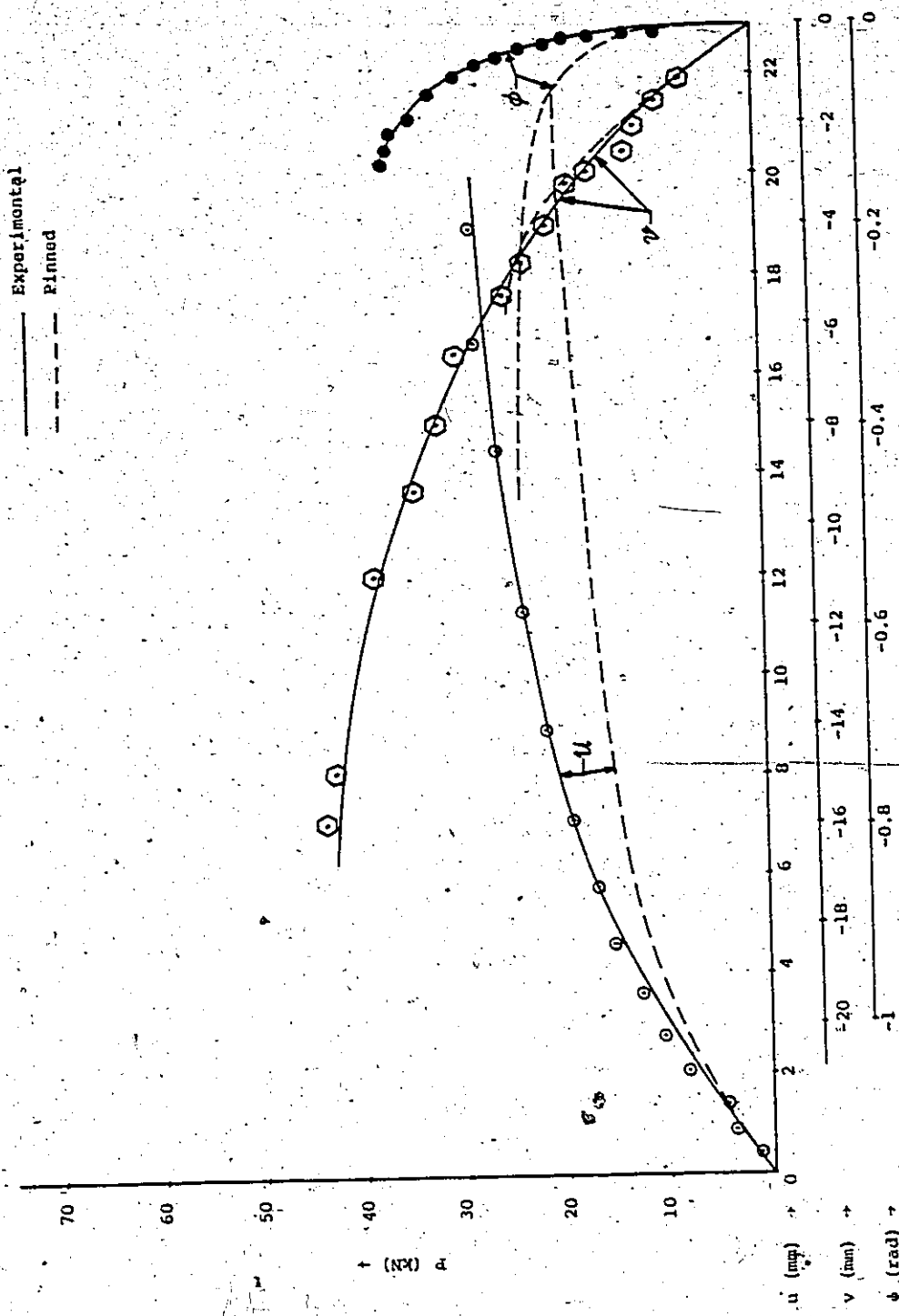


Figure 6.2 Load-deflection and load-rotation curves at midspan for Specimen ES65-3-2

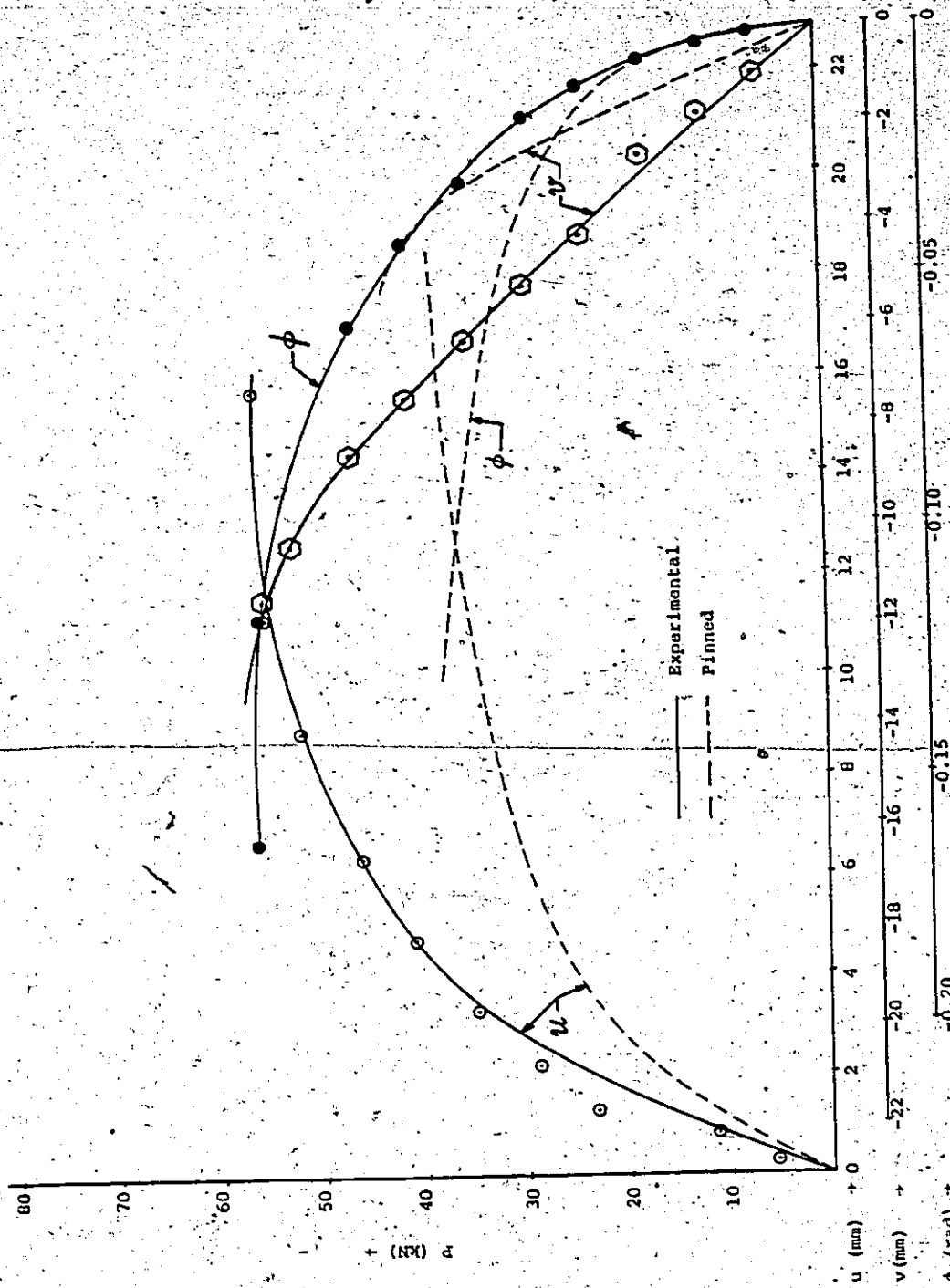


Figure 6.3 Load-deflection and load-rotation curves at midspan for Specimen PS65-2-2

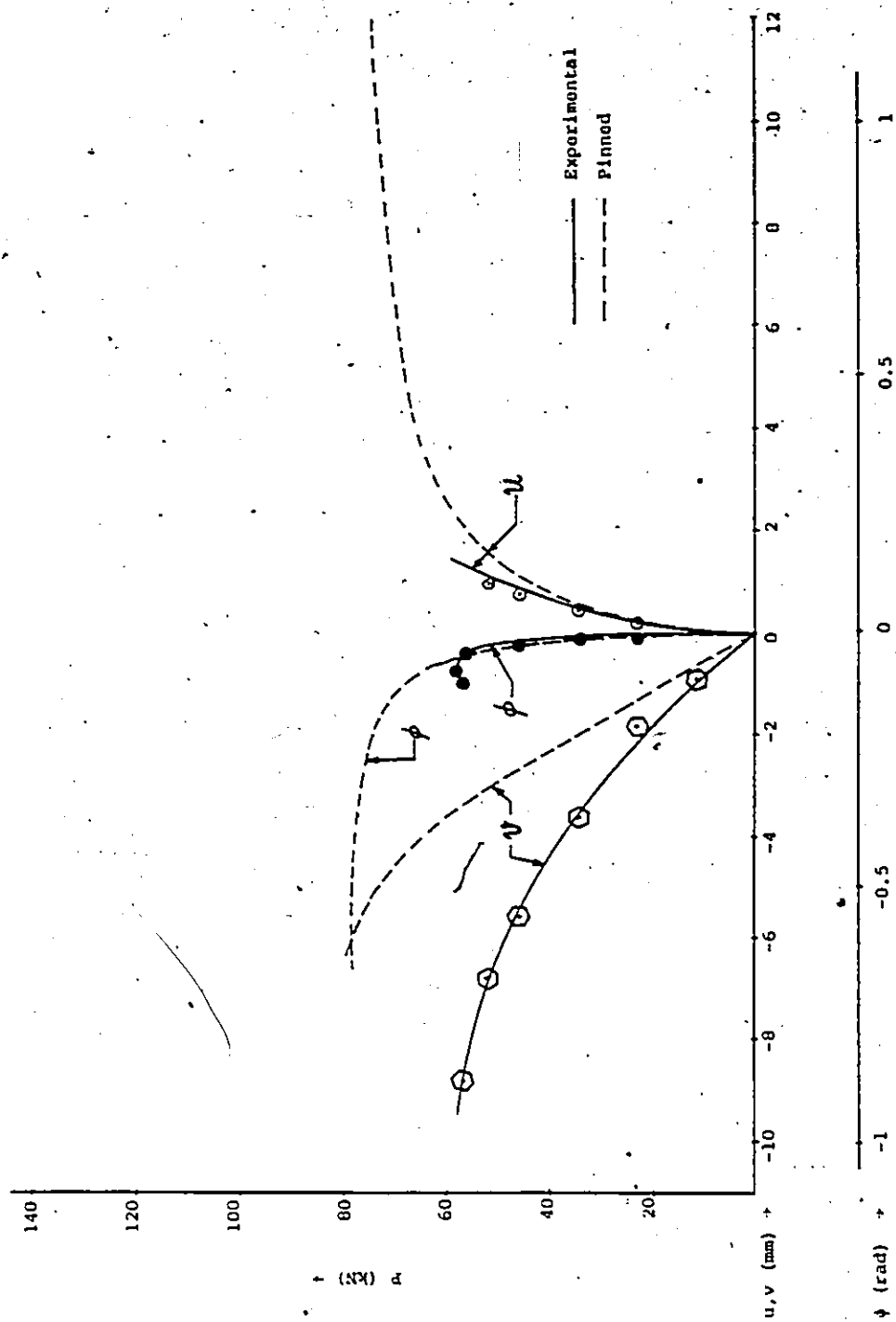


Figure 6.4 Load-deflection and load-rotation curves at midspan for Specimen ES55-1-1

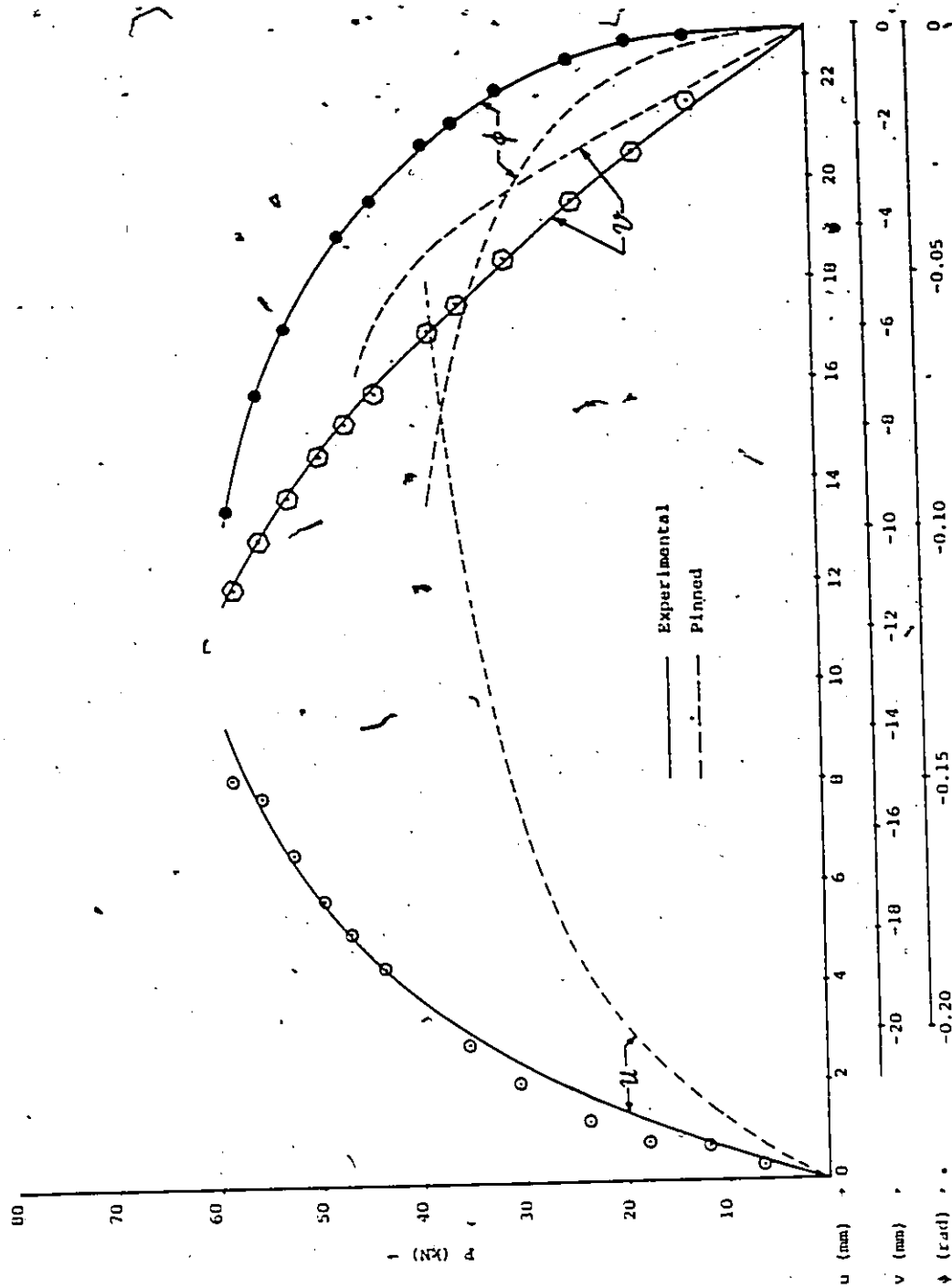


Figure 6.5 Load-deflection and load-rotation curves at midspan for Specimen ES55-2-2

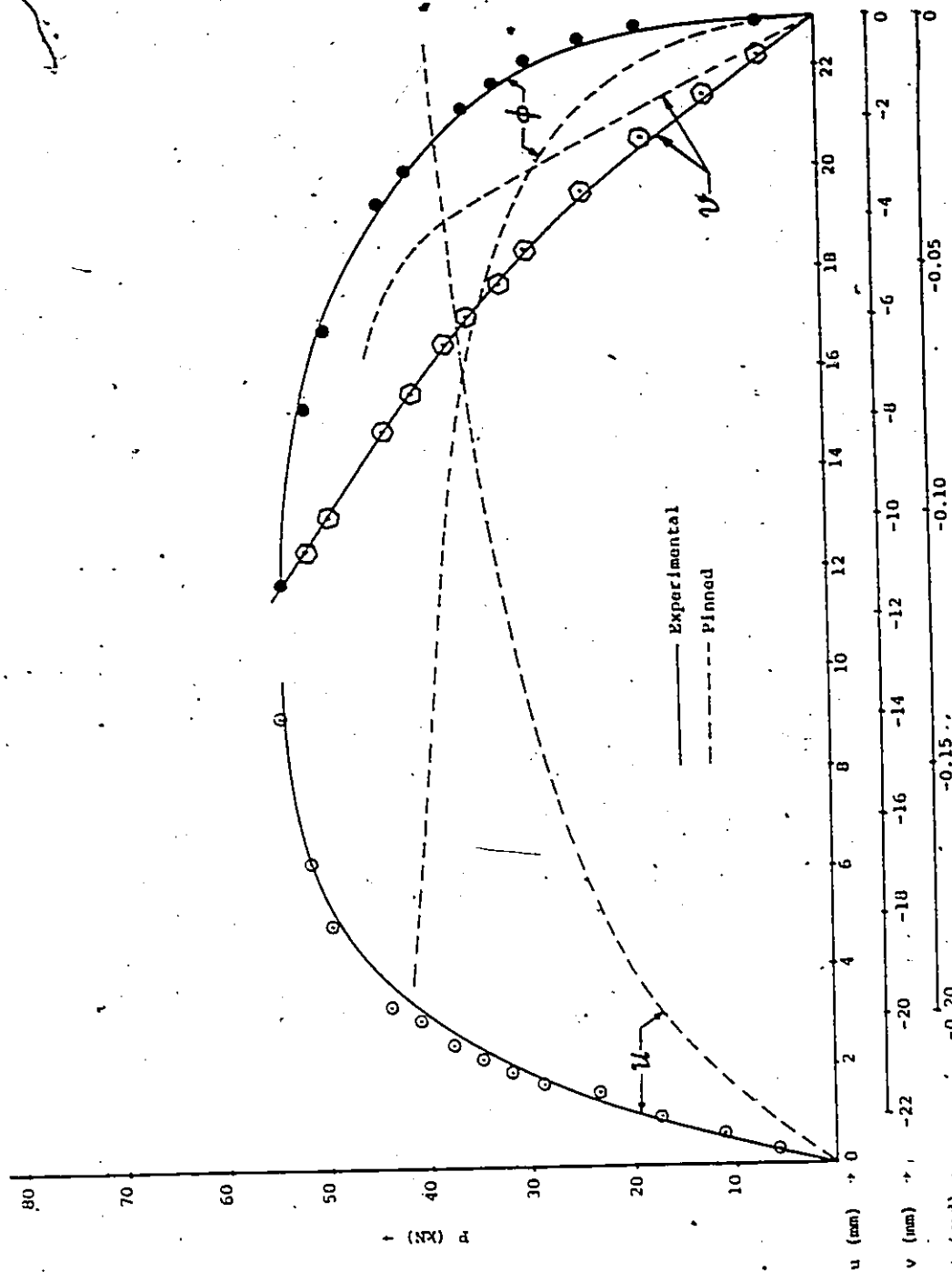


Figure 6.6 Load-deflection and load-rotation curves at midspan for Specimen ES55-2-1

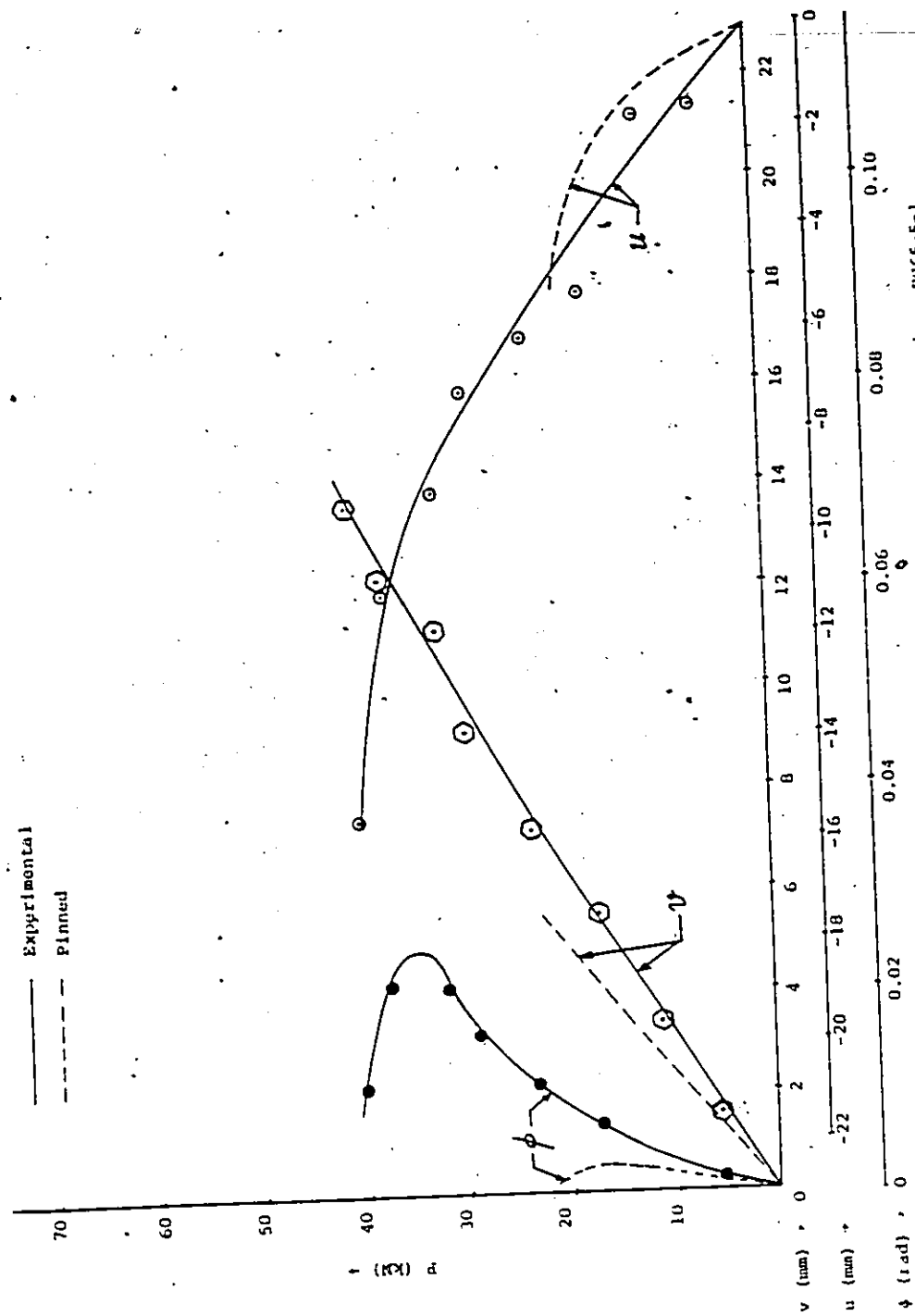


Figure 6.7 Load-deflection and load-rotation curves at midspan for Specimen ES65-5-1

APPENDIX 1

THEORETICAL FORMULATION FOR THE
CROSS-SECTIONAL PROPERTIES OF
COLD-FORMED ANGLES

APPENDIX 1

THEORETICAL FORMULATION FOR THE CROSS-SECTIONAL
PROPERTIES OF COLD-FORMED ANGLES

The formulas for the calculation of the cross-sectional properties are as given below:

1. Area (Ref. Fig. 1)

$$[1] \quad A = (c_1 + c_2) t + \frac{\pi}{4} [(r + t)^2 - r^2]$$

2. Location of Centroid (Ref. Fig. 1)

$$[2] \quad \bar{x} = \frac{A_1 x_1 + A_2 x_2 + A_3 x_3 - A_4 x_4}{A_1 + A_2 + A_3 - A_4}$$

$$[3] \text{ and } \bar{y} = \frac{A_1 y_1 + A_2 y_2 + A_3 y_3 - A_4 y_4}{A_1 + A_2 + A_3 - A_4}$$

where $A_1 = c_1 t$

$$A_2 = c_2 t$$

$$A_3 = \frac{\pi}{4} (r+t)^2$$

$$A_4 = \frac{\pi}{4} r^2$$

$$x_1 = y - c_1/2$$

$$x_2 = t/2$$

$$x_3 = (r+t) - \frac{4(r+t)}{3\pi}$$

$$x_4 = (r+t) - \frac{4r}{3\pi}$$

$$y_1 = t/2$$

$$y_2 = x - c_2/2$$

$$y_3 = (r+t) - \frac{4(r+t)}{3\pi}$$

$$y_4 = (r+t) - \frac{4r}{3\pi}$$

3. Moments of inertia (Ref. Fig. 1)

Final expressions for I_{xx} , I_{yy} and P_{xy} are as follows:

$$\begin{aligned}
 [4] \quad I_{xx} = & \frac{c_1^3 t^3}{12} + c_1 t (\bar{y} - t/2)^2 + \frac{c_2^3 t^3}{12} + c_2 t (x - \bar{y} - c_2/2)^2 \\
 & + \left\{ \frac{1}{16} \pi (r+t)^4 - \frac{\pi (r+t)^2}{4} \left[\frac{4(r+t)}{3\pi} \right]^2 + \frac{\pi (r+t)^2}{4} \left[\bar{y} - (r+t) + \frac{4(r+t)}{3\pi} \right]^2 \right\} \\
 & - \left\{ \frac{1}{16} \pi r^4 - \frac{\pi r^2}{4} \left(\frac{4r}{3\pi} \right)^2 + \frac{\pi r^2}{4} \left[\bar{y} - (r+t) + \frac{4r}{3\pi} \right]^2 \right\}
 \end{aligned}$$

$$\begin{aligned}
 [5] \quad I_{yy} = & \frac{c_1^3 t^3}{12} + c_1 t (y - \bar{x} - c_1/2)^2 + \frac{c_2^3 t^3}{12} + c_2 t (\bar{x} - t/2)^2 \\
 & + \left\{ \frac{1}{16} \pi (r+t)^4 - \frac{\pi (r+t)^2}{4} \left[\frac{4(r+t)}{3\pi} \right]^2 + \frac{\pi (r+t)^2}{4} \left[\bar{x} - (r+t) + \frac{4(r+t)}{3\pi} \right]^2 \right\} \\
 & - \left\{ \frac{1}{16} \pi r^4 - \frac{\pi r^2}{4} \left(\frac{4r}{3\pi} \right)^2 + \frac{\pi r^2}{4} \left[\bar{x} - (r+t) + \frac{4r}{3\pi} \right]^2 \right\}
 \end{aligned}$$

$$[6] \text{ and } P_{xy} = c_1 t [-(\bar{y} - t/2)] (y - \bar{x} - c_1/2) + c_2 t [-(\bar{x} - t/2)] (x - \bar{y} - c_2/2)$$

$$+ \frac{\pi(r+t)^2}{4} \left\{ \left[d_2 + \frac{4(r+t)}{3\pi} \right] \left[d_1 + \frac{4(r+t)}{3\pi} \right] \right\}$$

$$- \frac{\pi r^2}{4} \left[\left(d_2 + \frac{4r}{3\pi} \right) \left(d_1 + \frac{4r}{3\pi} \right) \right] + \frac{(r+t)^4}{8} - \frac{r^4}{8} - \frac{\pi(r+t)^2}{4} \left[\frac{4(r+t)}{3\pi} \right]^2$$

$$+ \frac{\pi r^2}{4} \left(\frac{4r}{3\pi} \right)^2$$

Minimum and maximum moments of inertia are computed by using the following expressions:

$$[7] \quad I_{\min} = \frac{I_{xx} + I_{yy}}{2} - \sqrt{\left(\frac{I_{xx} - I_{yy}}{2} \right)^2 + P_{xy}^2}$$

$$[8] \text{ and } I_{\max} = I_{xx} + I_{yy} - I_{\min}$$

4. Inclination of major principal axis to horizontal

The angle α between the major principal axis (u-u axis) and the horizontal (x-x axis) is calculated as follows:

$$[9] \quad \tan 2\alpha = \frac{2P_{xy}}{I_{xx} - I_{yy}}$$

5. Minimum radius of gyration.

$$[10] \quad r_{\min} = \sqrt{\frac{I_{\min}}{\text{Area}}}$$

6. Torsional constant (Ref. Fig. 1)

St. Venant's torsional constant has been computed by using the following expression:

$$[11] \quad J = \frac{1}{3} b t^3 \quad \text{where } b = \text{centre-line length of the cross-section}$$

$$= c_1 + c_2 + \pi(r+t/2)/2$$

and t = thickness of the section.

7. Location of shear centre (Ref. Fig. 2 to 13)

(a) v-coordinate (Bending about v-v axis) (Ref. Figs. 2 to 10)

Depending on the size of the angle, thickness and inside bend radius, there are several possible cases as shown in Table I

Case I - Figure 2

$$[12] \quad m_1 = (\bar{y} - t/2)t \cos \alpha \quad l_1^3 / (3I_{\min})$$

$$[13] \quad m_2 = (\bar{y} - t/2)t \cos \alpha \quad l_2(l_1^2 - l_2^2/3) / (2I_{\min})$$

$$[14] \quad m_3 = (\bar{x} - t/2)t \sin \alpha \quad l_3^3 / (3I_{\min})$$

$$[15] \quad m_4 = (\bar{x} - t/2)t \sin \alpha \quad l_4(l_3^2 - l_4^2/3) / (2I_{\min})$$

$$[16] \quad m_5 = \int_0^{\pi/4} \{ r_{oc1}^2 + r_{oc1} d\theta \sin(\pi/2 - \phi + \theta) - r_{oc1}^3 \cos(\alpha + \phi - \pi/2)\theta /$$

$$I_{\min} - \frac{2r_{oc1}^4}{I_{\min}} \sin \theta/2 \sin(\alpha + \theta/2)$$

$$- \frac{r_{oc1}^2 t \sin(\pi/2 - \phi + \theta)}{I_{\min}} \cos(\alpha + \phi - \pi/2)\theta$$

$$- \frac{2r_{oc1}^3 t d\theta}{I_{\min}} [\sin \theta/2 \sin(\alpha + \theta/2) \sin(\pi/2 - \phi + \theta)] d\theta$$

$$\begin{aligned}
 [17] \quad \text{and } m_6 = & \int_0^{\pi/4} \{ r_o^2 q_{c2} + r_o dq_{c2} \cos(\pi/2 - \phi - \theta) - \frac{r_o^3 dt \cos(\pi/2 - \alpha - \phi)}{I_{\min}} \theta \\
 & - \frac{2r_o^4 t}{I_{\min}} \sin \theta/2 \sin(\pi/2 - \alpha + \theta/2) - \frac{r_o^2 d^2 t}{I_{\min}} \cos(\pi/2 - \alpha - \phi) \theta \cos(\pi/2 - \phi - \theta) \\
 & - \frac{2r_o^3 dt}{I_{\min}} [\cos(\pi/2 - \phi - \theta) \sin \theta/2 \sin(\pi/2 - \alpha + \theta/2)] \} d\theta
 \end{aligned}$$

$$[18] \quad \therefore v_s = m_1 + m_2 + m_5 - m_3 - m_4 - m_6$$

Case II - Figure 3

m_1, m_2, m_3, m_4 = same as eqn. nos. [12], [13], [14] and [15], respectively.

$$\begin{aligned}
 [19] \quad m_5 = & \int_0^{\pi/4} \{ r_o^2 q_{c1} - r_o dq_{c1} \sin(\pi/2 - \phi + \theta) + \frac{r_o^3 td \cos(\alpha + \phi - \pi/2)}{I_{\min}} \theta \\
 & - \frac{2r_o^4 t}{I_{\min}} \sin \theta/2 \sin(\alpha + \theta/2) - \frac{r_o^2 d^2 t \sin(\pi/2 - \phi + \theta)}{I_{\min}} \cos(\alpha + \phi - \pi/2) \theta \\
 & + \frac{2r_o^3 td}{I_{\min}} [\sin \theta/2 \sin(\alpha + \theta/2) \sin(\pi/2 - \phi + \theta)] \} d\theta
 \end{aligned}$$

$$\begin{aligned}
 [20] \quad \text{and } m_6 = & \int_0^{\pi/4} \{ r_o^2 q_{c2} - r_o dq_{c2} \cos(\pi/2 - \phi - \theta) + \frac{r_o^3 dt \cos(\pi/2 - \alpha - \phi)}{I_{\min}} \theta \\
 & - \frac{2r_o^4 t}{I_{\min}} \sin \theta/2 \sin(\pi/2 - \alpha + \theta/2) - \frac{r_o^2 d^2 t}{I_{\min}} \cos(\pi/2 - \alpha - \phi) \theta \cos(\pi/2 - \phi - \theta) \\
 & + \frac{2r_o^3 dt}{I_{\min}} [\cos(\pi/2 - \phi - \theta) \sin \theta/2 \sin(\pi/2 - \alpha + \theta/2)] \} d\theta
 \end{aligned}$$

$$[21] \quad \therefore v_s = m_1 + m_2 + m_5 - m_3 - m_4 - m_6$$

Case III - Figure 4

$$[22] \quad m_1 = (\bar{y} - t/2)t \cos \alpha \frac{l_1^2(l_1'/2 - l_1/6)}{I_{\min}}$$

$$[23] \quad m_3 = (\bar{x} - t/2)t \sin \alpha \frac{l_3^2(l_3'/2 - l_3/6)}{I_{\min}}$$

$$[24] \quad m_5 = \int_0^{\beta} (\text{Integrand same as eqn. no. [19]})$$

$$[25] \quad m_6 = \int_0^{\pi/4-\beta} \{r_o^2 q_{c3} - r_o dq_{c3} \sin(\pi/2 - \phi + \theta + \beta) + \frac{r_o^3 t d \cos(\alpha + \phi - \pi/2)}{I_{\min}} \theta$$

$$- \frac{2r_o^4 t}{I_{\min}} \sin \theta/2 \sin(\alpha + \beta + \theta/2) - \frac{r_o^2 d^2 t \sin(\pi/2 - \phi + \theta + \beta)}{I_{\min}} \theta \cos(\alpha + \phi - \pi/2)$$

$$+ \frac{2r_o^3 t d}{I_{\min}} [\sin \theta/2 \sin(\alpha + \beta + \theta/2) \sin(\pi/2 - \phi + \theta + \beta)] d\theta$$

$$[26] \quad m_7 = \int_0^{\beta} (\text{Integrand same as eqn. no. [20]})$$

$$[27] \quad \text{and } m_8 = \int_0^{\pi/4-\beta} \{r_o^2 q_{c4} - r_o dq_{c4} \cos(\pi/2 - \phi - \theta - \beta) + \frac{r_o^3 t d \cos(\pi/2 - \alpha - \phi)}{I_{\min}} \theta$$

$$- \frac{2r_o^4 t}{I_{\min}} \sin \theta/2 \sin(\pi/2 - \alpha + \beta + \theta/2) - \frac{r_o^2 d^2 t}{I_{\min}} \cos(\pi/2 - \alpha - \phi) \theta \cos(\pi/2$$

$$- \phi - \theta - \beta)$$

$$+ \frac{2r_o^3 t d}{I_{\min}} [\sin \theta/2 \sin(\pi/2 - \alpha + \beta + \theta/2) \cos(\pi/2 - \phi - \theta - \beta)] d\theta$$

$$[28] \quad \therefore v_s = m_1 + m_5 + m_6 - m_3 - m_7 - m_8$$

Case IV - Figure 5

m_1, m_3 = same as eqn. nos. [22] and [23], respectively.

$$[29] \quad m_5 = \int_0^{\beta} (\text{Integrand same as eqn. no. [19]})$$

$$[30] \quad m_6 = \int_0^{\delta} (\text{Integrand same as eqn. no. [25]})$$

$$[31] \quad m_7 = \int_0^{\nu} (\text{Integrand same as eqn. no. [20]})$$

$$[32] \quad m_8 = \int_0^{\pi/2 - \beta - \nu - \delta} (\text{Integrand same as eqn. no. [27]})$$

$$[33] \quad \therefore v_s = m_1 + m_5 + m_6 - m_3 - m_7 - m_8$$

Case Va - Figure 6

m_1, m_2, m_3, m_4 = same as eqn. nos. [12], [13], [14], and [15], respectively.

$$[34] \quad m_5 = \int_0^{\delta} (\text{Integrand same as eqn. no. [19]})$$

$$[35] \quad \text{and } m_6 = \int_0^{\pi/2 - \delta} (\text{Integrand same as eqn. no. [20]})$$

$$[36] \quad \therefore v_s = m_1 + m_2 + m_5 - m_3 - m_4 - m_6$$

Case Vb - Figure 6

m_1, m_2, m_3 = same as eqn. nos. [12], [13], and [14], respectively.

$$[37] \quad m_4 = (\bar{x} - t/2)t \sin \alpha (l_4 - x') [l_3^2 - (l_4 - x')^2/3] / (2I_{\min})$$

$$[38] \quad m_{4a} = (\bar{x} - t/2)q_{c5}x' \left(1 + \frac{x'^2}{3c'} + \frac{x'b'}{2c'}\right)$$

$$\text{where } b' = -2l_4$$

$$\text{and } c' = 2q_{c5}I_{\min}/(t \sin \alpha)$$

$$[39] \quad m_5 = \int_0^{\pi/2} (\text{Integrand same as eqn. no. [19]})$$

$$[40] \quad \therefore v_s = m_1 + m_2 + m_{4a} + m_5 - m_3 - m_4$$

Case VIa - Figure 7

m_1, m_2, m_3, m_4 = same as eqn. nos. [12], [13], [14] and [15], respectively.

$$[41] \quad m_5 = \int_0^{\delta} \left\{ r_o^2 q_{c1} + \frac{r_o^3 t d \cos(\pi/2 + \alpha + \phi)}{I_{\min}} \theta - \frac{2r_o^4 t}{I_{\min}} \sin \theta/2 \sin(\alpha + \theta/2) \right.$$

$$\left. - r_o dq_{c1} \cos(\pi + \phi - \theta) - \frac{r_o^2 d^2 t}{I_{\min}} \cos(\pi/2 + \alpha + \phi) \theta \cos(\pi + \phi - \theta) \right.$$

$$\left. + \frac{2r_o^3 t d}{I_{\min}} [\sin \theta/2 \sin(\alpha + \theta/2) \cos(\pi + \phi - \theta)] \right\} d\theta$$

$$[42] \quad \text{and } m_6 = \int_0^{\pi/2 - \delta} \left\{ r_o^2 q_{c2} + \frac{r_o^3 t d \cos(\pi/2 + \alpha + \phi)}{I_{\min}} \theta - \frac{2r_o^4 t}{I_{\min}} \sin \theta/2 \sin(\pi/2 - \alpha + \theta/2) \right.$$

$$\left. - r_o dq_{c2} \sin(-\theta - \phi) - \frac{r_o^2 d^2 t \cos(\pi/2 + \alpha + \phi)}{I_{\min}} \theta \sin(-\theta - \phi) \right.$$

$$\left. + \frac{2r_o^3 t d}{I_{\min}} [\sin \theta/2 \sin(\pi/2 - \alpha + \theta/2) \sin(-\theta - \phi)] \right\} d\theta$$

$$[43] \quad \therefore v_s = m_1 + m_2 + m_5 - m_3 - m_4 - m_6$$

Case VIb - Figure 7

$m_1, m_2, m_3, m_4, m_{4a}$ = same as eqn. nos. [12], [13], [14], [37] and [38], respectively.

$$[44] \quad m_5 = \int_0^{\pi/2} (\text{Integrand same as eqn. no. [41]})$$

$$[45] \quad \therefore v_s = m_1 + m_2 + m_{4a} + m_5 - m_3 - m_4$$

Case VIIa - Figure 8

m_1, m_3, m_4 = same as eqn. nos. [22], [14] and [15], respectively.

$$[46] \quad m_5 = \int_0^\beta \{ r_o^2 q_{c1} + r_o dq_{c1} \sin(\pi/2 + \phi - \theta) - \frac{r_o^3 td \sin(\alpha + \phi)}{I_{\min}} \theta \\ - \frac{2r_o^4 t}{I_{\min}} \sin \theta/2 \sin(\alpha + \theta/2) - \frac{r_o^2 d^2 t \sin(\alpha + \phi)}{I_{\min}} \theta \sin(\pi/2 + \phi - \theta) \\ - \frac{2r_o^3 td}{I_{\min}} [\sin \theta/2 \sin(\alpha + \theta/2) \sin(\pi/2 + \phi - \theta)] \} d\theta$$

$$[47] \quad m_6 = \int_0^\delta \{ r_o^2 q_{c3} + \frac{r_o^3 dt \cos(\pi/2 + \alpha + \phi)}{I_{\min}} \theta - \frac{2r_o^4 t}{I_{\min}} \sin \theta/2 \sin(\alpha + \beta + \theta/2) \\ - r_o dq_{c3} \cos(\pi + \phi - \beta - \theta) - \frac{r_o^2 d^2 t \cos(\pi/2 + \alpha + \phi) \cos(\pi + \phi - \beta - \theta)}{I_{\min}} \theta \\ + \frac{2r_o^3 td}{I_{\min}} [\sin \theta/2 \sin(\alpha + \theta/2 + \beta) \cos(\pi + \phi - \beta - \theta)] \} d\theta$$

$$[48] \quad \text{and } m_7 = \int_0^{\pi/2 - \beta - \delta} (\text{Integrand same as eqn. no. [42]})$$

$$[49] \quad \therefore v_s = m_1 + m_5 + m_6 - m_3 - m_4 - m_7$$

Case VIIb - Figure 8

m_1, m_3, m_4, m_{4a} = same as eqn. nos. [22], [14], [37] and [38], respectively.

$$[50] \quad m_5 = \int_0^\beta (\text{Integrand same as eqn. no. [46]})$$

$$[51] \quad \text{and } m_6 = \int_0^{\pi/2 - \beta} (\text{Integrand same as eqn. no. [47]})$$

$$[52] \quad \therefore v_s = m_1 + m_{4a} + m_5 + m_6 - m_3 - m_4$$

Case VIIIa - Figure 9

m_1, m_3, m_4 = same as eqn. nos. [22], [14] and [15], respectively.

$$[53] \quad m_5 = \int_0^8 \quad (\text{Integrand same as eqn. no. [19]})$$

$$[54] \quad m_6 = \int_0^{\delta} \quad (\text{Integrand same as eqn. no. [25]})$$

$$[55] \quad \text{and } m_7 = \int_0^{\pi/2-\delta} \quad (\text{Integrand same as eqn. no. [20]})$$

$$[56] \quad \therefore v_s = m_1 + m_5 + m_6 - m_3 - m_4 - m_7$$

Case VIIIb - Figure 9

m_1, m_3, m_4, m_{4a} = same as eqn. nos. [22], [14], [37] and [38], respectively.

$$[57] \quad m_5 = \int_0^8 \quad (\text{Integrand same as eqn. no. [19]})$$

$$[58] \quad \text{and } m_6 = \int_0^{\pi/2-\delta} \quad (\text{Integrand same as eqn. no. [25]})$$

$$[59] \quad \therefore v_s = m_1 + m_{4a} + m_5 + m_6 - m_3 - m_4$$

Case IXa - Figure 10

m_1, m_2, m_3, m_4 = same as eqn. nos. [12], [13], [14] and [15], respectively.

$$[60] \quad m_5 = \int_0^{\delta} \quad (\text{Integrand same as eqn. no. [16]})$$

$$[61] \quad \text{and } m_6 = \int_0^{\pi/2-\delta} \quad (\text{Integrand same as eqn. no. [17]})$$

$$[62] \quad \therefore v_s = m_1 + m_2 + m_5 - m_3 - m_4 - m_6$$

Case IXb - Figure 10

$m_1, m_2, m_3, m_4, m_{4a}$ = same as eqn. nos. [12], [13], [14], [37] and [38], respectively.

$$[63] \quad \text{and } m_5 = \int_0^{\pi/2} (\text{Integrand same as eqn. no. [16]})$$

$$[64] \quad \therefore v_s = m_1 + m_2 + m_{4a} + m_5 - m_3 - m_4$$

(b) u-coordinate (Bending about u-u axis) (Ref. Fig. 11 to 13)

Depending on the location where the u-u axis intersects the centre-line of the cross-section, one of the following cases will be applicable.

Case I - Figure 11 [u-u axis intersects the centre-line of the cross-section just at the beginning of curve]

$$[65] \quad m_1 = \frac{(\bar{y} - t/2)t c_1^2}{2I_{\max}} \left[\frac{\bar{y} - t/2}{\cos^2 \alpha} + \left(l_1 - \frac{c_1}{3} \right) \sin \alpha \right]$$

$$[66] \quad m_2 = (\bar{x} - t/2)t \cos \alpha c_2^3 / (3I_{\max})$$

$$[67] \quad \text{and } m_3 = \int_0^{\pi/2} \left\{ r_o^2 q_{c6} + r_o dq_{c6} \sin(\theta + \phi) + \frac{r_o^3 t d \cos(\alpha + \phi)}{I_{\max}} \theta \right. \\ \left. + \frac{r_o^2 d^2 \sin(\theta + \phi) \theta \cos(\alpha + \phi)}{I_{\max}} + \frac{2r_o^4 t}{I_{\max}} \sin \theta/2 \sin(\pi/2 - \alpha - \theta/2) \right. \\ \left. + \frac{2r_o^3 t d}{I_{\max}} [\sin \theta/2 \sin(\theta + \phi) \sin(\pi/2 - \alpha - \theta/2)] \right\} d\theta$$

$$[68] \quad \therefore u_s = m_1 + m_2 + m_3$$

Case II - Figure 12 [u-u axis intersects the centre-line of the cross-section in the curved portion]

m_1 = same as eqn. no. [65].

$$[69] \quad m_2 = (\bar{x} - t/2)t \cos \alpha c_2^2 (l_5 - c_2/3) / (2I_{\max})$$

$$[70] \quad m_3 = \int_0^{\beta} (\text{Integrand same as eqn. no. [67]})$$

$$[71] \quad \text{and } m_4 = \int_0^{\pi/2-\beta} \left\{ r_o^2 q_{c7} - \frac{r_o^3 t d \cos(\alpha + \phi)}{I_{\max}} \theta + \frac{2r_o^4 t}{I_{\max}} \sin \theta/2 \sin(\alpha - \theta/2) \right. \\ \left. + r_o^2 q_{c7} d \sin(\theta + \phi) - \frac{r_o^2 d^2 t \cos(\alpha + \phi)}{I_{\max}} \theta \sin(\theta + \phi) \right. \\ \left. + \frac{2r_o^3 t d}{I_{\max}} [\sin(\theta + \phi) \sin \theta/2 \sin(\alpha - \theta/2)] \right\} d\theta$$

$$[72] \quad \therefore u_s = m_1 + m_2 + m_3 + m_4.$$

However, if $d_1 < 0$, the eqn. nos. [70] and [71] shall be replaced by eqn. nos. [73] and [74], respectively.

$$[73] \quad m_3 = \int_0^{\theta} \{ r_o^2 q_{c6} - r_o d q_{c6} \sin(\theta + \phi) - \frac{r_o^3 t d \cos(\alpha + \phi)}{I_{\max}} \theta + \frac{r_o^2 d^2 t \sin(\theta + \phi) \theta \cos(\alpha + \phi)}{I_{\max}} + \frac{2r_o^4 t}{I_{\max}} [\sin \theta/2 \sin(\pi/2 - \alpha - \theta/2)] - \frac{2r_o^3 t d}{I_{\max}} [\sin \theta/2 \sin(\theta + \phi) \sin(\pi/2 - \alpha - \theta/2)] \} d\theta$$

$$[74] \quad \text{and } m_4 = \int_0^{\pi/2 - \theta} \{ r_o^2 q_{c7} + \frac{r_o^3 t d \cos(\alpha + \phi)}{I_{\max}} \theta - r_o q_{c7} d \sin(\theta + \phi) - \frac{r_o^2 d^2 t \cos(\alpha + \phi)}{I_{\max}} \theta \sin(\theta + \phi) + \frac{2r_o^4 t}{I_{\max}} [\sin \theta/2 \sin(\alpha - \theta/2)] - \frac{2r_o^3 t d}{I_{\max}} [\sin(\theta + \phi) \sin \theta/2 \sin(\alpha - \theta/2)] \} d\theta$$

Case III - Figure 13 [u-u axis intersects the centre-line of the cross-section in the straight portion of the long leg]

$$m_1 = \text{same as eqn. no. [65]}$$

$$[75] \quad m_2 = -(\bar{x} - t/2) t \cos \alpha \ell_6^3 / (3I_{\max})$$

$$[76] \quad m_3 = (\bar{x} - t/2) \ell_5 [t \cos \alpha \ell_5^2 / (3I_{\max}) + q_{c8}]$$

$$[77] \quad \text{and } m_4 = \int_0^{\pi/2} (\text{Integrand same as eqn. no. [67]})$$

$$[78] \quad \therefore u_s = m_1 + m_2 + m_3 + m_4$$

8. Polar moment of inertia about the shear centre

$$[79] \quad I_{ps} = I_{\max} + I_{\min} + \text{Area}(u_s^2 + v_s^2)$$

where u_s and v_s are the computed u- and v-coordinates of the shear centre.

9. Warping constant (Ref. Fig. 14)

The following are the basic expressions used in the calculation of the magnitude of warping constant:

$$[80] \quad w_{s_1} = - \int_0^s r_1 ds \quad 0 \leq s \leq c_1$$

$$[81] \quad w_{s_2} = -r_1 c_1 - \int_0^\theta r_2 (x + t/2) d\theta \quad 0 \leq \theta \leq \pi/2$$

$$[82] \quad w_{s_3} = -r_1 c_1 - (x + t/2)^2 \pi/2 - r' (x + t/2) [\cos(v + \pi/2) - \cos v] - \int_0^s r_3 ds$$

$$0 \leq s \leq c_2$$

$$[83] \quad w_s = \frac{1}{[c_1 + c_2 + \pi(x + t/2)/2]} \left[\int_0^{c_1} w_{s_1} ds + \int_0^{\pi/2} w_{s_2} (x + t/2) d\theta + \int_0^{c_2} w_{s_3} ds \right]$$

$$= \frac{1}{[c_1 + c_2 + \pi(x + t/2)/2]} \left\{ -r_1 c_1 [c_1 + \pi(x + t/2)]/2 + c_2 (c_3 - r_3 c_2/2) \right.$$

$$\left. - \frac{\pi^2 (x + t/2)^3}{8} - r' (x + t/2)^2 [\sin(v + \pi/2) - \sin v - \pi/2 \cos v] \right\}$$

$$\text{where } c_3 = -r_1 c_1 - (x + t/2)^2 \pi/2 - r' (x + t/2) [\cos(v + \pi/2) - \cos v]$$

[84] and finally warping constant,

$$C_w = \int (w_s^- - w_s)^2 t ds$$

$$= \int_0^{c_1} (w_s^- - w_{s_1})^2 t ds + \int_0^{c_2} (w_s^- - w_{s_3})^2 t ds + \int_0^{\pi/2} (w_s^- - w_{s_2})^2 t (x + t/2) d\theta$$

which becomes

$$\begin{aligned}
 & t[w_s^2 + r_1^2 c_1^2/3 + w_s r_1 c_1]c_1 + t[w_s^2 + c_3^2 + r_3^2 c_2^2/3 \\
 & - c_3 r_3 c_2 - 2w_s c_3 + w_s r_3 c_2]c_2 + \{[w_s^2 + r_1^2 c_1^2 + r'^2 (r + t/2)^2 \\
 & \cos^2 v - 2r_1 c_1 r' (r + t/2) \cos v + 2w_s r_1 c_1 - 2w_s r' (r + t/2) \cos v] \\
 & + (r + t/2)^4 \pi^3/24 + r'^2 (r + t/2)^2 (\pi/4 - .5 \sin 2v) - [-r_1 c_1 (r + t/2)^2 \\
 & + r' (r + t/2)^3 \cos v - w_s (r + t/2)^2] \pi^2/4 - [-2r_1 c_1 r' (r + t/2) + \\
 & 2r'^2 (r + t/2)^2 \cos v - 2w_s r' (r + t/2)] [\sin(v + \pi/2) - \sin v] + \\
 & 2(r + t/2)^3 r' [.5 \pi \sin(v + \pi/2) + \cos(v + \pi/2) - \cos v] \} t(r + t/2)
 \end{aligned}$$

10. β_1 and β_2 (Ref. Fig. 15 and 16)

(a) For long leg only (Ref. Fig. 15)

$$[85] \quad x_{\ell\ell} = [x'_\beta - p_\ell] \cos(\pi/2 - \alpha) - q_1 - y_1 \cos(\pi/2 - \alpha)$$

$$[86] \quad y_{\ell\ell} = [x'_\beta - p_\ell] \sin(\pi/2 - \alpha) - y_1 \sin(\pi/2 - \alpha)$$

$$[87] \quad \text{and } dA = tdp_\ell$$

where p_ℓ varies from 0 to $(x'_\beta - r_o)$

(b) For short leg only (Ref. Fig. 15)

$$[88] \quad x_{s\ell} = [y'_\beta - p_s] \cos \alpha - y_1 \cos(\pi/2 - \alpha) - q_1$$

$$[89] \quad y_{s\ell} = -\{(y'_\beta - p_s) \sin \alpha + y_1 \sin(\pi/2 - \alpha)\}$$

$$[90] \quad \text{and } dA = tdp_s$$

where p_s varies from 0 to $(y'_\beta - r_o)$

(c) For curved portion only (Ref. Fig. 16)

$$[91] \quad x_{cp} = -[\bar{x}' - r_o + r_o \sin \theta]$$

$$[92] \quad y_{cp} = -[\bar{y}' - r_o + r_o \cos \theta]$$

$$[93] \quad x_c = y_{cp} \cos \alpha + x_{cp} \sin \alpha$$

$$[94] \quad y_c = x_{cp} \cos \alpha - y_{cp} \sin \alpha$$

$$[95] \quad \text{and } dA = r_o t d\theta$$

where θ varies from 0 to $\pi/2$

Finally, β_1 and β_2 are given by the following expressions:

$$[96] \quad \beta_1 = \left(\int_0^{\bar{y}' - r_o} (y_{ll}^3 + x_{ll}^2 y_{ll}) t dp_l + \int_0^{\bar{y}' - r_o} (y_{sl}^3 + x_{sl}^2 y_{sl}) t dp_s \right. \\ \left. + \int_0^{\pi/2} (y_c^3 + x_c^2 y_c) r_o t d\theta \right) / I_{\max} - 2v_s$$

$$[97] \quad \text{and } \beta_2 = \left(\int_0^{\bar{x}' - r_o} (x_{ll}^3 + y_{ll}^2 x_{ll}) t dp_l + \int_0^{\bar{x}' - r_o} (x_{sl}^3 + y_{sl}^2 x_{sl}) t dp_s \right. \\ \left. + \int_0^{\pi/2} (x_c^3 + y_c^2 x_c) r_o t d\theta \right) / I_{\min} - 2u_s$$

The integrals are evaluated by adaptive quadrature technique using Simpson's

rule [Ref.: Johnson, L.W. and Riess, R.D. 1982. Numerical Analysis.

Addison-Wesley Publishing Company, Don Mills, Ontario. pp. 313-317].

List of Symbols

d = distance between the centre of curvature and the centroid

d_1 = $\bar{y} - (r + t)$

d_2 = $\bar{x} - (r + t)$

q_{cl} = shear flow at the beginning of the curve from the short leg (bending about v-v axis)

- q_{c2} = shear flow at the beginning of the curve from the long leg (bending about v-v axis)
- q_{c3} = shear flow at the point where the v-v axis intersects the short leg, if it is in the curved portion, i.e. at the end of angle β [Ref. Fig. 5] (bending about v-v axis)
- q_{c4} = shear flow at the point where the v-v axis intersects the long leg, if it is in the curved portion, i.e., at the end of angle γ [Ref. Fig. 5] (bending about v-v axis)
- q_{c5} = shear flow at the end of the curve from the short leg (bending about v-v axis)
- q_{c6} = shear flow at the beginning of the curve from the short leg (bending about u-u axis)
- q_{c7} = shear flow at the beginning of the curve from the long leg (bending about v-v axis)
- q_{c8} = shear flow at the end of the curve from the short leg (bending about u-u axis)
- r_o = $r + t/2$
- x' = distance of the point of zero shear flow from the end of the curve, if it lies in the straight portion of the long leg

Table I

Case	Figure	Coordinates of centre of curvature		v-v axis intersects	Location of point of zero shear flow		Remarks
		x-coord.	y-coord.		long leg	short leg	
Equal leg angles							
I	2	-	-	straight portion	curved portion		
II	3	+	+	"	"		"
III	4	+	+	curved portion	curved portion		
Unequal leg angles							
IV	5	+	+	"	"		The angle $\delta + \beta$ from short leg gives the point of zero shear flow
Va	6	+	+	straight portion	straight portion		The angle δ from short leg gives the point of zero shear flow
Vb	6	+	+	"	"		
VIa	7	+	-	"	curved portion		"
VIIb	7	+	-	"	straight portion		-
VIIa	8	+	-	"	curved portion		The angle $\delta + \beta$ from short leg gives the point of zero shear flow
VIIIb	8	+	-	"	straight portion		-
VIIIa	9	+	+	"	curved portion		"
VIIIf	9	+	+	"	straight portion		-
IXa	10	-	-	straight portion	curved portion		The angle δ from short leg gives the point of zero shear flow
IXb	10	-	-	"	straight portion		-

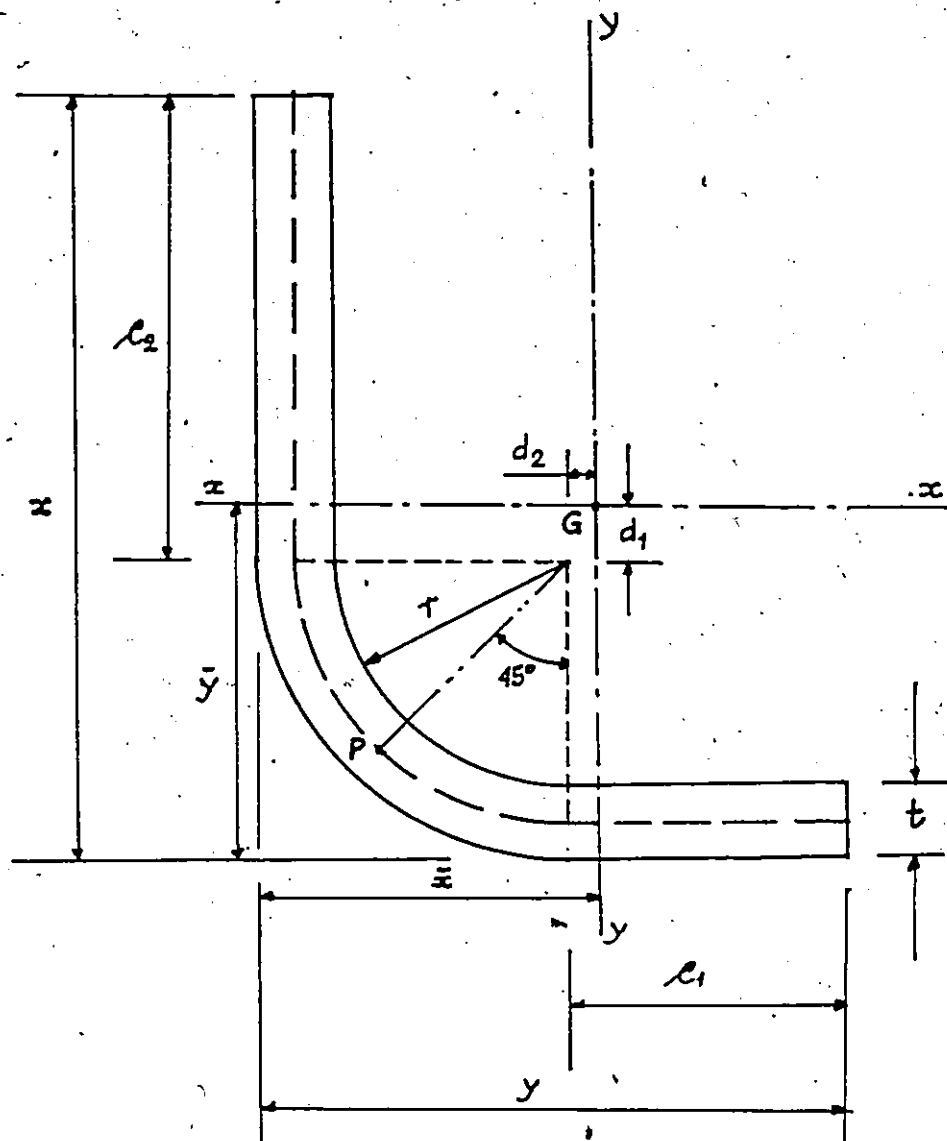


Figure 1

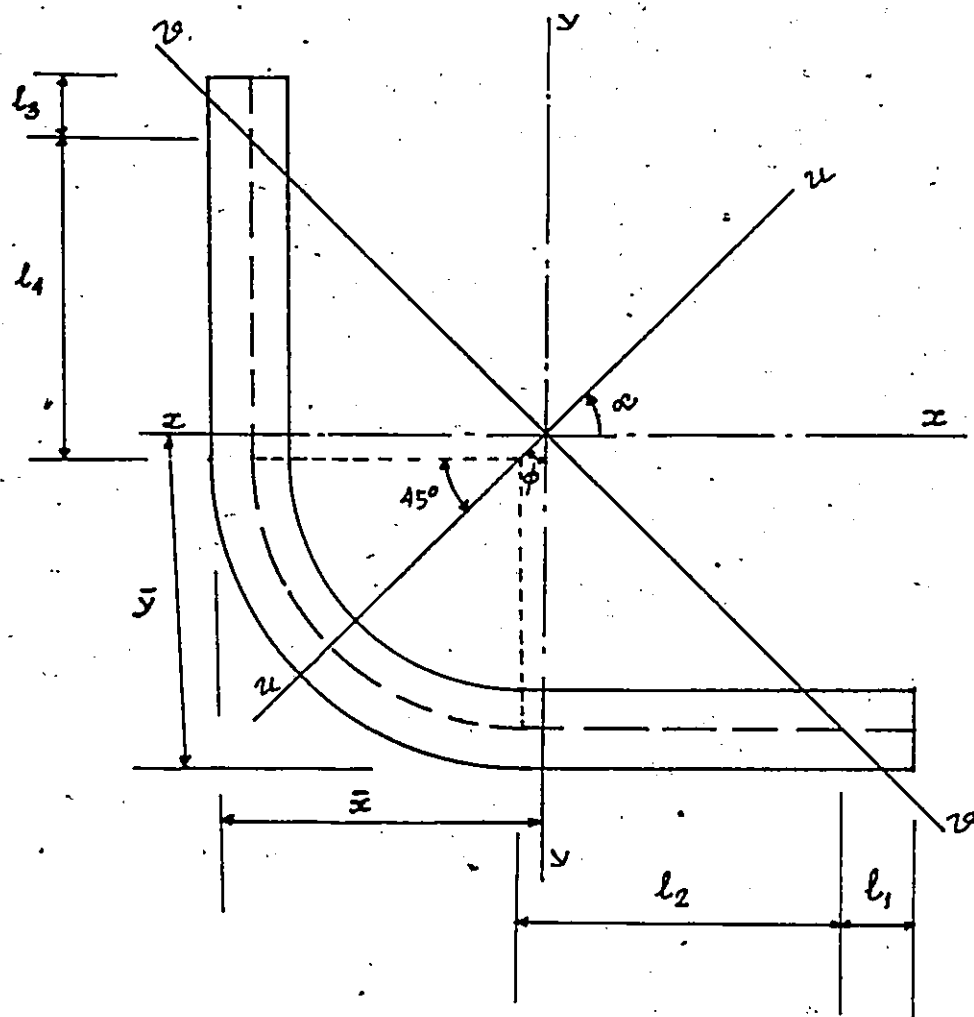


Figure 2

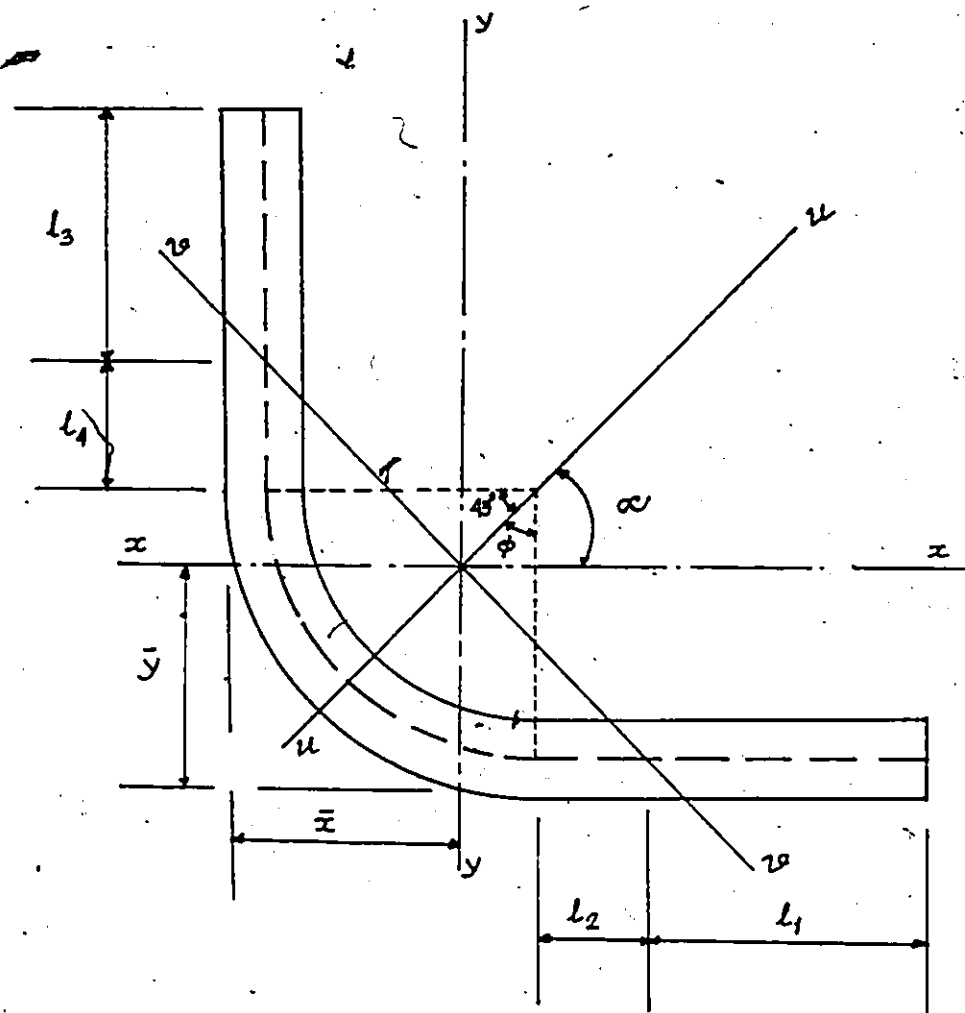


Figure 3

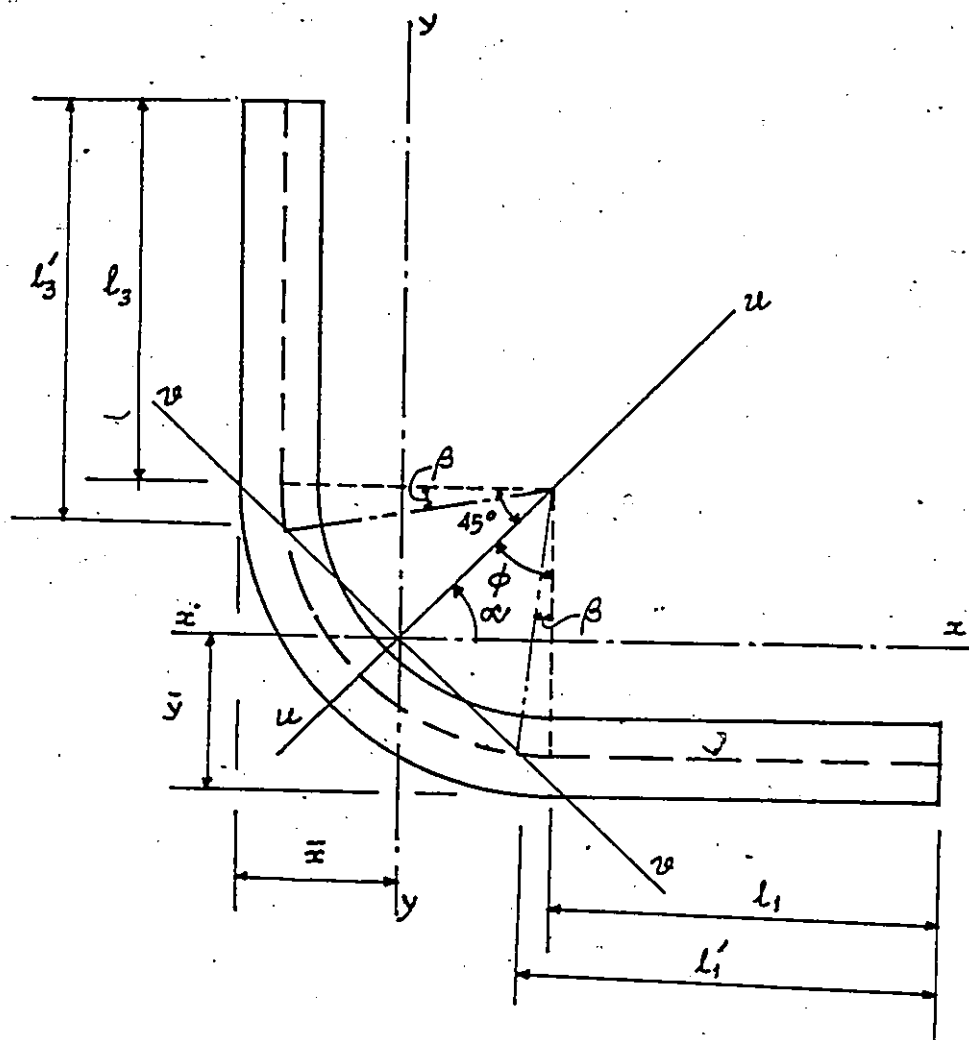


Figure 4

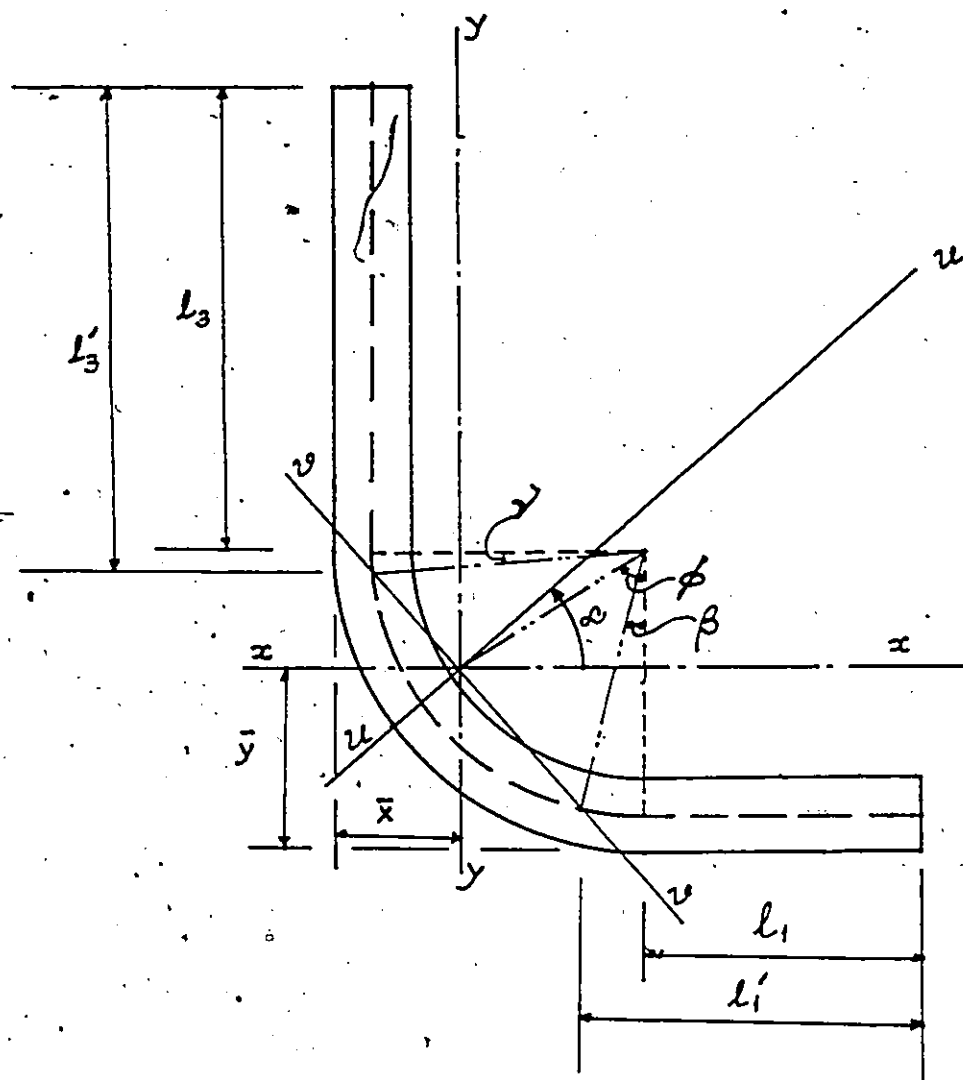


Figure 5

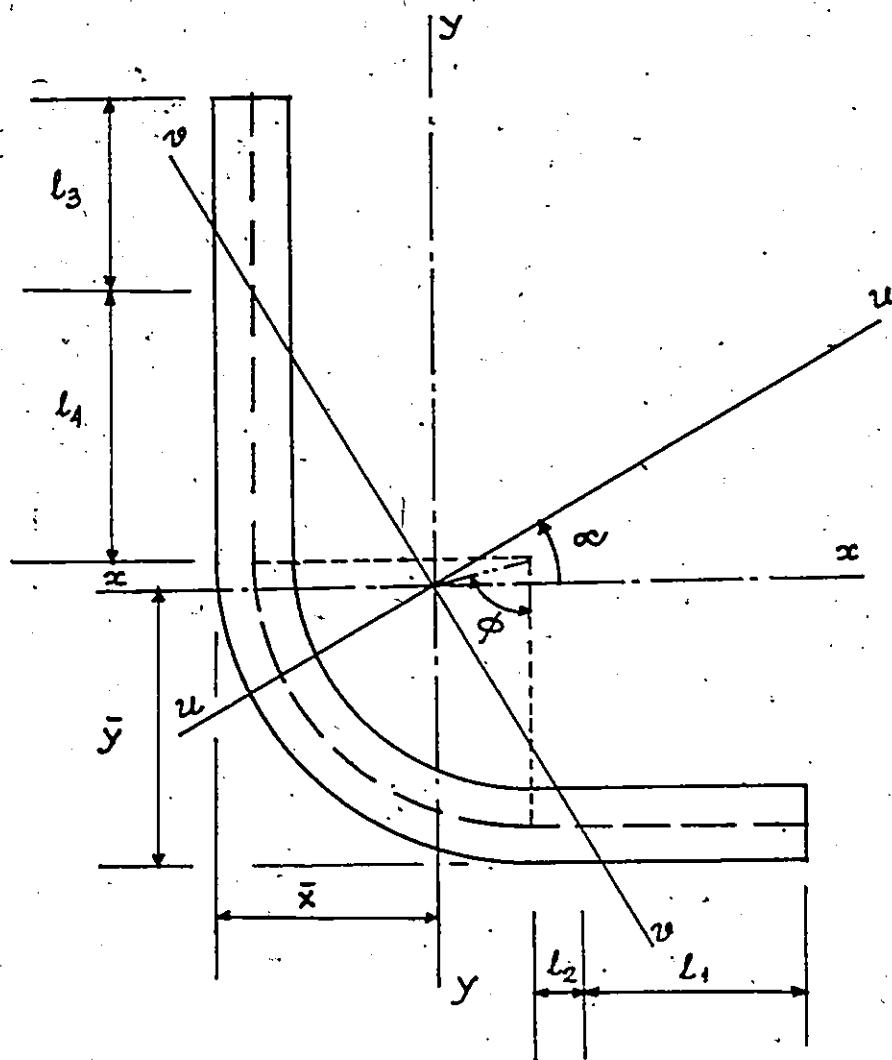


Figure 6

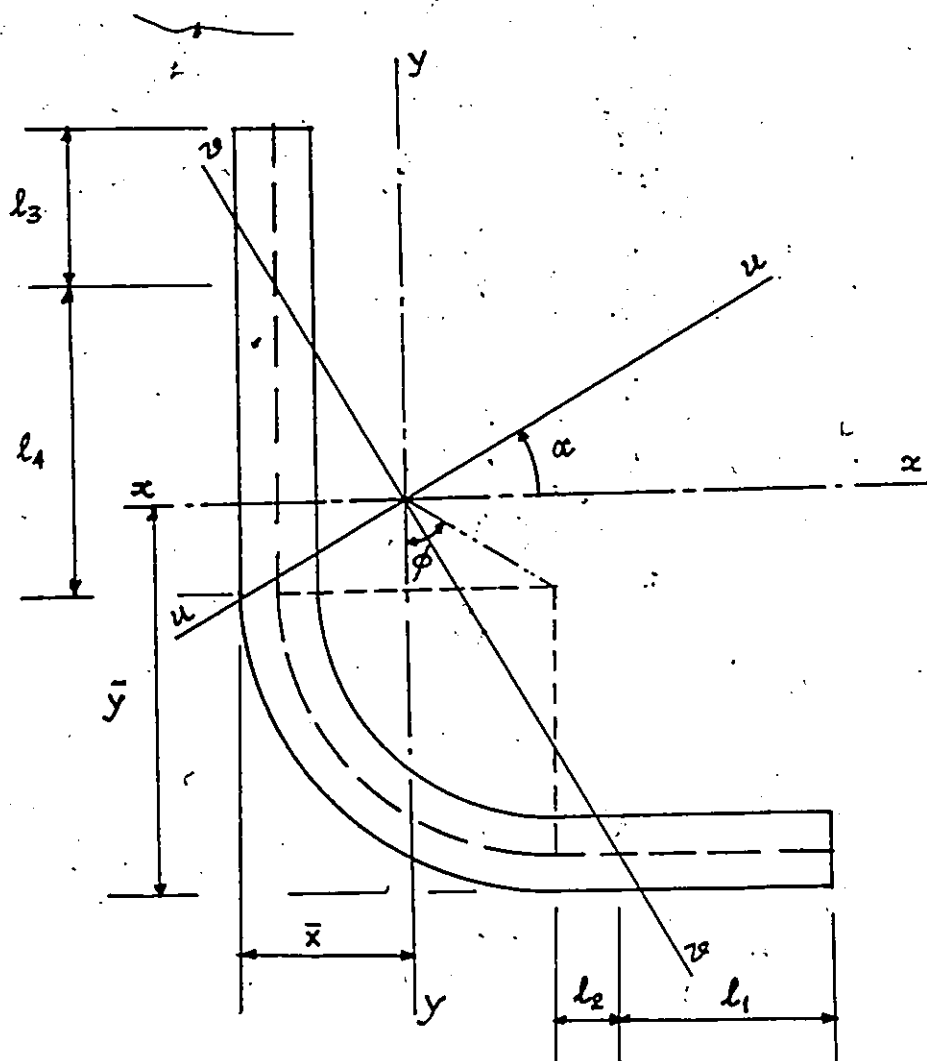


Figure 7

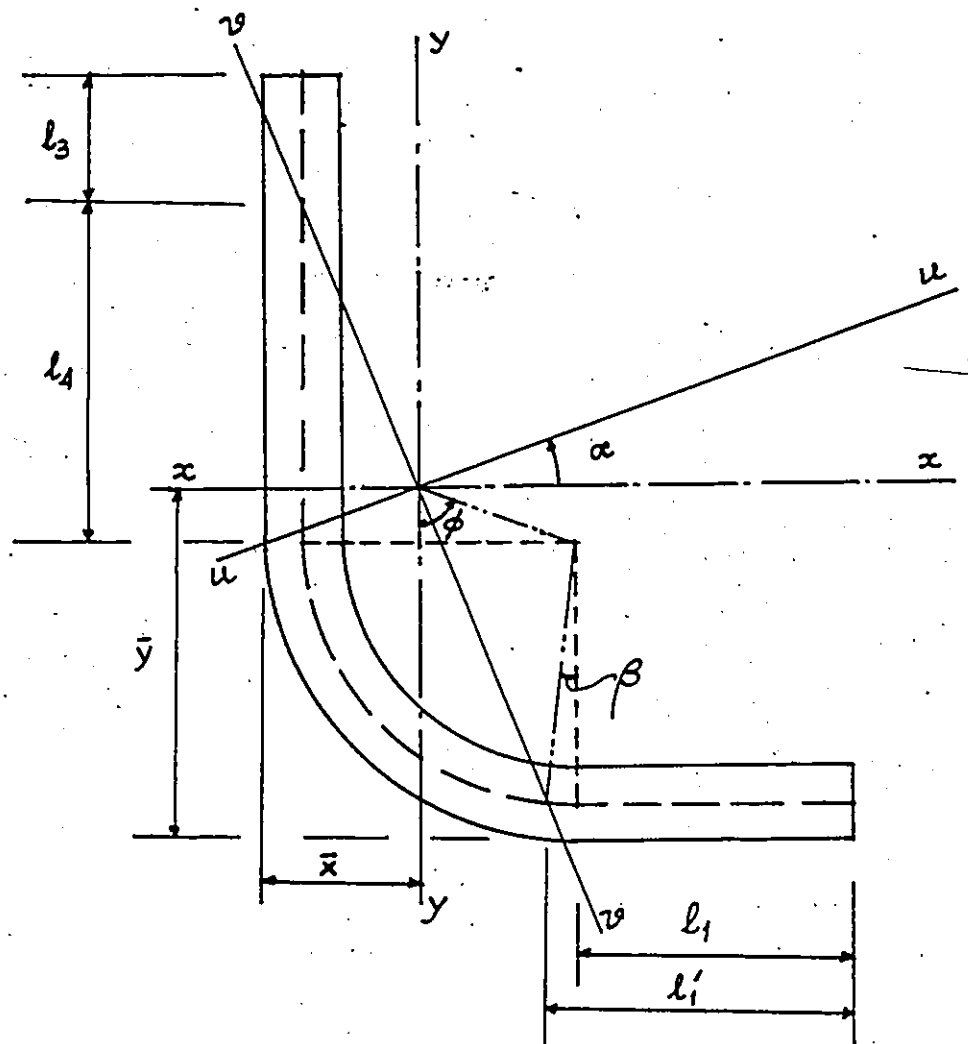


Figure 8

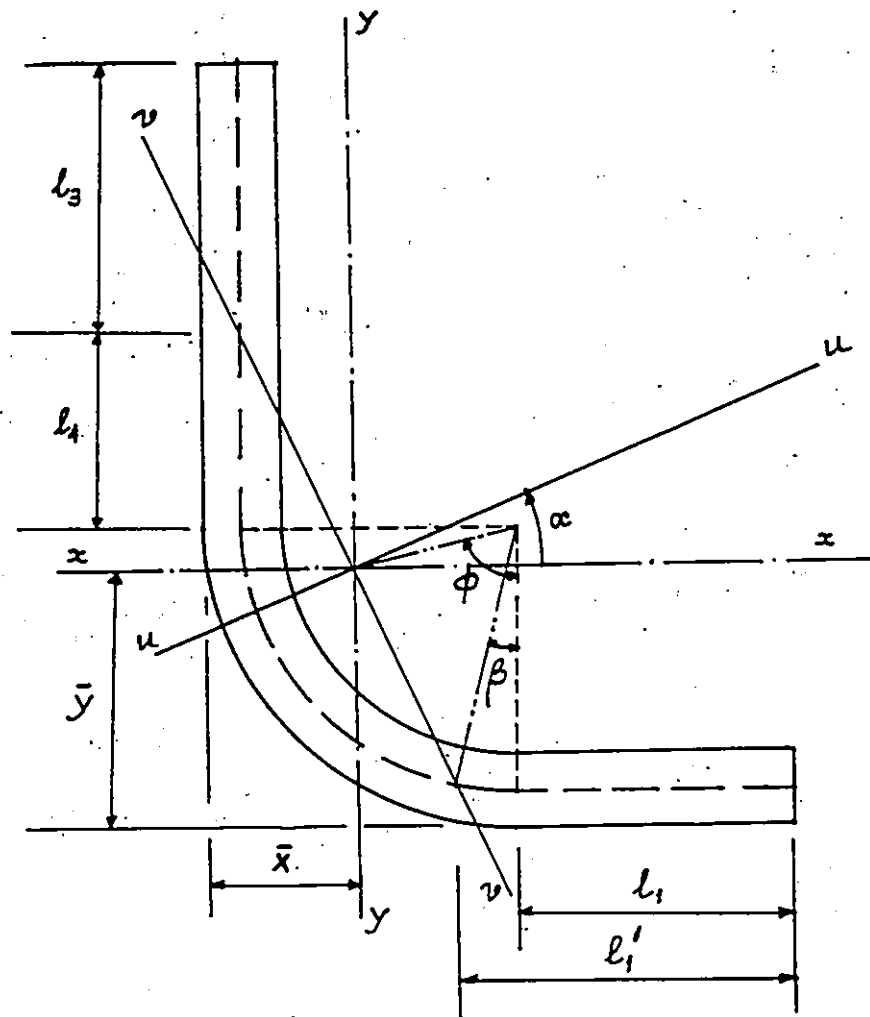


Figure 9

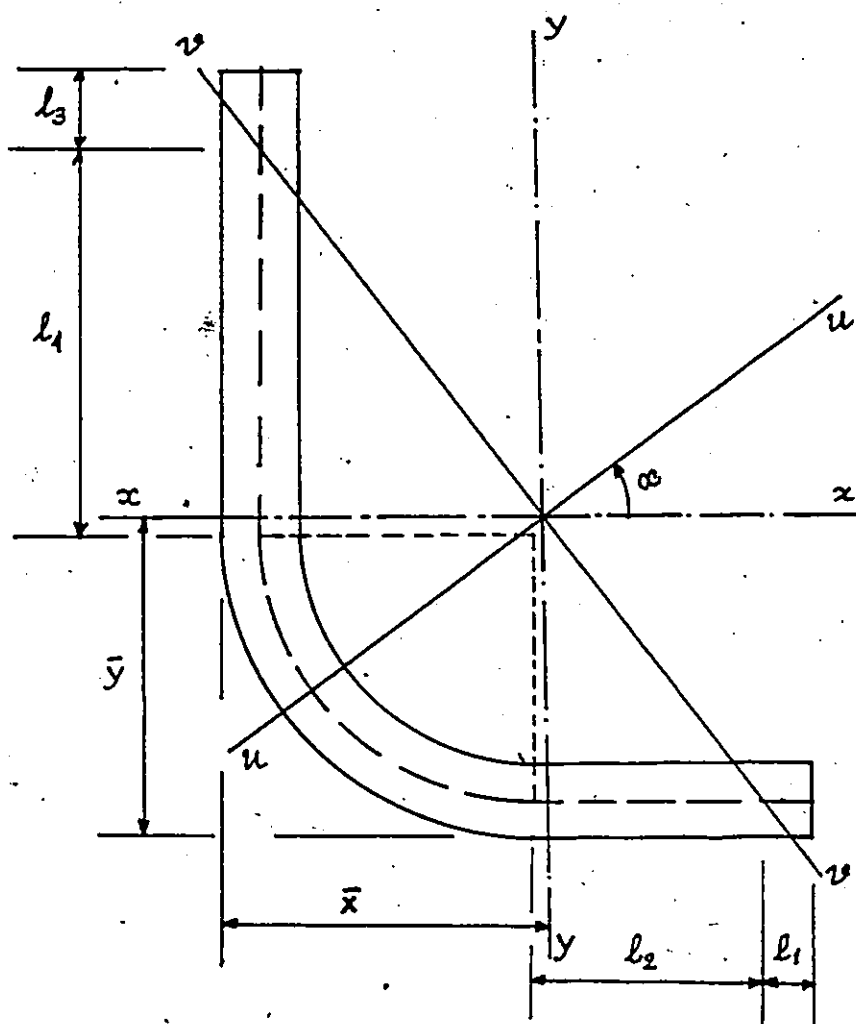


Figure 10

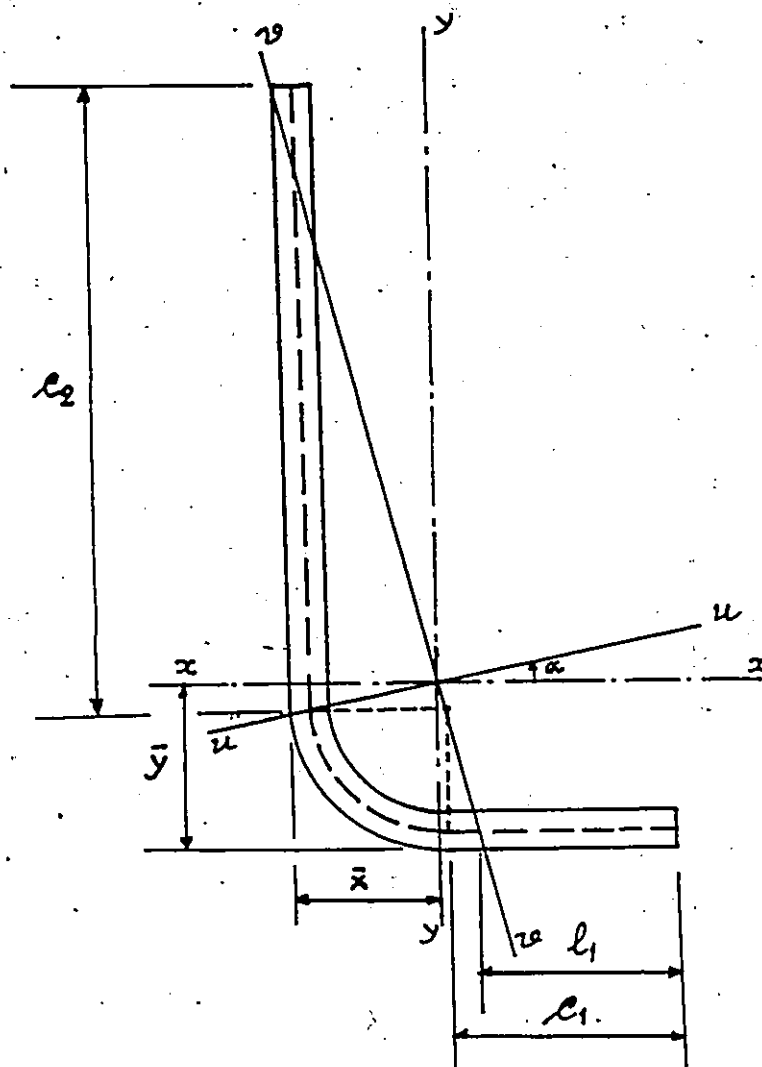


Figure 11

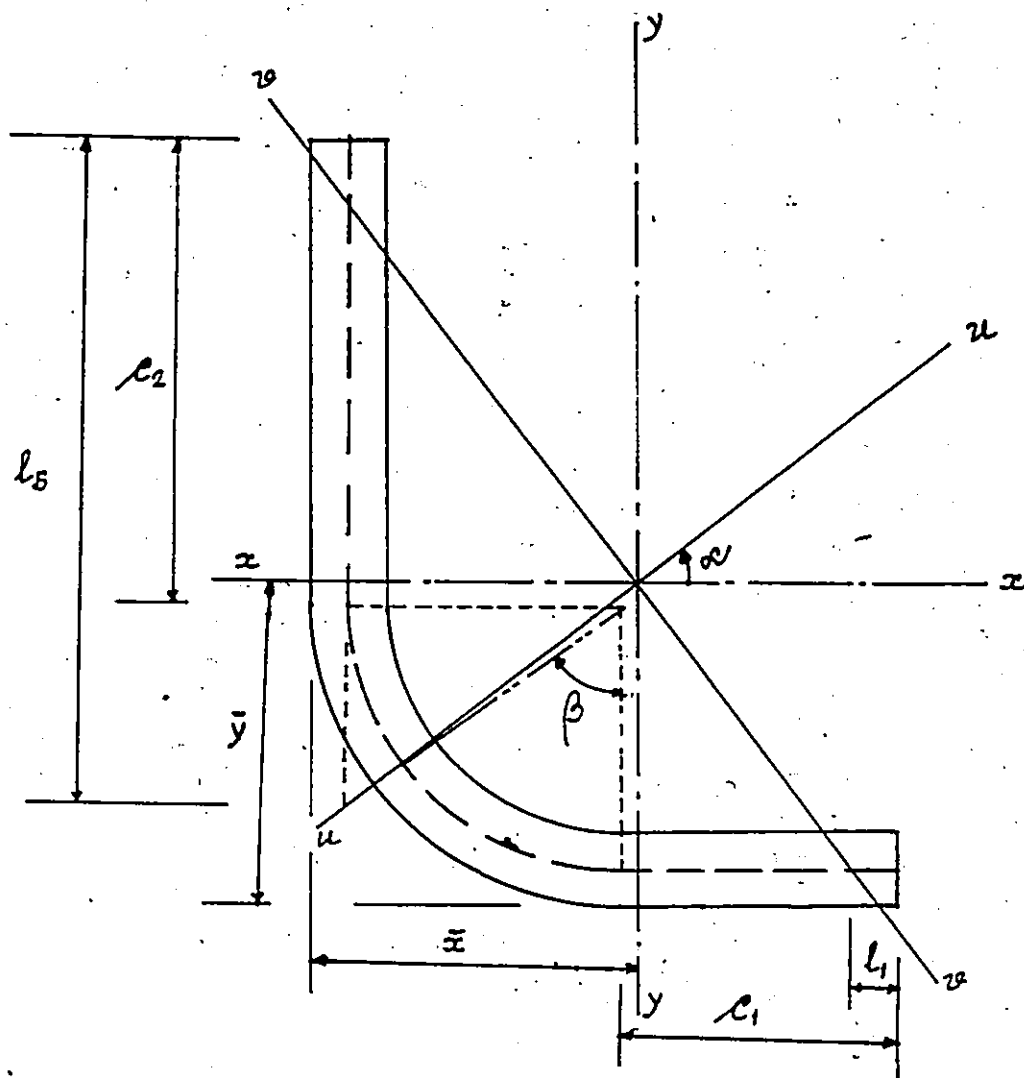


Figure 12

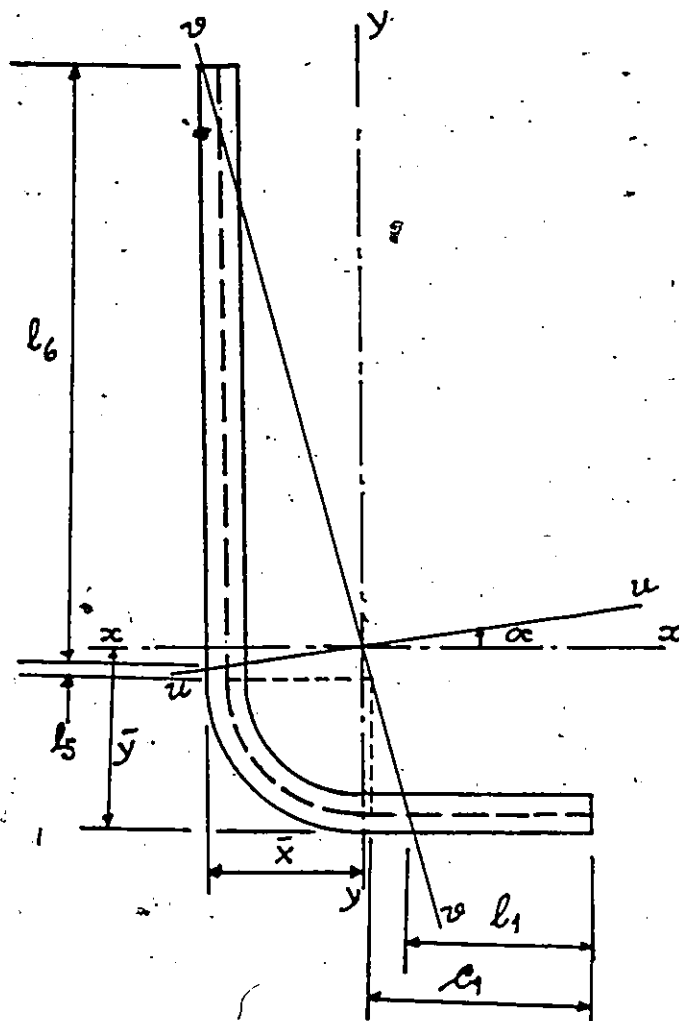


Figure 13

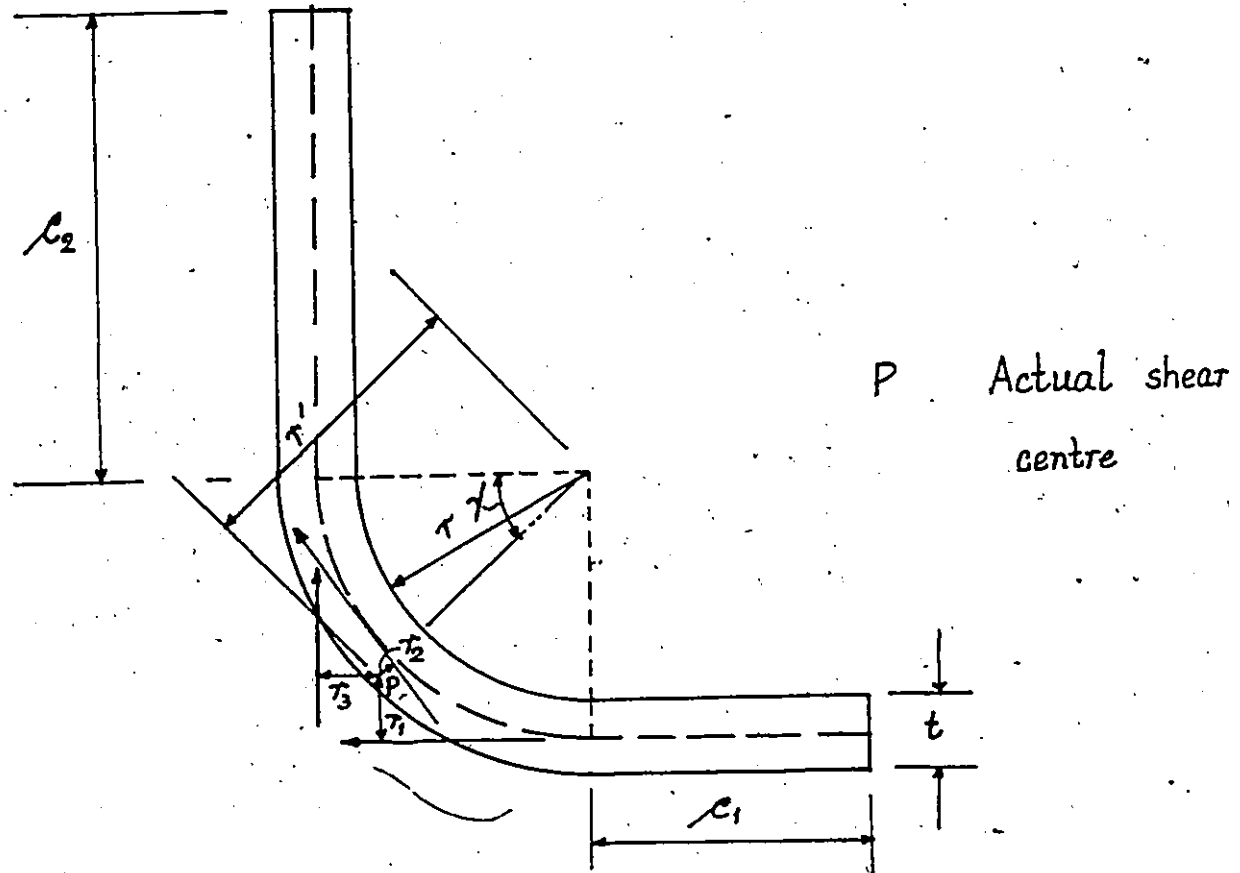


Figure 14

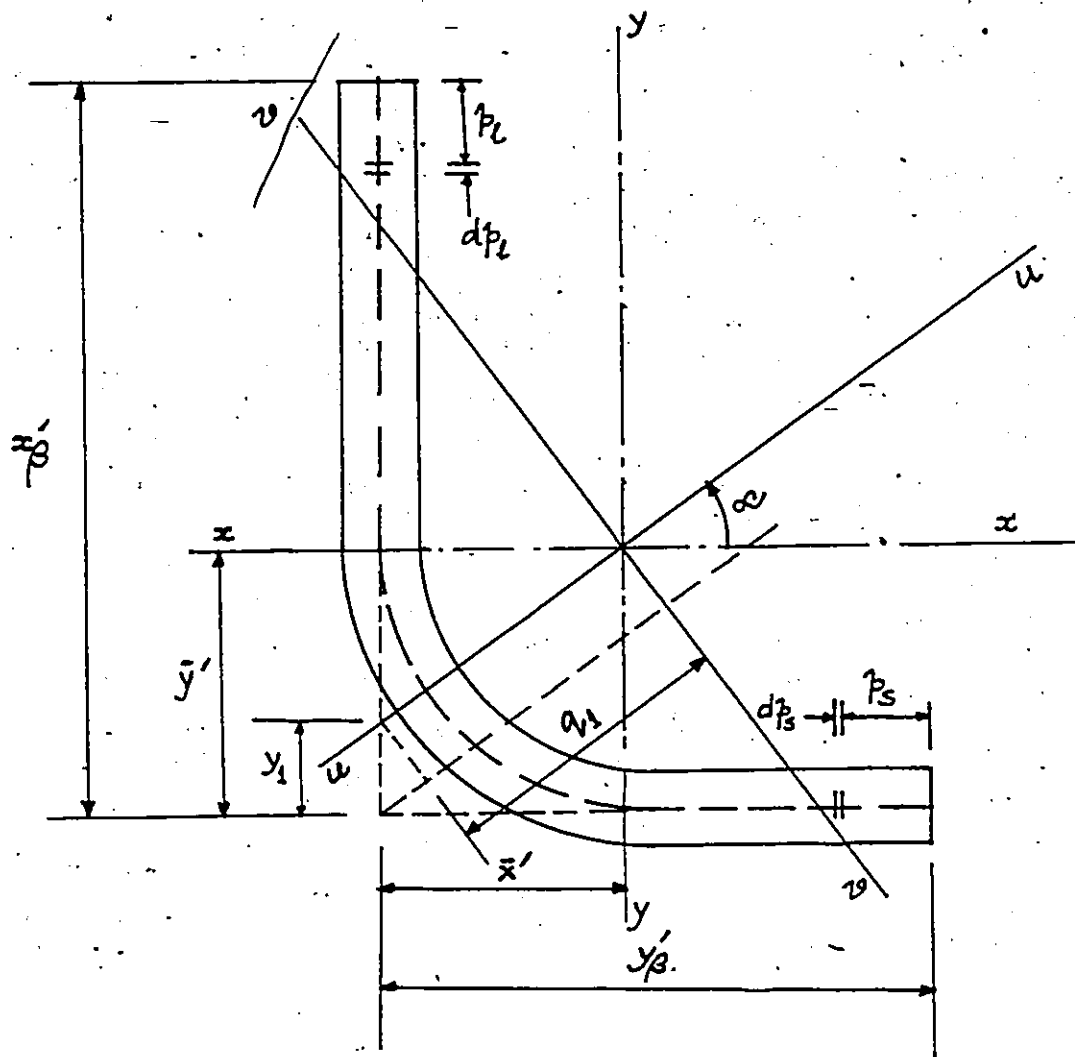


Figure 15

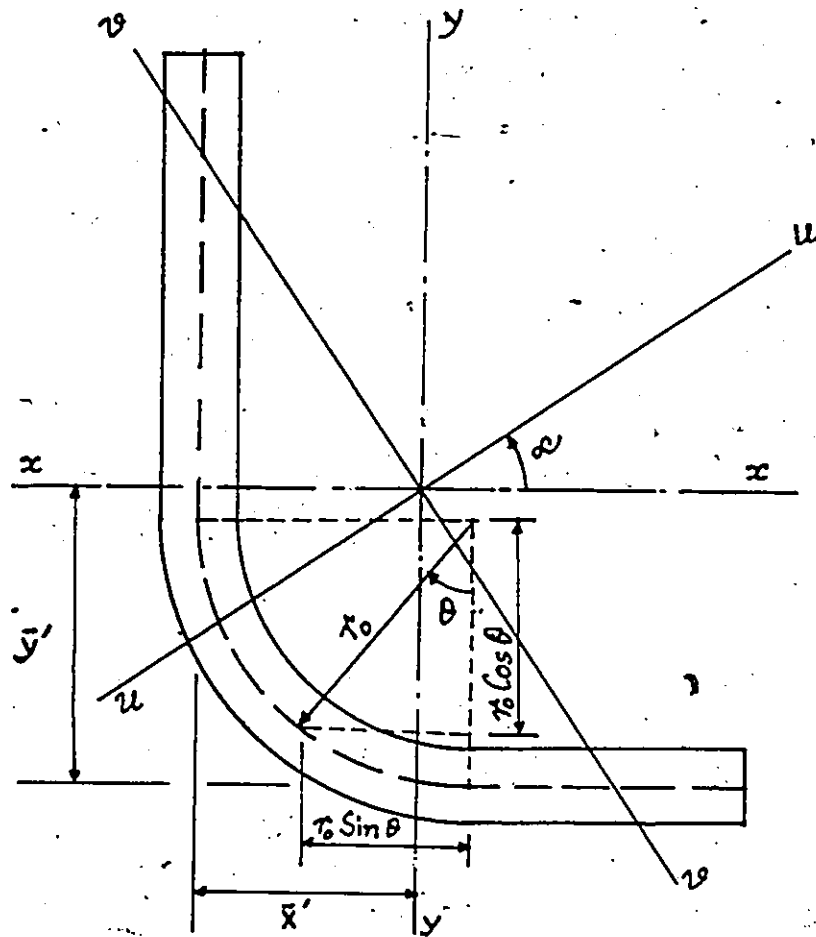


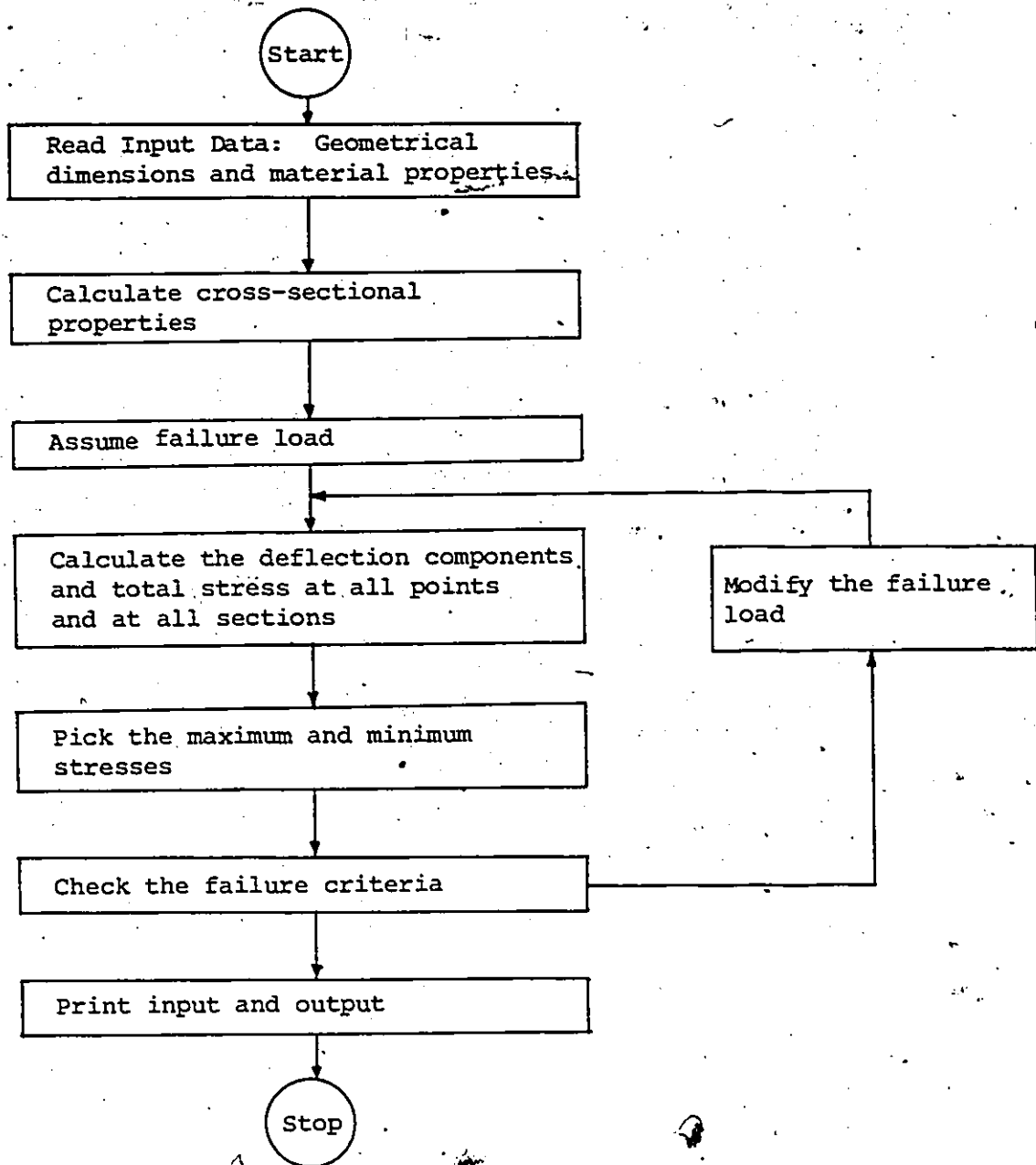
Figure 16

APPENDIX 2

FLOW CHART OF COMPUTER PROGRAM

APPENDIX 2

FLOW CHART OF COMPUTER PROGRAM



APPENDIX 3

SOURCE LISTING OF COMPUTER PROGRAM

RAY, SUJIT KUMAR

SENSITIVITY ANALYSIS

 * THIS PROGRAM CALCULATES THE THEORETICAL CRITICAL LOAD *
 * OF A COLD-FORMED ANGLE COLUMN, UNDER TORSIONAL- *
 * FLEXURAL BUCKLING, FOR DIFFERENT VALUES OF WARPING *
 * CONSTANT, SHEAR CENTER LOCATION & SLENDERNESS RATIO. THE *
 * ASSUMPTIONS MADE ARE MENTIONED IN THE RESPECTIVE PARTS *
 * OF THE PROGRAM. HOWEVER, THE BASIC ASSUMPTION OF THIS *
 * ANALYSIS IS THE CONSIDERATION OF THE CURVED PORTION *
 * OF THE ANGLE SECTION AS LINE ELEMENT. *
 * *****

INPUT DATA

X=LONG LEG OF THE ANGLE SECTION
 Y=SHORT LEG OF THE ANGLE SECTION
 T=THICKNESS, ASSUED CONSTANT THROUGHOUT
 R=INTERNAL RADIUS OF CURVED PORTION
 GPLATE=THICKNESS OF THE CONNECTED GUSSET PLATE
 CONLEG=SIZE OF THE CONNECTED LEG, X OR Y
 GAGDIS=LOCATION OF THE BOLT HOLE
 SIGMAY=YIELD STRESS OF THE MATERIAL
 (NOTE : ALL INPUTS SHALL BE IN N AND MM ONLY)

VARIABLE IDENTIFICATION

C=SECTIONAL AREA, MM**2
 Y11=DISTANCE OF CENTROID ALONG X-X AXIS, MM
 X11=DISTANCE OF CENTROID ALONG Y-Y AXIS, MM
 IXX=MOMENT OF INERTIA ABOUT X-X AXIS, MM**4
 (X-X AXIS BEING THE AXIS PARALLEL TO
 SHORT LEG)
 IYY=MOMENT OF INERTIA ABOUT Y-Y AXIS, MM**4
 (Y-Y AXIS BEING THE AXIS PARALLEL TO
 LONG LEG)
 PXY=PRODUCT OF INERTIA, MM**4
 IMIN=MOMENT OF INERTIA ABOUT V-V AXIS, MM**4
 (V-V AXIS BEING THE AXIS MAKING AN ANGLE
 ALPHA WITH Y-Y AXIS)
 IMAX=MOMENT OF INERTIA ABOUT U-U AXIS, MM**4
 (U-U AXIS BEING THE AXIS MAKING AN ANGLE
 ALPHA WITH X-X AXIS)
 APHD=THE ANGLE ALPHA BETWEEN THE X-X AXIS & U-U

```

*****
      AXIS, MEASURED COUNTER-CLOCKWISE FROM X-X AXIS
      UZRACT,VZRACT=U- & V- COORDINATES OF THE ACTUAL
      LOCATION OF THE SHEAR CENTER, MM
      UZRAS1,VZRAS1,UZRAS2,VZRAS2=U- & V- COORDINATES OF THE
      ASSUMED LOCATION OF THE
      SHEAR CENTER, MM
      RMIN=MINIMUM RADIUS OF GYRATION, MM
      J3=TORSIONAL CONSTANT, MM**4
      EU,EV=U- & V- ECCENTRICITIES OF THE POINT OF THE
      LOAD APPLICATION, MM
      BETA1,BETA2=PARAMETERS REQD. FOR THE CALCULATION
      OF THE CRITICAL LOAD, MM
      CTRACT=ACTUAL MAGNITUDE OF THE WARPING CONSTANT,
      MM**6
      PXE=EULER LOAD OF THE MEMBER ( BENDING ABOUT U-U
      AXIS ), N
      PYE=EULER LOAD OF THE MEMBER ( BENDING ABOUT V-V
      AXIS ), N
      POE=CRITICAL LOAD OF THE MEMBER ( UNDER PURE
      TORSION ), N
      CBILOD=CRITICAL LOAD UNDER TORSIONAL-FLEXURAL
      BUCKLING, N
*****
      IMPLICIT REAL*8 (A-Z)
      INTEGER I,J,K,L,M,N,MM,IK,IJ,IL,KL,MNP
      DIMENSION DP(16),VP(16),U(11),V(11),BETA(11),PHIDER(11),
      DCH(11),VCH(11),BETACH(11)
      READ(5,55555) N
      DO 10 I=1,N
      READ(5,33333) X,Y,T,R,GELATE,CONLEG,GAGDIS,SIGMAI
55555  FORMAT(I3)
33333  FORMAT(8F6.2)
      X1=X-T
      C1=Y-X1
      C2=X-X1
      C3=T-.5
      C4=C1*C3*T
      C5=C2*C3*(X+X1)
      C6=C1*C3*(Y+X1)
      C7=C2*C3*T
      C8=(R+C3)*1.570796327
*****
      * CALCULATION OF THE SECTIONAL AREA
*****
      C=(C1+C2+C8)*T
*****
      * CALCULATION OF THE IBAR & YBAR
*****
      CXY=(X1-C8*.405284734)*C8*T
      CY=C6+C7*CXY
      CX=C4+C5*CXY
      Y11=CY/C
      X11=CX/C
*****
      * CALCULATION OF IXX, IYY & PXY
*****
      CYY=C1*T*((X+X1)*.5-Y11)**2+T*C2*(Y11-C3)**2
      CXX=C2*T*((X+X1)*.5-X11)**2+T*C1*(X11-C3)**2
      P=Y11-X1+C8*.405284734
      Q=X11-X1+C8*.405284734
      C9=.14877839*(R+C3)**3*T
      C10=T/12.
      C11=T*T*C10
      ISI=C1**3*C10+C2*C11+C9+C3*T*P**2
      IYY=ISI+CYT
      IS2=C2**3*C10+C1*C11+C9+C3*T*Q**2
      IXX=IS2+CXX
      C12=R+C3

```



```

511 C13=X2L2-7*C12*C12*DCOS(APHR+TT)/LMIN
    C14=T*C12*D3*DSIN(APHR+PHI)/LMIN
    IF(D1.LT.0.0)C14=-C14
    C15=T*C12*C12/LMIN
    THT=1.570796327
    IF(D2.LT.0.0.AND.L10.GT.C1) THT=1.570796327-TT
C   *****
C   * FINDING THE POINT OF ZERO SHEAR FLOW
C   *****
    AA=C13-C14*THT+C15*DCOS(THT+APHR+TT)
    IF(AA.GE.0.0) GO TO 51
    THT1=0.0
    DTH=.1
    THT2=THT1+DTH
15  A=C13-C14*THT1+C15*DCOS(APHR+THT1+TT)
    B=C13-C14*THT2+C15*DCOS(APHR+THT2+TT)
    IF(A.GT.0.0.AND.B.LT.0.0) GO TO 20
    THT1=THT2
    THT2=THT2+DTH
    GO TO 15
20  THT1=THT1+.01
    DTH=DTH+.1
    THT2=THT1+DTH
25  A=C13-C14*THT1+C15*DCOS(APHR+THT1+TT)
    B=C13-C14*THT2+C15*DCOS(APHR+THT2+TT)
    IF(A.LT.0.0.AND.B.LT.0.0) GO TO 38
    IF(A.GT.0.0.AND.B.LT.0.0) GO TO 30
    THT1=THT2
    THT2=THT2+DTH
    GO TO 25
38  THT1=THT1-.1
30  THT1=THT1+.001
    DTH=DTH+.1
    THT2=THT1+DTH
35  A=C13-C14*THT1+C15*DCOS(APHR+THT1+TT)
    B=C13-C14*THT2+C15*DCOS(APHR+THT2+TT)
    IF(A.LT.0.0.AND.B.LT.0.0) GO TO 42
    IF(A.GT.0.0.AND.B.LT.0.0) GO TO 40
    THT1=THT2
    THT2=THT2+DTH
    GO TO 35
40  CONTINUE
C   *****
C   * THE FOLLOWING THT, WHICH IS THE ANGLE MEASURED
C   * CLOCKWISE FROM SHORT LEG, GIVES THE POINT OF ZERO
C   * SHEAR FLOW.
C   *****
    THT=.5*(THT1+THT2)
    ULMT=THT
    LLMT=0.0
    GO TO 45
42  THT=THT1-.001
    ULMT=THT
    LLMT=0.0
    GO TO 45
51  IF(D1.GT.0.0.AND.D2.LT.0.0) GO TO 502
    IF(TT.NE.0.0.AND.D1.LT.0.0.AND.D2.LT.0.0) GO TO 559
C   *****
C   * CALCULATION OF THE MOMENT OF THE CURVED PORTION
C   * ABOUT CENTROID
C   *****
    JLMT=1.570796327
    LLMT=0.0
    C16=T/LMIN
    INT1=C12*C12*X2L2*ULMT
    INT2=C12*X2L2*D3*(-CPHI-SPHI)
    INT3=C12*B*C16*.5*D3*DSIN(APHR+PHI)*JLMT*ULMT
    INT4=C12*B*C16*(ULMT*APH2-DSIN(APHR+ULMT)*APH1)
    INT5=C12*C12*C16*DSIN(APHR+PHI)*D3*D3*(SPHI+
    -570796327*CPHI)
    INT6=C12*B*C16*D3*(APH2*(SPHI+CPHI)-DCOS(APHR+PHI)
    *ULMT*.5*.5*DSIN(APHR+PHI))
C   *****
C   * MXCP GIVES THE MOMENT OF THE CURVED PORTION ABOUT
C   * CENTROID
C   *****
    IF(D1.LT.0.0) GO TO 528
    MXCP=INT1-INT2-INT3-INT4-INT5-INT6
    GO TO 112
528  MXCP=INT1+INT2+INT3+INT4+INT5+INT6

```

```

559 GO TO 112
19989 *B112(6.19999)
112 L3=X-X11-(Y11-C3)/APH3
L4=X-L3-X1
IF(AA.GT.0.0) GO TO 52
*****
C * CALCULATION OF THE MOMENT OF THE STRAIGHT PORTION OF
C * THE LONG LEG
C *****
COX=T*APH1/(2.*IMIN)
OX3L3=COX*L3*L3
MCX=(Y11-C3)*T*APH1/(2.*IMIN)
MX3=MCX*(L3**3)*2./3.
OX4L4=COX*(L3+L4)*(L3-L4)
MX4=MCX*L4*(L3-L4+L4/3.)
IF(AA.EQ.0.0) GO TO 35
IF(D1.LT.0.0.AND.D2.LT.0.0) GO TO 908
IF(D1.LT.0.0.AND.L3.GT.C2) GO TO 655
LLMT=0.0
ULMT=1.5708-PHI
IF(D2.LT.0.0.AND.L10.GT.C1) ULMT=ULMT-TT
TT2=0.
IF(L4.GT.0.0) GO TO 656
*****
C * CALCULATION OF THE MOMENT OF THE CURVED PORTION
C * ABOUT CENTROID
C *****
352 INT1=C12*C12*OX4L4*ULMT
INT2=C12**3*T*D3*DSIN(APH1+PHI)/IMIN*ULMT*ULMT*.5
INT3=C12*D3*OX4L4*(DSIN(1.570796-ULMT-PHI)-CPHI)
INT4=C12*C12*D3*D3*T*DSIN(APH1+PHI)/IMIN*(-ULMT*DSIN(1.570796-ULMT
-PHI)+DSIN(ULMT+PHI)-SPHI)
INT5=C12**4*T/IMIN*(-DSIN(1.570796-APH1+ULMT)+APH1*ULMT+APH2)
INT6=2.*C12**3*T*D3/IMIN*(-.5*APH1*(DSIN(1.570796-ULMT-PHI)-CPHI)
+.25*DCOS(APH1+PHI)*ULMT-.325*(DSIN(2.*ULMT+PHI-APH1)-CSIN
(PHI-APH1)))
C *****
C * MXCRV GIVES THE MOMENT OF THE CURVED PORTION ABOUT
C * CENTROID
C *****
IF(D1.LT.0.0) GO TO 339
MXCRV=INT1+INT2+INT3+INT4+INT5+INT6
GO TO 340
339 MXCRV=INT1+INT2+INT3+INT4+INT5+INT6
340 MXCP=MXCRV-MXCLV
IF(ULMT.EQ.TT2) GO TO 656
*****
C * VZRACT GIVES THE V- COORDINATE OF THE ACTUAL SHEAR
C * CENTER
C *****
95 VZRACT=-(MX1+MX2+MXCP-MX3-MX4)
GO TO 14
655 CONTINUE
*****
C * CALCULATION OF THE MOMENT OF THE STRAIGHT PORTION OF
C * THE LONG LEG
C *****
L11=L3
L3=C2
OX4L4=COX*2.*L3*(L11-L3*.5)
MX3=MCX*2.*L3*L3*(L11-.5-L3/6.)
MX4=0.
L4=0.
C *****
C * CALCULATION OF THE ANGLE "TT2"
C *****
TT2=DARCOS(DABS(X11)/C12)
ULMT=TT2
LLMT=0.
GO TO 352
656 CONTINUE
*****
C * CALCULATION OF THE MOMENT OF THE CURVED PORTION ABOUT
C * CENTROID IF THE CENTROID LIES IN THE SECOND QUADRANT
C * WITH RESPECT TO CENTER OF CURVATURE AND IF THE POINT
C * OF ZERO SHEAR FLOW IS IN THE CURVED PORTION
C *****
ULMT=1.5708-PHI-TT-TT2
LLMT=0.

```

```

C400=QX3L4-C12*C12*T/IMIN*APH1
C401=C12*D3*T*DSIN(APHR+PHI)/IMIN
C402=T*C12*C12/IMIN
Q3=C400+C401*TT2-C402*DSIN(TT2-APHR)
INT1=C12*C12*Q3*ULMT
INT2=C12*D3*T*DSIN(APHR+PHI)/IMIN*.5*ULMT*ULMT
INT3=C12*D3*Q3*(DSIN(1.570796-PHI-ULMT-TT2)-DSIN(1.570796-PHI-
TT2))
INT4=C12*D3*D3*T/IMIN*DSIN(APHR+PHI)*(-ULMT*DSIN(
1.570796-PHI-ULMT-TT2)+DCOS(1.570796-PHI-ULMT-TT2))
INT5=C12*D3*T/IMIN*(DSIN(APHR-TT2)*ULMT-DSIN(-APHR+ULMT+TT2
+1.570796)+DSIN(1.570796-APHR+TT2))
INT6=2.*C12*D3*T*DSIN(-.125*(DSIN(2.*ULMT+PHI-APHR+2.*TT2)-
DSIN(PHI-APHR+2.*TT2))+.25*DCOS(APHR+PHI)*ULMT-.5*DSIN
(APHR-TT2)*(DSIN(1.570796-ULMT-PHI-TT2)-DSIN(1.570796-PHI-
TT2)))
*****
C C C C
* MYCEV GIVES THE MOMENT OF THE CURVED PORTION ABOUT *
* CENTROID *
*****
IF(D1.GT.0.0.AND.D2.GT.0.0)GO TO 658
MYCEV=INT1+INT2+INT3+INT4+INT5+INT6
MYCP=MYC2-MYCEV
GO TO 95
658 MYCEV=INT1+INT2+INT3+INT4+INT5+INT6
MYCP=MYCP-MYCEV
GO TO 95
52 CONTINUE
C C C C
* CALCULATION OF THE POINT OF ZERO SHEAR FLOW IF IT *
* LIES BEYOND THE CURVED PORTION THAT IS, IN THE *
* STRAIGHT PORTION OF THE LONG LEG *
*****
AQ=1.
BQ=-2.*L3
CQ=2.*L1*IMIN/(T*APH1)
DISC=BQ*BQ-4.*AQ*CQ
XPP=(-BQ+DSQRT(DISC))/2.*AQ
XPS=(-BQ-DSQRT(DISC))/2.*AQ
XP=XPS
*****
C C C C
* CALCULATION OF THE MOMENT OF THE STRAIGHT PORTION OF *
* THE LONG LEG *
*****
MCX=Y11-C3
MX=MCX*AA*XP*(1.+(XP*XP/(3.*CQ)))+(XP*BQ/(2.*CQ))
CQX=T*APH1/(2.*IMIN)
QX3L3=CQX*L3*L3
MX3=2.*MCX*(L3**3)*CQX/3.
QX4L4=CQX*(L3*L3-(L4-XP)*(L3-L3-(L4-XP)*(L4-XP)/3.))
MX4=MCX*CQX*(L4-XP)*(L3-L3-(L4-XP)*(L4-XP)/3.))
*****
C C C C
* VZRACT GIVES THE V-COORDINATE OF THE ACTUAL SHEAR *
* CENTER *
*****
VZRACT=-(MX1+MX2+MYCP+MX-MX3-MX4)
GO TO 14
45 CONTINUE
C C C C
* CALCULATION OF THE MOMENT OF THE CURVED PORTION *
* ABOUT CENTROID *
*****
IF(D1.GT.0.0.AND.D2.LT.0.0)GO TO 905
C16=T/IMIN
INT1=C12*C12*QX2L2*(ULMT-LLMT)
INT2=C12*QX2L2*D3*(DCOS(1.570796+TT+ULMT-PHI)-DCOS(1.570796+TT-
LLMT-PHI))
INT3=C12*D3*C16*.5*D3*DCOS(APHR+PHI-1.570796)*(ULMT*ULMT-LLMT
*LLMT)
INT4=C12*D3*C16*((ULMT-LLMT)*DCOS(APHR+TT)-DSIN(ULMT+TT+APHR)
+DSIN(APHR+LLMT+TT))
INT5=C12*D3*C16*D3*DCOS(APHR+PHI-1.570796)*(-ULMT*DCOS(
1.570796
-PHI+ULMT+TT)+LLMT*DCOS(1.570796-PHI+LLMT+TT)+DSIN(1.570796
-PHI+TT+ULMT)-DSIN(1.570796-PHI+TT+LLMT))
INT6=C12*D3*C16*D3*(-DCOS(APHR+TT)*(DCOS(1.570796-PHI+ULMT+TT)-
DCOS
(1.570796-PHI+LLMT+TT))+.25*(DCOS(1.570796+2.*ULMT+2.*TT+APHR
-PHI)-DCOS(1.570796+2.*LLMT+2.*TT+APHR-PHI))-.5*DSIN(1.570796

```



```

C *****-APHR-PHI)*(ULMT-LLMT))*****
C * XICP GIVES THE MOMENT OF THE CURVED PORTION ABOUT *
C * CENTROID *****
C IP(D1-LT.0.0)GO TO 525
XICP=-INT6-INT5-INT4+INT1-INT2-INT3
GO TO 526
525 XICP=INT1+INT2+INT3-INT4-INT5+INT6
526 IP(D2-LT.0.0.AND.L10.GT.C1)GO TO 555
GO TO 112
555 LLMT=0.0
ULMT=TT
C *****
C * CALCULATION OF THE MOMENT OF THE CURVED PORTION ABOUT*
C * CENTROID *****
C INT1=C12*C12*Q1*(ULMT-LLMT)
INT2=C12*Q1*D3*(DSIN(-ULMT+PHI)-DSIN(-LLMT+PHI))
INT3=C12*Q3*C16*.5*D3*DSIN(APHR+PHI)*(ULMT-ULMT-LLMT
*LLMT)
INT4=C12*Q4*C16*((ULMT-LLMT)*APH2-DSIN(ULMT+APHR)
*DSIN(APHR+LLMT))
INT5=C12*C12*C16*D3*D3*DSIN(APHR+PHI)*(-ULMT*DSIN
*(-ULMT+PHI)+DCOS(-ULMT+PHI)+LLMT*DSIN(PHI-LLMT)-DCOS(PHI-
LLMT))
INT6=C12*Q3*C16*D3*(-APH2*DSIN(-ULMT+PHI)-DSIN(-LLMT
+PHI))-D3*DSIN(1.570796-APHR-PHI)*(ULMT-LLMT)+.25*(DCOS(2.*
ULMT+1.570796+APHR-PHI)-DCOS(2.*LLMT+APHR-PHI+1.570796)))
C *****
C * XICP GIVES THE MOMENT OF THE CURVED PORTION ABOUT *
C * CENTROID *****
C XICP=INT1+INT2+INT3-INT4-INT5+INT6+XICP
GO TO 112
902 CONTINUE
C *****
C * CALCULATION OF THE MOMENT OF THE CURVED PORTION ABOUT*
C * CENTROID IF THE CENTROID LIES IN THE SECOND QUADRANT *
C * WITH RESPECT TO CENTER OF CURVATURE AND IF POINT OF *
C * ZERO SHEAR FLOW IS NOT IN THE CURVED PORTION *****
C IP(TT.EQ.0.0)GO TO 904
C * HERE, L1.GT.C1 *****
C ULMT=TT
LLMT=0.
CALL XICP78(C12,Q1,D3,T,APHR,PHI,IMIN,ULMT,LLMT,NXX)
XICP=NXX
ULMT=1.570796-TT
LLMT=0.
CALL XICP12(C12,QX2L2,D3,T,APHR,PHI,IMIN,ULMT,LLMT,NXX,IT)
XICP=XICP+NXX
GO TO 112
904 CONTINUE
C *****
C * HERE, L1.LE.C1 *****
C ULMT=1.570796
LLMT=0.
CALL XICP12(C12,QX2L2,D3,T,APHR,PHI,IMIN,ULMT,LLMT,NXX,TT)
XICP=NXX
GO TO 112
905 CONTINUE
C *****
C * CALCULATION OF THE MOMENT OF THE CURVED PORTION ABOUT*
C * CENTROID IF THE CENTROID LIES IN THE SECOND QUADRANT *
C * WITH RESPECT TO CENTER OF CURVATURE AND IF THE POINT *
C * OF ZERO SHEAR FLOW IS IN THE CURVED PORTION *****
C IP(TT.EQ.0.0)GO TO 906
C * HERE, L1.GT.C1 *****
C ULMT=TT
LLMT=0.
CALL XICP78(C12,Q1,D3,T,APHR,PHI,IMIN,ULMT,LLMT,NXX)
XICP=NXX
ULMT=TT

```

```

      LLMT=0.
      CALL MXCP12(C12,QX2L2,D3,T,APHR,PHI,ININ,ULMT,LLMT,MXX,TT)
      MXCP=MXCP+MXX
      GO TO 112
906  CONTINUE
      * HERE, L1-LE.C1
      *
      ULMT=THT
      LLMT=0.
      CALL MXCP12(C12,QX2L2,D3,T,APHR,PHI,ININ,ULMT,LLMT,MXX,TT)
      MXCP=MXCP+MXX
      GO TO 112
908  CONTINUE
      * CALCULATION OF THE MOMENT OF THE CURVED PORTION ABOUT
      * CENTROID IF THE CENTROID LIES IN THE SECOND QUADRANT *
      * WITH RESPECT TO CENTER OF CURVATURE AND IF POINT OF *
      * ZERO SHEAR FLOW IS IN THE CURVED PORTION *
      *
      ULMT=1.570796-THT-TT
      LLMT=0.
      CALL MXCP34(C12,QX4L4,D3,T,APHR,PHI,ININ,ULMT,LLMT,MXX)
      MXCRV=MXX
      MXCP=MXCP-MXCRV
      GO TO 95
14   CONTINUE
      * CALCULATION OF U-COORDINATE OF THE ACTUAL SHEAR
      * CENTER
      *
      * CALCULATION OF THE MOMENT OF THE STRAIGHT PORTION
      * OF THE SHORT LEG
      *
      Y1SC=T*C1*((X11-C3)/APH2+(L1-C1-.5)*APH1)/INAX
      Y1=(X11-C3)*T*C1*.5*((X11-C3)/APH2+(L1-C1/3.)*
      * APH1)/LDA1
      C18=T/INAX
      CO1=(Y11-C3)*APH3
      IF(IX1.EQ.IYY)GO TO 31
      * FINDING THE POINT AT WHICH U-U AXIS INTERSECTS THE
      * CENTER-LINE OF THE CROSS-SECTION
      *
      IF(CO1.LE.D1)GO TO 32
      AB=1.570796327-PHI-APHR
      IF(D1.GT.0.0)GO TO 330
      CC=1.570796327+PHI+APHR
      BB=DARSIN((D3*DSIN(CC))/(R+C3))
      AB1=AB-BB
      THTA=1.570796327-AB1-PHI
      GO TO 332
330  BB=DARSIN((D3*DSIN(AB))/(R+C3))
      CC=3.141592654-AB-BB
      CO2=(R+C3)*DSIN(CC)/DSIN(AB)
      * THE FOLLOWING THTA, WHICH IS THE ANGLE MEASURED
      * COUNTER-CLOCKWISE FROM THE LONG LEG, GIVES THE POINT
      * AT WHICH U-U AXIS INTERSECTS THE CENTER-LINE OF THE
      * CROSS-SECTION
      *
      THTA=DARCCOS((CO2*APH2-D2)/(R+C3))
332  LLMT=0.0
      ULMT=1.570796327-THTA
      GO TO 32
31   LLMT=0.0
      ULMT=.785398163
      THTA=ULMT
32   CONTINUE
      * CALCULATION OF THE MOMENT OF THE CURVED PORTION ABOUT
      * CENTROID
      *
83   INT1=C12*C12*QY1SC*(ULMT-LLMT)
      INT2=C12*.3*.5*C18*.03*DCOS(APHR+PHI)*(ULMT*.2-LLMT*.2)
      INT3=C12*.4*C18*(-DCOS(ULMT+APHR)*DCOS(LLMT+APHR)
      * (LLMT-ULMT)*APH1)
      INT4=C12*D3*QY1SC*(-DCOS(ULMT+PHI)+DCOS(LLMT+PHI))
      INT5=C12*C12*C18*D3*DCOS(PHI+APHR)*(-ULMT*DCOS(
      * ULMT+PHI)-LLMT*DCOS(LLMT+PHI)+DSIN(ULMT+PHI)-DSIN(LLMT+PHI))

```

```

      INT6=C12**3*2.*C18*D3*(-.125*(-DSIN(2.*ULMT+APHR+PHI)
      +DSIN(2.*LLMT+APHR+PHI))+.25*(ULMT-LLMT)*DCOS(APHR-PHI)
      +.5*APH1*(DCOS(ULMT+PHI)-DCOS(LLMT+PHI)))
*****
* MYC1 GIVES THE MOMENT OF THE CURVED PORTION ABOUT *
* CENTROID *
*****
      IF(D1.LT.0.0)GO TO 530
      MYC1=INT1+INT2+INT3+INT4+INT5+INT6
      GO TO 539
530 MYC1=INT1+INT3+INT5+INT6-INT2-INT4
539 IF(ULMT.EQ.1.5708)GO TO 602
      GO TO 603
62 ULMT=1.5708
      LLMT=0.0
      GO TO 63
602 IF(CO1.NE.D1)GO TO 605
*****
* CALCULATION OF THE MOMENT OF THE STRAIGHT PORTION OF *
* THE LONG LEG IF U-U AXIS INTERSECTS THE CENTER-LINE *
* OF THE CROSS-SECTION JUST AT THE END OF THE CURVED *
* PORTION *
*****
      MY2=(Y11-C3)*T*APH2/IMAX*C2**3/3.
*****
* UZRACT GIVES THE U- COORDINATE OF THE ACTUAL SHEAR *
* CENTER *
*****
      UZRACT=-(MY1+MY2+MYC1)
      GO TO 100
605 CONTINUE
*****
* CALCULATION OF THE MOMENT OF THE STRAIGHT PORTION OF *
* THE LONG LEG IF U-U AXIS INTERSECTS THE CENTER-LINE *
* OF THE CROSS-SECTION IN THE STRAIGHT PORTION OF THE *
* LONG LEG *
*****
      L5=D1-CO1
      C20=.785398164-APHR
      C21=D3*DCOS(APHR+PHI)+.900316316*C12*DSIN(
      C20)
      QAT90=QY1SC+C18*C21*C12*1.570796327
      MY3=(Y11-C3)*L5*(T*APH2*L5*L5/(3.*IMAX)+QAT90)
      L6=X1-L5
      MY2=(Y11-C3)*T*APH2*L6**3/(3.*IMAX)
*****
* UZRACT GIVES THE U- COORDINATE OF THE ACTUAL SHEAR *
* CENTER *
*****
      UZRACT=-(MY1+MY2+MY3+MYC1)
      GO TO 100
603 CONTINUE
*****
* CALCULATION OF THE MOMENT OF THE STRAIGHT PORTION OF *
* THE LONG LEG IF U-U AXIS INTERSECTS THE CENTER-LINE *
* OF THE CROSS-SECTION IN THE CURVED PORTION *
*****
      L5=C2+CO1-D1
      JL=T*C2*APH2/IMAX*(L5-C2*.5)
      MY2=(Y11-C3)*T*APH2*.5/IMAX*C2*C2*(L5-C2/3.)
      LLMT=0.0
      ULMT=THTA
*****
* CALCULATION OF THE MOMENT OF THE CURVED PORTION ABOUT *
* CENTROID *
*****
      INT1=Q1*C12*C12*ULMT
      INT2=C12**3*C18*D3*.5*DCOS(PHI+APHR)*ULMT*ULMT
      INT3=C12**4*C18*(DSIN(ULMT-APHR)-ULMT*APH2+APH1)
      INT4=C12*D3*Q1*(-DCOS(ULMT+PHI)-CPHI)
      INT5=C12*C12*C18*D3*D3*(-ULMT*DCOS(ULMT+PHI)+DSIN(ULMT+PHI)-SPHI)
      *DCOS(APHR+PHI)
      INT6=C12**3*2.*C18*D3*(-.125*(-DCOS(2.*ULMT-APHR+PHI)
      +DCOS(APHR-PHI))+.25*DSIN(APHR+PHI)*ULMT+.5*APH2*
      (DCOS(ULMT+PHI)-CPHI))
*****
* MYC2 GIVES THE MOMENT OF THE CURVED PORTION ABOUT *
* CENTROID *
*****
      IF(D1.LT.0.0)GO TO 540

```

```

MYC2=INT1-INT2+INT3+INT4-INT5+INT6
GO TO 542
540 MYC2=INT1+INT3-INT5-INT6+INT2-INT4
*****
* UZRACT GIVES THE U- COORDINATE OF THE ACTUAL SHEAR
* CENTER
*****
542 UZRACT=-(MY1+MY2+MYC1+MYC2)
100 CONTINUE
*****
* CALCULATION OF THE BETA1 & BETA2 (REFERENCE: PAGE 245
* OF "THEORY OF ELASTIC STABILITY" BY TIMOSHENKO)
*****
* CALCULATION FOR LONG LEG
*****
C400=(Y11-C3)/APH2
C401=X11-C01-C3
C402=X-C3
C403=Y-C3
MM=1
CALL INTGRL(0,X-X1,SUM11,MM,C400,C401,C402,C403,APH1,APH2,T,
X11,Y11,R,IMIN)
MM=2
CALL INTGRL(0,X-X1,SUM12,MM,C400,C401,C402,C403,APH1,APH2,T,
X11,Y11,R,IMIN)
*****
* CALCULATION FOR SHORT LEG
*****
MM=3
CALL INTGRL(0,Y-Y1,SUM21,MM,C400,C401,C402,C403,APH1,APH2,T,
X11,Y11,R,IMIN)
MM=4
CALL INTGRL(0,Y-Y1,SUM22,MM,C400,C401,C402,C403,APH1,APH2,T,
X11,Y11,R,IMIN)
*****
* CALCULATION FOR CURVED PORTION
*****
MM=5
ULMT=1.5707963
CALL INTGRL(0,ULMT,SUM31,MM,C400,C401,C402,C403,APH1,
APH2,T,X11,Y11,R,IMIN)
MM=6
CALL INTGRL(0,ULMT,SUM32,MM,C400,C401,C402,C403,APH1,
APH2,T,X11,Y11,R,IMIN)
26 SUM1=SUM11+SUM21+SUM31
27 SUM2=SUM12+SUM22+SUM32
GAMMA1=1.570796327-PHI-APHA
GAMMA2=.785398163-APHA
*****
* JZRAS1,VZRAS1,UZRAS2 & VZRAS2 GIVE THE U- & V-
* COORDINATES OF THE ASSUMED SHEAR CENTERS
*****
IF(D1-GT-0.0) GO TO 370
VZRAS1=-(C12*DSIN(GAMMA2)+D3*DSIN(GAMMA1))
UZRAS1=-(C12*DCOS(GAMMA2)+D3*DCOS(GAMMA1))
GO TO 374
370 VZRAS1=-(C12*DSIN(GAMMA2)+D3*DSIN(GAMMA1))
UZRAS1=-(C12*DCOS(GAMMA2)+D3*DCOS(GAMMA1))
374 H1=X11-C1-C01
H2=(Y11-C3)/APH2
VZRAS2=-H1*APH2
UZRAS2=-(H2+H1*APH1)
*****
* XC1,YC1,XC2 & YC2 GIVE THE X- & Y- COORDINATES OF THE
* ASSUMED SHEAR CENTERS
*****
XC1=UZRAS1*APH2-VZRAS1*APH1
YC1=UZRAS1*APH1+VZRAS1*APH2
XC2=UZRAS2*APH2-VZRAS2*APH1
YC2=UZRAS2*APH1+VZRAS2*APH2
*****
* CALCULATION OF THE CO-ORDINATES OF THE CRITICAL
* POINTS, ON THE CBCSS-SECTION, FOR THE FUSECS2 OF
* CHECKING STRESSES
*****
UP(1)=(X-X11)*APH1-(Y11-T)*APH2
VP(1)=(X-X11)*APH2+(Y11-T)*APH1
UP(2)=(X-X11)*APH1-Y11*APH2
VP(2)=(X-X11)*APH2+Y11*APH1
UP(3)=-(X11-T)*APH1+(Y-Y11)*APH2

```

```

VP(3) = -(X11-T)*APH2-(Y-Y11)*APH1
UP(4) = -X11*APH1+(Y-Y11)*APH2
VP(4) = -X11*APH2-(Y-Y11)*APH1
UP(5) = -(Y11-T)*APH2-(X11-X1)*APH1
VP(5) = -(X11-X1)*APH2+(Y11-T)*APH1
UP(6) = -Y11*APH2-(X11-X1)*APH1
VP(6) = -(X11-X1)*APH2+Y11*APH1
UP(7) = -(Y11-X1)*APH2-(X11-T)*APH1
VP(7) = -(X11-T)*APH2+(Y11-X1)*APH1
UP(8) = -(Y11-X1)*APH2-X11*APH1
VP(8) = -X11*APH2+(Y11-X1)*APH1
PRJ1=Y11*APH2/APH1
PRJ2=(Y11-T)*APH2/APH1
DX1=X11+PRJ1
DY2=X11+PRJ2
DLX=DX1-X1
IF(DLY-LE.0.) GO TO 7010
UP(11) = -Y11*APH2+PRJ1*APH1
VP(11) = Y11*APH1+PRJ1*APH2
GO TO 7011
7010 UP(11)=0.
      VP(11)=0.
7011 DLX=DX2-X1
      IF(DLY-LE.0.) GO TO 7012
UP(10) = -(Y11-T)*APH2+PRJ2*APH1
VP(10) = (Y11-T)*APH1+PRJ2*APH2
GO TO 7014
7012 UP(10)=0.
      VP(10)=0.
7014 IF(DABS(UP(10)).LE.1.0D-07.AND.DABS(VP(11)).LE.1.0D-07) GO TO 7015
      WRITE(6,7879)
7879 FORMAT(/,10X,'POINT MARKED 10 AND 11 ARE NOT CORRECTLY',
            * IDENTIFIED',/)
      GO TO 10
7015 UP(10)=0.
      UP(11)=0.
      PRJ3=Y11*APH1/APH2
      PRJ4=(Y11-T)*APH1/APH2
      DY3=X11-PRJ3
      DY4=X11-PRJ4
      DLY=DY3-X1
      IF(DLY-LE.0.) GO TO 7016
UP(15) = -Y11*APH2-PRJ3*APH1
VP(15) = -PRJ3*APH2+Y11*APH1
GO TO 7017
7016 UP(15)=0.
      VP(15)=0.
7017 DLX=DX4-X1
      IF(DLY-LE.0.) GO TO 7018
UP(14) = -(Y11-T)*APH2-PRJ4*APH1
VP(14) = -PRJ4*APH2+(Y11-T)*APH1
GO TO 7019
7018 UP(14)=0.
      VP(14)=0.
7019 IF(DABS(VP(14)).LE.1.0D-07.AND.DABS(VP(15)).LE.1.0D-07) GO TO 7020
      WRITE(6,7879)
78799 FORMAT(/,10X,'POINT MARKED 14 AND 15 ARE NCT CORRECTLY',
            * IDENTIFIED',/)
      GO TO 10
7020 VP(14)=0.
      VP(15)=0.
      PRJ5=X11*APH1/APH2
      PRJ6=(X11-T)*APH1/APH2
      DX1=Y11+PRJ5
      DX2=Y11+PRJ6
      DLI=DX1-X1
      IF(DLI-LE.0.) GO TO 7021
UP(13) = PRJ5*APH2-X11*APH1
VP(13) = -X11*APH2-PRJ5*APH1
GO TO 7022
7021 UP(13)=0.
      VP(13)=0.
7022 DLX=DX2-X1
      IF(DLI-LE.0.) GO TO 7023
UP(12) = PRJ6*APH2-(X11-T)*APH1
VP(12) = -(X11-T)*APH2-PRJ6*APH1
GO TO 7024
7023 UP(12)=0.
      VP(12)=0.
7024 IF(DABS(UP(12)).LE.1.0D-07.AND.DABS(UP(13)).LE.1.0D-07) GO TO 7025

```

```

78781 WRITE(6,78781)
      FORMAT(//,10X,'POINT MARKED 12 AND 13 ARE NOT CORRECTLY',
      * IDENTIFIED',/)
      GO TO 10
7025 UP(12)=0.
      UP(13)=0.
      D11=X-DY1
      D10=X-DY2
      D14=X-DY4
      D15=X-DY3
      D12=Y-DI2
      D13=Y-DX1
      VZERO=VZRAC
      UZERO=UZRAC
      *****
      * CALCULATION OF THE TORSIONAL CONSTANT, MINIMUM RADIUS
      * OF GYRATION & POLAR MOMENT OF INERTIA.
      *****
      * ASSUMPTION MADE: 1) TORSIONAL CONSTANT,  $J_3 = B \cdot T^{3/3}$ 
      * WHERE, T=THICKNESS
      * B=CENTER-LINE LENGTH OF
      * THE CROSS-SECTION
      *****
      J3=C*T*T/3.
      RMIN=DSQRT(IMIN/C)
      IF(IXL.EQ.IYY) GO TO 28
      IABSC=IMIN+IMAX+C*(UZERO-UZERO+VZERO-VZERO)
      GO TO 29
28 IABSC=IMIN+IMAX+C*UZERO-UZERO
29 CONTINUE
      *****
      * CALCULATION OF THE COORDINATES OF THE CENTER OF
      * THE CURVED PORTION
      *****
      IF(IXL.EQ.IYY) GO TO 310
      AB=1.570796327-PHI-APHR
      IF(D1.IT.0.0) GO TO 360
      GO TO 361
360 UCPR=-D3*DCOS(AB)
      VCPR=-D3*DSIN(AB)
      GO TO 303
361 UCPR=D3*DCOS(AB)
      VCPR=D3*DSIN(AB)
      GO TO 303
310 IF(D1.IT.0.0.AND.D2.IT.0.0) GO TO 320
      UCPR=-D3
      VCPR=0.0
      GO TO 303
320 UCPR=D3
      VCPR=0.0
303 CONTINUE
      *****
      * CALCULATION OF THE DISTANCE BETWEEN THE SHEAR CENTER
      * AND THE CENTER OF THE CURVED PORTION
      *****
      RPR=DSQRT((VZERO-VCPR)**2+(UZERO-UCPR)**2)
      IF(IXL.EQ.IYY) GO TO 315
      JPPR=UCPR-C12*APR2
      VPPR=C12*APR1+VCPR
      RRR=DSQRT((UPPR-UCPR)**2+(VPPR-VZERO)**2)
      LMT=DARCOS((RPR*HPR+C12*C12-RRR*RRR)/(2.*C12*RPR))
      *****
      * XC & YC GIVE THE X- & Y- COORDINATES OF THE ACTUAL
      * SHEAR CENTER
      *****
      YC=-(D1+RPR*JSIN(LMT))
      XC=-(D2+RPR*DCOS(LMT))
      GO TO 313
315 CONTINUE
      *****
      * XC & YC GIVE THE X- & Y- COORDINATES OF THE ACTUAL
      * SHEAR CENTER
      *****
      YC=-(D2+RPR*.70710678)
      XC=-(D1+RPR*.70710678)
      LMT=.785398163
333 WRITE(6,200)
      * WRITE(6,300) X,Y,T,B,C,T11,X11,CONLEG,GAGDIS,SPLATE,SIGMAY,IXX,IYY,
      * IMAX,IMIN,PIY,PMIN,APHO,J3,IABSC

```

```

200 FORMAT(///,10X,19(' '),SECTIONAL PROPERTIES,19(' '),10X,12
308 FORMAT(///,15X,'SIZE OF THE ANGLE',10X,'P6.2',
*      'P6.2',P6.2,15X,'INTERNAL RADIUS',14X,
*      'P5.2',P5.2,15X,'AREA OF THE CROSS-SECTION',
*      'P12.2',MM**2,15X,'DIST. OF CENTROID ALONG X-AXIS',
*      'P12.2',MM,15X,'DIST. OF CENTROID ALONG Y-AXIS',
*      'P12.2',MM,
*      '15X,'CONNECTED LEG',16X,'P12.2',MM,15X,
*      'GAUGE DISTANCE',15X,'P12.2',MM,15X,
*      'THICKNESS OF GUSSET PLATE',P12.2,MM,15X,
*      'ASSUMED MATERIAL YIELD STRESS',P12.2,N/MM**2,15X,
*      '15X,M. I. ABOUT X-X AXIS',6X,'P10.0',3X,MM**4,
*      '15X,M. I. ABOUT Y-Y AXIS',6X,'P10.0',3X,MM**4,
*      '15X,M. I. ABOUT U-U AXIS',P10.0,
*      '3X,MM**4,15X,M. I. ABOUT V-V AXIS',P10.0,
*      '15X,PRODUCT OF INERTIA',10X,'P10.0',
*      'MM**4,15X,'MINIMUM RADIUS OF GYRATION',
*      'P12.2',MM,15X,'ALPHA MEASURED FROM X AXIS',
*      'P12.2',DEGREES,15X,'TORSIONAL CONSTANT',11X,'P12.2',
*      'P12.2',MM**4,15X,'POLAR M. I. ABOUT SHEAR CENTR',
*      'P10.0',MM**4,
*      WRITE(6,3088)UZRACT,VZRACT,UZRAS1,VZRAS1,UZRAS2,VZRAS2,XC,YC,
3088 FORMAT(///,15X,'IN U & V SYSTEM OF AXES',
*      '15X,LOC OF ACTUAL SHEAR CENTER',F7.2,F7.2,
*      '15X,LOC OF ASSUMED SHEAR CENTER 1',F7.2,F7.2,
*      '15X,LOC OF ASSUMED SHEAR CENTER 2',F7.2,F7.2,
*      '15X,IN X & Y SYSTEM OF AXES',
*      'LOC OF ACTUAL SHEAR CENTER',F7.2,F7.2,
*      '15X,LOC OF ASSUMED SHEAR CENTER 1',F7.2,F7.2,
*      '15X,LOC OF ASSUMED SHEAR CENTER 2',F7.2,F7.2,
*      '10X,50(' '),
*      CALL CFACTL(RPB,C12,X11,C3,YC,XC,Y11,LMT,C1,C2,C8,T,CFACT,
*      'AVOMGS,ASC1,ASC2)
*      IF (CONLEG.EQ.X) GO TO 701
C *****
C * EU & EV GIVE THE CO-ORDINATES OF THE POINT OF THE *
C * LOAD APPLICATION *
C *****
EU=(GAGDIS-Y11)*APH2-(Y11+.5*GPLATE)*APH1
EV=-(X11+.5*GPLATE)*APH2-(GAGDIS-Y11)*APH1
GO TO 702
701 EU=-(Y11+.5*GPLATE)*APH2+(GAGDIS-Y11)*APH1
EV=(GAGDIS-X11)*APH2+(Y11+.5*GPLATE)*APH1
C *****
C * ASSUMPTIONS MADE : *
C * 1) MODULUS OF SHEAR RIGIDITY=77000 N/MM**2 *
C * 2) MODULUS OF ELASTICITY=205000 N/MM**2 *
C * *
C * THE MEMBER IS ASSUMED TO BE INITIALLY STRAIGHT AND *
C * STRESS FREE. *
C * THE MEMBER IS ASSUMED TO FAIL OR REACH CRITICAL *
C * LOAD IF THE MAXIMUM STRESS AT ANY POINT OF THE *
C * CROSS-SECTION REACHES THE YIELD STRESS OF THE MATERIAL *
C * OR THE DEFLCTION COMPONENTS CHANGE THEIR SIGN *
C *****
702 G=.77D 05
PLAS=.205D 06
IL=1
790 BETA1=SUN1/IMAX-2.*VZERO
BETA2=SUN2/IMIN-2.*VZERO
WRITE(6,400)UZZERO,VZERO,BETA1,BETA2
400 FORMAT(///,10X,50(' '),10X,17(' '),TABLE OF CRITICAL LOADS,
*      '17(' '),10X,50(' '),21X,'SHEAR CENTER CONSIDERED',
*      'P6.2',F6.2,15X,'BETA1',F9.2,9X,'BETA2',
*      'P9.2)
IABSC=IMIN+IMAX+C*(UZZERO*UZZERO+VZERO*VZERO)
CCC=(Y11-C3)-DABS(XC)
CCD=-((X11-C3)-DABS(YC))
77 FORMAT(///,25X,I3,22X,F10.1)
C70=UZZERO-EU
C71=VZERO-EV
C72=IABSC/C+BETA1*2V+BETA2*EU
IJ=1
C=CFACT
786 SR=20.
WRITE(6,7879)C
7879 FORMAT(///,28X,'C=',D15.6,MM**6,10X,50(' '),18X,
*      'SLENDERNESS RATIO',12X,'CRITICAL LOAD',53X,

```

```

770 * CLENTH=SR*MIN
    C73=9.869604404/(CLENTH*CLENTH)
    PYE=ELAS*IMIN=C73
    PIX=ELAS*IMAX=C73
    POE=(4.130221794*ELAS*CH=C73+1.001870909*G*J3)/C72
C *****
C * FOR FIRST ITERATION, CRITICAL LOAD IS ASSUMED TO BE *
C * 0.1% OF THE MINIMUM OF PIX, PYE & POE *
C *****
    IF(PYE.GT.PO2)GO TO 705
    CRILOD=PYE
    GO TO 706
705 IF(POE.LT.J.)GO TO 7899
    CRILOD=PO2
    GO TO 706
7899 CRILOD=PYE
706 INCR=CRILOD/10.
    CRILOD=.001*CRILOD
    MNP=1
762 CALL DEPROT(PYE,PYE,POE,CRILOD,C70,C71,C72,E0,EV,CLENTH,IMIN,
    IMAX,ELAS,U,V,BETA,PHIDER)
    CALL SIGMA(CRILOD,E0,EV,UP,VP,C,IMIN,IMAX,MXSTR,SIGMAX,
    MNSTR,U,V,BETA,VZERO,VZERO,ELAS,PHIDER,AVOIGS,
    WSC1,WSC2,LMT,C12,RPR,C1,X1,APH1,APH2,D1,D2,C4,CCC,C2,
    R,D10,D11,C12,D13,D14,D15,CCD)
/ IF(MNP.EQ.1)GO TO 7585
C *****
C * CHECKING THE SIGNS OF THE DEPLETION COMPONENTS *
C *****
    DO 9898 KLM=2,10
    EEE=DABS(U(KLM))-DABS(UCH(KLM))
    IF(EEE.LT.0.)GO TO 761
    FPP=DABS(V(KLM))-DABS(VCH(KLM))
    IF(FPP.LT.0.)GO TO 761
    GGG=DABS(BETA(KLM))-DABS(BETACH(KLM))
    IF(GGG.LT.0.)GO TO 761
9898 CONTINUE
C *****
C * CHECKING THE MAXIMUM STRESS *
C *****
7585 IF(DABS(MXSTR).LT.DABS(MNSTR))MXSTR=DABS(MNSTR)
    IF(MXSTR.GT.SIGMAX)GO TO 761
    CRILOD=CRILOD*INCR
C *****
C * STORING THE CURRENT DEPLETION COMPONENTS FOR USE IN *
C * NEXT STEP OF ITERATION *
C *****
    DO 7789 KLM=1,11
    UCH(KLM)=U(KLM)
    VCH(KLM)=V(KLM)
    BETACH(KLM)=BETA(KLM)
7789 CONTINUE
    MNP=MNP+1
    GO TO 762
761 CRILOD=CRILOD-INCR
    INCR=INCR/10.
    MNP=1
764 CALL DEPROT(PYE,PYE,POE,CRILOD,C70,C71,C72,E0,EV,CLENTH,IMIN,
    IMAX,ELAS,U,V,BETA,PHIDER)
    CALL SIGMA(CRILOD,E0,EV,UP,VP,C,IMIN,IMAX,MXSTR,SIGMAX,
    MNSTR,U,V,BETA,VZERO,VZERO,ELAS,PHIDER,AVOIGS,
    WSC1,WSC2,LMT,C12,RPR,C1,X1,APH1,APH2,D1,D2,C4,CCC,C2,
    R,D10,D11,D12,D13,D14,D15,CCD)
/ IF(MNP.EQ.1)GO TO 7586
C *****
C * CHECKING THE SIGNS OF THE DEPLETION COMPONENTS *
C *****
    DO 9897 KLM=2,10
    EEE=DABS(U(KLM))-DABS(UCH(KLM))
    IF(EEE.LT.0.)GO TO 763
    FPP=DABS(V(KLM))-DABS(VCH(KLM))
    IF(FPP.LT.0.)GO TO 763
    GGG=DABS(BETA(KLM))-DABS(BETACH(KLM))
    IF(GGG.LT.0.)GO TO 763
9897 CONTINUE
C *****
C * CHECKING THE MAXIMUM STRESS *
C *****
7586 IF(DABS(MXSTR).LT.DABS(MNSTR))MISTR=DABS(MNSTR)

```



```

IF(NXSTR.GT.SIGMAY) GO TO 763
CRILOD=CRILOD+INCR
*****
C * STORING THE CURRENT DEFLECTION COMPONENTS FOR USE IN *
C * NEXT STEP OF ITERATION *
*****
DO 7788 KLM=1,11
UCH(KLM)=U(KLM)
VCH(KLM)=V(KLM)
BETACH(KLM)=BETA(KLM)
7788 CONTINUE
MNP=MNP+1
GO TO 764
763 CRILOD=CRILOD-INCR
INCR=INCR/10.
MNP=1
765 CALL DEFROT(PYE,PXE,POE,CRILOD,C70,C71,C72,EU,EV,CLENTN,IMIN,
IMAX,ELAS,U,V,BETA,PHIDER)
CALL SIGMA(CRILOD,EU,EV,UP,VP,C,IMIN,IMAX,MXSTR,SIGMAY,
MNSTR,U,V,BETA,UZERO,VZERO,ELAS,PHIDER,AVOJGS,
WSC1,WSC2,LIT,C12,REP,C1,X1,APH1,APH2,D1,D2,C,CCC,C2,
R,D10,D11,D12,D13,D14,D15,CCD)
IF(MNP.EQ.1) GO TO 7587
*****
C * CHECKING THE SIGNS OF THE DEFLECTION COMPONENTS *
C * *
*****
DO 9896 KLM=2,10
EEE=DABS(U(KLM))-DABS(UCH(KLM))
IF(EEE.LT.0.) GO TO 766
PPP=DABS(V(KLM))-DABS(VCH(KLM))
IF(PPP.LT.0.) GO TO 766
GGG=DABS(BETA(KLM))-DABS(BETACH(KLM))
IF(GGG.LT.0.) GO TO 766
9896 CONTINUE
*****
C * CHECKING THE MAXIMUM STRESS *
*****
7587 IF(DABS(MXSTR).LE.DABS(MNSTR)) MXSTR=DABS(MNSTR)
IF(MXSTR.GT.SIGMAY) GO TO 766
CRILOD=CRILOD+INCR
*****
C * STORING THE CURRENT DEFLECTION COMPONENTS FOR USE IN *
C * NEXT STEP OF ITERATION *
*****
DO 7787 KLM=1,11
UCH(KLM)=U(KLM)
VCH(KLM)=V(KLM)
BETACH(KLM)=BETA(KLM)
7787 CONTINUE
MNP=MNP+1
GO TO 765
766 CRILOD=CRILOD-INCR
INCR=INCR/10.
MNP=1
768 CALL DEFROT(PYE,PXE,POE,CRILOD,C70,C71,C72,EU,EV,CLENTN,IMIN,
IMAX,ELAS,U,V,BETA,PHIDER)
CALL SIGMA(CRILOD,EU,EV,UP,VP,C,IMIN,IMAX,MXSTR,SIGMAY,
MNSTR,U,V,BETA,UZERO,VZERO,ELAS,PHIDER,AVOJGS,
WSC1,WSC2,LIT,C12,REP,C1,X1,APH1,APH2,D1,D2,C,CCC,C2,
R,D10,D11,D12,D13,D14,D15,CCD)
IF(MNP.EQ.1) GO TO 7588
*****
C * CHECKING THE SIGNS OF THE DEFLECTION COMPONENTS *
C * *
*****
DO 9895 KLM=2,10
EEE=DABS(U(KLM))-DABS(UCH(KLM))
IF(EEE.LT.0.) GO TO 769
PPP=DABS(V(KLM))-DABS(VCH(KLM))
IF(PPP.LT.0.) GO TO 769
GGG=DABS(BETA(KLM))-DABS(BETACH(KLM))
IF(GGG.LT.0.) GO TO 769
9895 CONTINUE
*****
C * CHECKING THE MAXIMUM STRESS *
*****
7588 IF(DABS(MXSTR).LE.DABS(MNSTR)) MXSTR=DABS(MNSTR)
IF(MXSTR.GT.SIGMAY) GO TO 769
CRILOD=CRILOD+INCR
*****
C * STORING THE CURRENT DEFLECTION COMPONENTS FOR USE IN *
C * *
*****

```

```

C * NEXT STEP OF ITERATION
C *****
DO 7786 KLM=1,11
UCH(KLM)=U(KLM)
VCH(KLM)=V(KLM)
BETACH(KLM)=BETA(KLM)
7786 CONTINUE
MNP=MNP+1
GO TO 768
769 CRILOD=CRILOD-INCR
INCR=INCR/10.
MNP=1
7707 CALL DEFROT(PYE,PKZ,POE,CRILOD,C70,C71,C72,EO,EV,CLNTH,IMIN,
      INAX,ELAS,J,V,BETA,PHIDR)
      CALL SIGMA(CRILOD,EO,EV,UP,VP,C,IMIN,INAX,MISTR,SIGMAT,
      MNSTR,U,V,BETA,UZERO,VZERO,ELAS,PHIDR,AVONGS,
      WSC1,WSC2,LMT,C12,APR,C1,X1,APH1,APH2,D1,D2,C2,CCC,C2,
      R,D10,D11,D12,D13,D14,D15,C6D)
      IF(MNP.EQ.1) GO TO 7575
C *****
C * CHECKING THE SIGNS OF THE DEFLECTION COMPONENTS
C *****
DO 9801 KLM=2,10
EEZ=DABS(U(KLM))-DABS(UCH(KLM))
IF(EEZ.LT.0.) GO TO 7698
FFF=DABS(V(KLM))-DABS(VCH(KLM))
IF(FFF.LT.0.) GO TO 7698
GGG=DABS(BETA(KLM))-DABS(BETACH(KLM))
IF(GGG.LT.0.) GO TO 7698
9801 CONTINUE
C *****
C * CHECKING THE MAXIMUM STRESS
C *****
7575 IF(DABS(MISTR).LE.DABS(MNSTR)) MISTR=DABS(MNSTR)
      IF(MISTR.GT.SIGMAT) GO TO 7698
      CRILOD=CRILOD+INCR
C *****
C * STORING THE CURRENT DEFLECTION COMPONENTS FOR USE IN
C * NEXT STEP OF ITERATION.
C *****
DO 7701 KLM=1,11
UCH(KLM)=U(KLM)
VCH(KLM)=V(KLM)
BETACH(KLM)=BETA(KLM)
7701 CONTINUE
MNP=MNP+1
GO TO 7707
C *****
C * CRILOD GIVES THE CRITICAL LOAD FOR THE SECTION AND
C * SLENDERNESS RATIO
C *****
7698 IK=SR
      WRITE(6,77) IK,CRILOD
      IF(SR.GE.240.) GO TO 782
C *****
C * CHANGE TO NEXT HIGHER SLENDERNESS RATIO
C *****
      SR=SR+10.
      GO TO 770
782 IF(IJ.EQ.2) GO TO 7852
C *****
C * USING THE MAGNITUDE OF WARPING CONSTANT = 0.0
C *****
      CZ=0.0
      IJ=2
      WRITE(6,882)
      FORMAT(//,10X,60(' '),//,10X,60(' '))
882 GO TO 789
7852 IF(IL-2) 787,788,1010
C *****
C * CHANGE TO ANOTHER LOCATION OF THE SHEAR-CENTER
C *****
787 UZERO=UZRAS1
      VZERO=VZRAS1
      IL=2
      WRITE(6,884)
      FORMAT(//,10X,60(' '),//,10X,60(' '),//,10X,60(' '))
884 GO TO 790
C *****
C * CHANGE TO ANOTHER LOCATION OF THE SHEAR-CENTER
C *****

```

```

C *****
788 JZZERO=JZRAS2
VZERO=VZRAS2
IL=3
WRITE(6,884)
GO TO 790
1010 WRITE(6,885)
885 FORMAT(//,10X,60(' '),//,10X,60('*'),//,10X,20('END'))
10 CONTINUE
STOP
END
C *****
C THIS SUBROUTINE COMPUTES THE MOMENT OF THE CURVED
C PORTION (NEEDED FOR THE CALCULATION OF V-COORDINATE
C OF ACTUAL SHEAR CENTER) IF THE CENTROID IS IN THE
C SECOND QUADRANT WITH RESPECT TO CENTER OF CURVATURE
C AND IS VALID BETWEEN THE LIMITS 0 AND THT FROM THE
C SHORT LEG
C *****
SUBROUTINE MXCP12(R,QX,D3,T,APHR,PHI,IMIN,ULMT,LLMT,MXX,TT)
IMPLICIT REAL*8 (A-Z)
INT1=R*R*QX*(ULMT-LLMT)
INT2=R*D3*QX*(DSIN(3.141592-TT+PHI-ULMT)-DSIN(3.141592-TT+PHI-
LLMT))
INT3=R*D3*T/IMIN*.5*DCOS(1.570796+APHR+PHI)*(ULMT*ULMT-LLMT*
LLMT)
INT4=R*D3*T/IMIN*(DCOS(APHR+TT)*(ULMT-LLMT)-DSIN(APHR+TT+ULMT)+
DSIN(APHR+TT+LLMT))
INT5=R*R*D3*D3*T/IMIN*DCOS(1.570796+APHR+PHI)*(-ULMT*DSIN(3.141592
-TT+PHI-ULMT)+LLMT*DSIN(3.141592+PHI-TT-LLMT)+DCOS(3.141592+
PHI-TT-ULMT)-DCOS(3.141592+PHI-TT-LLMT))
INT6=2.*R*D3*D3*T/IMIN*(-DCOS(APHR+TT)*.5*(DSIN(3.141592-TT+PHI-
ULMT)-DSIN(3.141592+PHI-TT-LLMT))-25*DCOS(3.141592+PHI+APHR)
*(ULMT-LLMT)-125*(DSIN(2.*ULMT+2.*TT+PHI-3.141592+APHR)-DSIN
(APHR-3.141592+2.*TT+PHI+2.*LLMT)))
MXX=INT1+INT2+INT3+INT4+INT5+INT6
RETURN
END
C *****
C THIS SUBROUTINE COMPUTES THE MOMENT OF THE CURVED
C PORTION (NEEDED FOR THE CALCULATION OF V-COORDINATE
C OF ACTUAL SHEAR CENTER) IF THE CENTROID IS IN THE
C SECOND QUADRANT WITH RESPECT TO CENTER OF CURVATURE
C AND IS VALID BETWEEN THE LIMITS 0 AND 90-THT-TT (IF
C TT.NE.0.0) OR 0 AND 90-THT (IF TT.EQ.0.0) FROM THE
C LONG LEG
C *****
SUBROUTINE MXCP34(R,QX,D3,T,APHR,PHI,IMIN,ULMT,LLMT,MXX)
IMPLICIT REAL*8 (A-Z)
INT1=R*R*QX*(ULMT-LLMT)
INT2=R*D3*T/IMIN*.5*DCOS(1.570796+APHR+PHI)*(ULMT*ULMT-LLMT
*LLMT)
INT3=R*D3*QX*(DCOS(-ULMT+PHI)-DCOS(-LLMT+PHI))
INT4=R*D3*T/IMIN*(DCOS(APHR-1.570796)*(ULMT-LLMT)-DSIN(1.570796
-APHR+ULMT)+DSIN(1.570796-APHR+LLMT))
INT5=R*R*D3*D3*T/IMIN*DCOS(1.570796+APHR+PHI)*(ULMT*DCOS(-ULMT+PHI)
-LLMT*DCOS(-LLMT+PHI)+DSIN(-ULMT+PHI)-DSIN(-LLMT+PHI))
INT6=2.*R*D3*D3*T/IMIN*(-.5*DCOS(APHR-1.570796)*(DCOS(-ULMT+PHI)
-DCOS(-LLMT+PHI))-25*DSIN(1.570796-APHR+PHI)*(ULMT-LLMT)
-125*(DCOS(2.*ULMT+PHI-APHR+1.570796)-DCOS(2.*LLMT+PHI-
APHR+1.570796)))
MXX=INT1+INT2+INT3+INT4+INT5+INT6
RETURN
END
C *****
C THIS SUBROUTINE COMPUTES THE MOMENT OF THE CURVED
C PORTION (NEEDED FOR THE CALCULATION OF V-COORDINATE
C OF ACTUAL SHEAR CENTER) IF THE CENTROID IS IN THE
C SECOND QUADRANT WITH RESPECT TO CENTER OF CURVATURE
C AND IS VALID BETWEEN THE LIMITS 0 AND TT FROM THE
C SHORT LEG
C *****
SUBROUTINE MXCP78(R,QX,D3,T,APHR,PHI,IMIN,ULMT,LLMT,MXX)
IMPLICIT REAL*8 (A-Z)
INT1=R*R*QX*(ULMT-LLMT)
INT2=R*D3*QX*(DCOS(1.570796+PHI-ULMT)-DCOS(1.570796+PHI-LLMT))
INT3=R*D3*T/IMIN*.5*DSIN(APHR+PHI)*(ULMT*ULMT-LLMT*LLMT)
INT4=R*D3*T/IMIN*(DCOS(APHR)*(ULMT-LLMT)-DSIN(APHR+ULMT)+DSIN
(APHR+LLMT))
INT5=R*R*D3*D3*T/IMIN*DSIN(APHR+PHI)*(ULMT*DCOS(1.570796+PHI-

```

```

      ULMT)-LLMT)*DCOS(1.570796+PHI-LLMT)+DSIN(1.570796+PHI
      -ULMT)-DSIN(1.570796+PHI-LLMT))
      INT6=2.*R**3*D3**T/IMIN*(.5*DCOS(APHR)*(DCOS(1.570796+PHI-ULMT)
      -DCOS(1.570796+PHI-LLMT))- .25*DSIN(1.570796+APHR+PHI)
      *(ULMT-LLMT)- .125*(DCOS(-APHR+1.570796+PHI-2.*ULMT)-DCOS
      (-APHR+PHI+1.570796-2.*LLMT)))
      MX=INT1+INT2-INT3-INT4-INT5-INT6
      RETURN
      END
C *****
C * THIS SUBROUTINE CALCULATES THE MAGNITUDE OF ACTUAL *
C * WARPING CONSTANT AND RETURNS THE VALUE IN THE *
C * VARIABLE CFACT *
C *****
      SUBROUTINE CFACTL(RPR,C12,X11,C3,YC,XC,Y11,LMT,C1,C2,C8,T,CFACT,
      AVOMGS,C300,C301)
      IMPLICIT REAL*8 (A-Z)
      C300=-((X11-C3)-DABS(YC))
      C300A=C12*C12
      C300B=2*PR*C12
      C300C=DCOS(1.570796+LMT)
      C300D=DSIN(1.570796+LMT)
      C300E=DCOS(LMT)
      C300F=DSIN(LMT)
      C301=C300*C1-(C300A=1.570796+C300B*(C300C-C300E))
      C302=(Y11-C3)-DABS(XC)
      AVOMGS=(C300*C1*.5*(C1+.141592*C12)+C2*(C301-C302*.5*C2)-C12*C300
      *.1.233701-C12*C300B*(C300D-C300E*1.570796-C300F))/(C1+C2+C
      8)
      C303=C300*C1
      C304=AVOMGS*AVOMGS
      C305=2.*AVOMGS
      PART1=(C304+C303*C303/3.-C305*C303*.5)*C1*T
      PART2=((C304+C301*C301+C302*C302-C2*C2/3.-C301*C302*C2-C305
      *(C301-C302*C2*.5))*C2*T
      PART3=((C304+C303*C303+C300B*C300B+C300E*C300E+2.*C303*C300B*C300E
      -C305*(C303+C300B*C300E))*1.570796+C300A*C300A*1.291928+C300
      9*C300B*(.785398163-.5*DSIN(2.*LMT))-C300A*(C303+C300B*C300E
      -AVOMGS)*2.-.467402-C300B*(2.*C303+2.*C300B*(C300E-C305)*(C300D
      -C300F)+2.*C300A*C300B*(1.570796+C300D+C300C-C300E))*T*C12
      CFACT=PART1+PART2+PART3
      RETURN
      END
C *****
C * THIS SUBROUTINE ESTIMATES THE VALUE OF AN INTEGRAL *
C * BY ADAPTIVE QUADRATURE TECHNIQUE USING SIMPSON'S *
C * RULE. *
C *****
      DESCRIPTION OF PARAMETERS:
      C      = LOWER LIMIT OF INTEGRATION
      D      = UPPER LIMIT OF INTEGRATION
      SIMP    = ESTIMATED VALUE OF THE INTEGRAL
      K      = NUMBER OF DIVISIONS INTO WHICH (C,D) IS PARTITIONED
      HMIN    = MINIMUM SUB-INTERVAL; THE ALGORITHM IS SAID TO HAVE
      FAILED IF THE ERROR TEST CANNOT BE SATISFIED WITH-
      OUT USING A SUBDIVISION SMALLER THAN 'HMIN'.
      IEHROB  = A FLAG DENOTING EITHER A SUCCESS OR FAILURE OF
      THE ALGORITHM
      SP      = ESTIMATE USING ONE-PANEL SIMPSON'S RULE
      SZP     = ESTIMATE USING TWO-PANEL COMPOSITE SIMPSON'S RULE
      C *****
      SUBROUTINE INTGRL(C,D,SIMP,HM,C400,C401,C402,C403,APH1,APH2,T,
      X11,Y11,B,IMIN)
      IMPLICIT REAL*8 (A-Z)
      INTEGER I,IEHROB,K,HM,II
      SIMP=0.0
      EST=0.0
      IEHROB=4
      K=50
      AINC=(D-C)/K
      A=C
      B=C+AINC
      HMIN=(B-A)/2.0E 19
      II=2
      IF(IMIN-GE.1.0E 06)II=4
      IF(IMIN-LE.1.0E 06.AND.IMIN-GE.1.0E 05)II=3
      TOL=10**(-II)/K

```

```

DO 500 I=1,K
CALL ADSIMP(A,B,HMIN,TOL,EST,IERRORE,MH,C400,C401,C402,C403,
*      APH1,APH2,T,X11,Y11,B)
SIMP=SIMP+EST
IF (IERRORE.EQ.1) GO TO 400
A=A+AINC
B=B+AINC
500 CONTINUE
GO TO 600
400 CONTINUE
11 WRITE(6,11) B
FORMAT(//,3X,'ALGORITHM COULD NOT INTEGRATE F(X) BEYOND ',D16.9)
600 CONTINUE
RETURN
END
C *****
C * THIS SUBROUTINE ESTIMATES THE VALUE OF AN INTEGRAL IN *
C * THE SUB-INTERVAL (A,B) *****
C *****
SUBROUTINE ADSIMP(A,B,HMIN,TOL,EST,IERRORE,MH,C400,C401,C402,C403,
*      APH1,APH2,T,X11,Y11,B)
*      IMPLICIT REAL*8 (A-Z)
*      INTEGER I,IERRORE,MH
*      DIMENSION ER(20),V(20),FR(20),PS(20),FT(20),FU(20),FV(20)
*      FUNCT1(P,PC1,PC2,PC3,PC4,PC5,T)=((PC1-P)*PC2-PC3-PC4*PC2)**2
*      * ((PC1-P)*PC3-PC4*PC5)*((PC1-P)*PC5-PC4*PC5)**3)*T
*      FUNCT2(P,PC1,PC2,PC3,PC4,PC5,T)=((PC1-P)*PC2-PC3-PC4*PC2)**3
*      * ((PC1-P)*PC2-PC3-PC4*PC2)*((PC1-P)*PC3-PC4*PC5)**2)*T
*      FUNCT3(P,PC1,PC2,PC3,PC4,PC5,T)=((PC1-P)*PC3-PC4*PC5)**3-((
*      PC1-P)*PC2*PC4*PC5)*((PC1-P)*PC5-PC3-PC4*PC2)**2)*T
*      FUNCT4(P,PC1,PC2,PC3,PC4,PC5,T)=((PC1-P)*PC5-PC3-PC4*PC2)**3
*      * ((PC1-P)*PC5-PC3-PC4*PC2)*((PC1-P)*PC2*PC4*PC5)**2)*T
*      FUNCT5(P,X11,Y11,B,T,APH1,APH2)=((-Y11-B-T*(B+T*.5)*DSIN(P))
*      * APH2*(X11-B-T*(B+T*.5)*DCOS(P))*APH1)**3+((-Y11-B-T*(B+
*      * .5)*T)*DSIN(P))*APH2*(X11-B-T*(B+T*.5)*DCOS(P))*APH1)*
*      * ((B+T*.5)*DCOS(P))*APH2*(X11-B-T*(B+T*.5)*DSIN(P))*APH1
*      * ((B+T*.5)*T*(B+T*.5)*DCOS(P))*APH1)**2)*T*(B+.5*T)
*      FUNCT6(P,X11,Y11,B,T,APH1,APH2)=((-Y11-B-T*(B+T*.5)*DCOS(P))
*      * APH2*(X11-B-T*(B+T*.5)*DSIN(P))*APH1)**3+((-Y11-B-T*(B+
*      * .5)*T)*DCOS(P))*APH2*(X11-B-T*(B+T*.5)*DSIN(P))*APH1)*
*      * ((Y11-B-T*(B+T*.5)*DSIN(P))*APH2*(X11-B-T*(B+.5*T)*
*      * DCOS(P))*APH1)**2)*T*(B+.5*T)
EST=0.0
I=1
RH(1)=A
V(1)=B
GO TO (11,12,13,14,15,16),MH
11 FR(1)=FUNCT1(A,C402,APH1,C400,C401,APH2,T)
PS(1)=FUNCT1(A+(B-A)/4.,C402,APH1,C400,C401,APH2,T)
FT(1)=FUNCT1(A+(B-A)/2.,C402,APH1,C400,C401,APH2,T)
FV(1)=FUNCT1(B,C402,APH1,C400,C401,APH2,T)
FU(1)=FUNCT1(A+3.*B/4.,C402,APH1,C400,C401,APH2,T)
GO TO 50
12 FR(1)=FUNCT2(A,C402,APH1,C400,C401,APH2,T)
PS(1)=FUNCT2(A+(B-A)/4.,C402,APH1,C400,C401,APH2,T)
FT(1)=FUNCT2(A+(B-A)/2.,C402,APH1,C400,C401,APH2,T)
FV(1)=FUNCT2(B,C402,APH1,C400,C401,APH2,T)
FU(1)=FUNCT2(A+3.*B/4.,C402,APH1,C400,C401,APH2,T)
GO TO 50
13 FR(1)=FUNCT3(A,C403,APH1,C400,C401,APH2,T)
PS(1)=FUNCT3(A+(B-A)/4.,C403,APH1,C400,C401,APH2,T)
FT(1)=FUNCT3(A+(B-A)/2.,C403,APH1,C400,C401,APH2,T)
FV(1)=FUNCT3(B,C403,APH1,C400,C401,APH2,T)
FU(1)=FUNCT3(A+3.*B/4.,C403,APH1,C400,C401,APH2,T)
GO TO 50
14 FR(1)=FUNCT4(A,C403,APH1,C400,C401,APH2,T)
PS(1)=FUNCT4(A+(B-A)/4.,C403,APH1,C400,C401,APH2,T)
FT(1)=FUNCT4(A+(B-A)/2.,C403,APH1,C400,C401,APH2,T)
FV(1)=FUNCT4(B,C403,APH1,C400,C401,APH2,T)
FU(1)=FUNCT4(A+3.*B/4.,C403,APH1,C400,C401,APH2,T)
GO TO 50
15 FR(1)=FUNCT5(A,X11,Y11,B,T,APH1,APH2)
PS(1)=FUNCT5(A+(B-A)/4.,X11,Y11,B,T,APH1,APH2)
FT(1)=FUNCT5(A+(B-A)/2.,X11,Y11,B,T,APH1,APH2)
FV(1)=FUNCT5(B,X11,Y11,B,T,APH1,APH2)
FU(1)=FUNCT5(A+3.*B/4.,X11,Y11,B,T,APH1,APH2)
GO TO 50
16 FR(1)=FUNCT6(A,X11,Y11,B,T,APH1,APH2)
PS(1)=FUNCT6(A+(B-A)/4.,X11,Y11,B,T,APH1,APH2)
FT(1)=FUNCT6(A+(B-A)/2.,X11,Y11,B,T,APH1,APH2)

```

50

51

52

53

54

55

56

60

200

100

71

72

71

74

75

```

76 GO TO 80
   PS(I-1) = FUNCT6 (RR(I-1) + ((V(I-1) - RR(I-1)) / 4.), X11, Y11, R, T, APH1,
   *          APH2)
   PU(I-1) = FUNCT6 (RR(I-1) + 3. * (V(I-1) - RR(I-1)) / 4., X11, Y11, R, T, APH1,
   *          APH2)
80  I=I-1
   GO TO 50
300 CONTINUE
800 CONTINUE
   RETURN
   END
CCCCC *****
* THIS SUBROUTINE CALCULATES THE DEFLECTIONS & ROTATION
* AT ANY CROSS-SECTION FOR ANY PARTICULAR VALUE OF LOAD
* USING GALERKIN METHOD.
*****
SUBROUTINE DEPROT (PYE, PXE, PCE, P, C13, C14, C15, EU, EV, CLENTH,
*                VVI, UUI, E, U, V, PHI, PHIDER)
* IMPLICIT REAL*8 (A-H, O-Z)
* DIMENSION A(3,3), B(3), WKAREA(80), U(11), V(11), PHI(11),
*          PHIDER(11)
  A(1,1) = PYE - P
  A(1,2) = 0.
  A(1,3) = -P * C14 * 1.419594418
  A(2,1) = 0.
  A(2,2) = PXE - P
  A(2,3) = P * C13 * 1.419594418
  A(3,1) = -P * C14 * .5507
  A(3,2) = P * C13 * .5507
  A(3,3) = C15 * (PCE - 1.001870809 * P)
  B(1) = -P * P / PYE * EU * 1.273239545
  B(2) = -P * P / PXE * EV * 1.273239545
  B(3) = -P * P * .650108904 * (EU * C14 / PYE - EV * C13 / PXE)
  IA = 3
  N = 1
  N = 3
  IDGT = 9
  CALL LEQT2F(A, N, N, IA, B, IDGT, WKAREA, IER)
  C1 = B(1)
  C2 = B(2)
  C3 = B(3)
  D0 = 4.73004 / CLENTH
  D1 = 3.1415927 / CLENTH
  D2 = P * EU / (2. * E * VVI)
  D3 = P * EV / (2. * E * UUI)
  Z = 0.
  DEL = CLENTH / 10.
  DO 25 I = 1, 11
    U(I) = D2 * Z * (Z - CLENTH) * C1 * DSIN(D1 * Z)
    V(I) = D3 * Z * (Z - CLENTH) * C2 * DSIN(D1 * Z)
    PHI(I) = C3 * (DSIN(D0 * Z) - DSINH(D0 * Z) - 1.017809411 * (DCOS(D0 * Z) - DCOSH(D0 * Z)))
    * PHIDER(I) = D0 * D0 * (-DSIN(D0 * Z) - DSINH(D0 * Z) + 1.017809411 * (DCOS(D0 * Z)
    * DCOSH(D0 * Z))) * C3
  Z = Z + DEL
25  CONTINUE
  U(11) = 0.
  V(11) = 0.
  PHI(11) = 0.
  RETURN
  END
CCCCC *****
* THIS SUBROUTINE CALCULATES THE STRESSES AT THE PRE-
* DEFINED 16 DIFFERENT POINTS OF EACH OF THE 11
* DIFFERENT CROSS-SECTIONS AND RETURNS THE MAXIMUM AND
* MINIMUM STRESSES, AT ANY OF THOSE 11 CROSS-SECTIONS
* AND 11 X 16 POINTS THROUGHOUT THE LENGTH OF THE COLUMN
*****
SUBROUTINE SIGMA (PLOAD, EU, EV, UP, VP, C, ININ, IMAX, JXSTR, SIGMAX,
*                MNSTR, U, V, BETA, UZERO, VZERO, Z, PHIDER, AVOMGS,
*                WSC1, WSC2, LMT, CO2, APR, C1, X1, APH1, APH2, D1, D2, CW,
*                CCC, C2, R, D10, D11, D12, D13, D14, D15, CCD)
* IMPLICIT REAL*8 (A-Z)
* INTEGER I, II, JX, JN, KK, JFK
* DIMENSION STRESS(16), VP(16), UP(16), S(16), U(11), V(11),
*          BETA(11), PHIDER(11), JXSTR(11), MINSTR(11)
  C10 = PLOAD / C
  DO 50 II = 1, 11
    C11 = (EV - V(II)) - (EU - UZERO) * BETA(II) * PLOAD / IMAX
    C12 = (EU - U(II)) + (EV - VZERO) * BETA(II) * PLOAD / IMIN

```

```

C13=E*PHIDEZ(LI)
C14=1.5707963
IF(CW.EQ.0.)GO TO 182
A=-C11*X1*APH1+C12*X1*APH2+C13*HPR*CO2*DSIN(LMT)
B=-C11*X1*APH2-C12*X1*APH1+C13*HPR*CO2*DCOS(LMT)
CONS=-C13*CO2*CO2
H=DNAX1(A,B,CONS)
A=A/H
B=B/H
CONS=CONS/H
CALL SOLVE2(A,B,CONS,THTA)
GO TO 75
182 A=-C11*X1*APH1+C12*X1*APH2
    B=-C11*X1*APH2-C12*X1*APH1
75  THTA=DATAH(-B/A)
    XP=-(D2*X1*DCOS(THTA))
    YP=-(D1*X1*DSIN(THTA))
    UP(9)=YP*APH1+XP*APH2
    VP(9)=YP*APH2-XP*APH1
    XP=-(D2*B*DCOS(THTA))
    YP=-(D1*B*DSIN(THTA))
    UP(16)=YP*APH1+XP*APH2
    VP(16)=YP*APH2-XP*APH1
    IF(CW.EQ.0.)GO TO 185
    DO 5 I=1,4
        STRESS(I)=C10+C11*VP(I)+C12*UP(I)+C13*AVONGS
    5  CONTINUE
    DO 25 I=7,8
        STRESS(I)=C10+C11*VP(I)+C12*UP(I)+C13*(AVONGS-WSC1*C1)
    25 CONTINUE
    DO 92 I=5,6
        STRESS(I)=C10+C11*VP(I)+C12*UP(I)+C13*(AVONGS-WSC2)
    92 CONTINUE
    WS(9)=AVONGS-(WSC1*C1-CO2*CO2*(C14-THTA)-RPR*CO2*
        *DCOS(LMT+(C14-THTA))-DCOS(LMT))
    STRESS(9)=C10+C11*VP(9)+C12*UP(9)+C13*WS(9)
    WS(16)=WS(9)
    STRESS(16)=C10+C11*VP(16)+C12*UP(16)+C13*WS(16)
    WS(10)=AVONGS-(WSC2-CCC*(C2-D10))
    WS(11)=AVONGS-(WSC2-CCC*(C2-D11))
    WS(14)=AVONGS-(WSC2-CCC*(C2-D14))
    WS(15)=AVONGS-(WSC2-CCC*(C2-D15))
    WS(12)=AVONGS-(CCD*D12)
    WS(13)=AVONGS-(CCD*D13)
    DO 1212 I=10,15
        STRESS(I)=C10+C11*VP(I)+C12*UP(I)+C13*WS(I)
    1212 CONTINUE
    GO TO 187
    185 DO 99 I=1,16
        STRESS(I)=C10+C11*VP(I)+C12*UP(I)
    99 CONTINUE
    187 DO 11 I=1,16
        IF(UP(I).EQ.0..AND.VP(I).EQ.0.)STRESS(I)=0.
    11 CONTINUE
C *****
C * SORTING OF THE MAXIMUM AND MINIMUM STRESSES AT A *
C * CROSS-SECTION *
C *****
    MAXSTR(11)=STRESS(1)
    MINSTR(11)=STRESS(1)
    DO 10 I=2,16
        IF(MAXSTR(11).GT.STRESS(I))GO TO 12
        MAXSTR(11)=STRESS(I)
    12 IF(MINSTR(11).LE.STRESS(I))GO TO 10
        MINSTR(11)=STRESS(I)
    10 CONTINUE
    50 CONTINUE
C *****
C * SORTING OF THE MAXIMUM AND MINIMUM STRESSES IN THE *
C * COLUMN *
C *****
    MIXSTR=MAXSTR(1)
    MINSTR=MINSTR(1)
    DO 90 II=2,11
        IF(MIXSTR.GT.MAXSTR(II))GO TO 95
        MIXSTR=MAXSTR(II)
    95 IF(MINSTR.LE.MINSTR(II))GO TO 90
        MINSTR=MINSTR(II)
    90 CONTINUE
    RETURN

```



```

C      END
C      *****
C      * THIS SUBROUTINE CALCULATES THE ANGLE THETA, THAT IS, THE *
C      * POINT OF MAXIMUM STRESS IN THE CURVED PORTION, IF ANY *
C      *****
C      SUBROUTINE SOLVE(A,B,C,THETA)
C      IMPLICIT REAL*8 (A-Z)
C      INTEGER I
C      I=1
C      THETA=0.
C      INCR=.1
5      Y=A*DSIN(THETA)+B*DCOS(THETA)+C
      Y=A*DSIN(THETA+INCR)+B*DCOS(THETA+INCR)+C
      IF((X.GT.0. .AND. Y.LT.0.) .OR. (X.LT.0. .AND. Y.GT.0.)) GO TO 10
      THETA=THETA+INCR
      IF(THETA.GT.1.5708) GO TO 100
      GO TO 5
10     GO TO (15,25,35,40),I
15     INCR=INCR/10.
      I=2
      GO TO 5
25     INCR=INCR/10.
      I=3
      GO TO 5
35     INCR=INCR/10.
      I=4
      GO TO 5
40     THETA=THETA+.5*INCR
      GO TO 101
100    THETA=0.
101    RETURN
      END

```



APPENDIX 4

DEFINITE INTEGRALS

APPENDIX 4

DEFINITE INTEGRALS

$$\int_0^l \sin \frac{\pi z}{l} dz = 0.6366 l$$

$$\int_0^l \sin^2 \frac{\pi z}{l} dz = 0.5000 l$$

$$\int_0^l \left[\sin \frac{\lambda z}{l} - \sinh \frac{\lambda z}{l} - \alpha' \left(\cos \frac{\lambda z}{l} - \cosh \frac{\lambda z}{l} \right) \right] dz = 0.8457 l$$

$$\int_0^l \left[\sin \frac{\lambda z}{l} - \sinh \frac{\lambda z}{l} - \alpha' \left(\cos \frac{\lambda z}{l} - \cosh \frac{\lambda z}{l} \right) \right]^2 dz = 1.0359 l$$

$$\int_0^l \sin \frac{\pi z}{l} \left[\sin \frac{\lambda z}{l} - \sinh \frac{\lambda z}{l} - \alpha' \left(\cos \frac{\lambda z}{l} - \cosh \frac{\lambda z}{l} \right) \right] dz = 0.7098 l$$

$$\int_0^l \sin \frac{\pi z}{l} \left[-\sin \frac{\lambda z}{l} - \sinh \frac{\lambda z}{l} + \alpha' \left(\cos \frac{\lambda z}{l} + \cosh \frac{\lambda z}{l} \right) \right] dz = -0.3131 l$$

$$\int_0^l \left[\sin \frac{\lambda z}{l} - \sinh \frac{\lambda z}{l} - \alpha' \left(\cos \frac{\lambda z}{l} - \cosh \frac{\lambda z}{l} \right) \right] \left[-\sin \frac{\lambda z}{l} - \sinh \frac{\lambda z}{l} \right.$$

$$\left. + \alpha' \left(\cos \frac{\lambda z}{l} + \cosh \frac{\lambda z}{l} \right) \right] dz = -0.5696 l$$

APPENDIX 5

SAMPLE CALCULATION FOR COMPUTATION OF
ACTUAL DIMENSIONS OF TEST SPECIMENS

APPENDIX 5

SAMPLE CALCULATION FOR COMPUTATION OF ACTUAL
DIMENSIONS OF TEST SPECIMENS

Nominal dimensions of the specimen: 55 x 55 x 4 mm

Mass = 3.713 kg

Length = 1.208 m

Mass density = 7850 kg/m³

Volume = $\frac{3.713}{7850} = 4.73 \times 10^{-4} \text{ m}^3$

Cross-sectional area = $\frac{\text{Volume}}{\text{Length}} = \frac{4.73 \times 10^{-4}}{1.208} = 3.9155 \times 10^{-4} \text{ m}^2$
 $= 3.9155 \times 10^2 \text{ mm}^2$

	1	2	3	4	5	6
Thickness (t) (in.)	0.156	0.160	0.158	0.155	0.155	0.155

Average thickness = 0.156 in = 3.96 mm

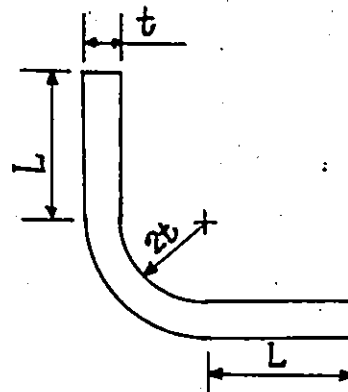
Centre line length of the cross-section of angle

$$= \frac{3.9155 \times 10^2}{3.96} = 98.13 \text{ mm}$$

From the figure,

$$L + L + \frac{\pi}{2} \times 2.5t = 98.13 \text{ mm}$$

or $L = 41.23 \text{ mm}$



Actual dimensions are

$(41.23 + 12) \times (41.23 + 12) \times 3.96$

i.e., $53.2 \times 53.2 \times 3.96$ mm.

APPENDIX 6

TYPICAL CALCULATIONS FOR THE DETERMINATION
OF FAILURE LOADS

APPENDIX 6

TYPICAL CALCULATIONS FOR THE DETERMINATION OF FAILURE LOADS

A6.1 According to ASCE Manual No. 52 (based on nominal dimensions)(a) Single-bolted specimen

Consider ES65-3-1

$$\left(\frac{b}{t}\right)_{\text{actual}} = \frac{65-12}{4} = 13.25; E = 205 \text{ GPa}; \sigma_y = 300 \text{ MPa}$$

$$\left(\frac{b}{t}\right)_{\text{limit}} = \frac{208}{\sqrt{\sigma_y}} = 12.01 = 12 < 13.25$$

$$\therefore \left(\frac{b}{t}\right)_{\text{limit}} < \left(\frac{b}{t}\right)_{\text{actual}}$$

$$\sigma_{y,\text{eff}} = \left[1.8 - \frac{0.8 \times 13.25}{12}\right] \times 300 = 275 \text{ MPa}$$

$$C_c = \pi \sqrt{\frac{2E}{\sigma_{y,\text{eff}}}} = 121.3$$

$$\frac{Kl}{r_y} = 171$$

$$\frac{Kl}{r_y} > C_c$$

$$\sigma_{cr} = \frac{\pi^2 \times 205\,000}{171^2} = 69.19 \text{ MPa}$$

$$\text{Failure Load} = 69.19 \times 426.83 = 29530 \text{ N} = 29.5 \text{ kN}$$

(b) Multiple-bolted specimen

Consider ES65-3-3

$$\frac{Kl}{r_y} = 46.2 + 0.615 \times 171 = 151.37$$

$$\frac{Kl}{r_y} > C_c$$

$$\sigma_{cr} = \frac{\pi^2 \times 205\,000}{151.37^2} = 88.30 \text{ MPa}$$

$$\text{Failure Load} = 88.30 \times 426.83 = 37690 \text{ N} = 37.7 \text{ kN}$$

A6.2 According to ECCS Recommendations (based on nominal dimensions)(a) Single-bolted specimen

Consider ES65-3-1

$$E = 210 \text{ GPa}; \sigma_y = 300 \text{ MPa}$$

$$\lambda = \frac{Kl}{r_y} = 171$$

$$\lambda_y = \pi \sqrt{\frac{E}{\sigma_y}} = \pi \sqrt{\frac{210\,000}{300}} = 83.12$$

$$\frac{\lambda}{\lambda_y} = \frac{171}{83.12} = 2.057 > 1.41$$

$$\left(\frac{\lambda}{\lambda_y} \right)_{\text{eff}} = \frac{\lambda}{\lambda_y}$$

$$\lambda_{\text{eff}} = \lambda = 171$$

$$\sigma_{\text{cr}} = 58.0 \text{ MPa}$$

$$\text{Failure Load} = 58.0 \times 426.83 = 24756 \text{ N} = 24.8 \text{ kN}$$

(b) Multiple-Bolted specimen

Consider ES65-3-3

$$\frac{\lambda}{\lambda_y} = 2.057$$

$$1.41 \leq \frac{\lambda}{\lambda_y} \leq 3.5$$

$$\left(\frac{\lambda}{\lambda_y} \right)_{\text{eff}} = 0.35 + 0.75 \times 2.057 = 1.893$$

$$\lambda_{\text{eff}} = 1.893 \times 83.12 = 157.35$$

$$\sigma_{\text{cr}} = 67.2 \text{ MPa}$$

$$\text{Failure Load} = 67.2 \times 426.83 = 28683 \text{ N} = 28.7 \text{ kN}$$